0-315-13255-8.

61165L

NAME OF AUTHOR/*NOM DE L'AUTEUR* _____ Philip Marsh

TITLE OF THESIS/*TITRE DE LA THÈSE* _____ "Ripening Processes and Meltwater Movement in

_____ Arctic Snowpacks"

UNIVERSITY/*UNIVERSITÉ* _____ McMaster University

DEGREE FOR WHICH THESIS WAS PRESENTED/
GRADE POUR LEQUEL CETTE THESE FUT PRÉSENTÉE _____ Ph.D.

YEAR THIS DEGREE CONFERRED/*ANNÉE D'OBTENTION DE CE DEGRÉ* _____ 1983

NAME OF SUPERVISOR/*NOM DU DIRECTEUR DE THÈSE* _____ Dr. M.K. Woo

DATED/*DATE* _____ January 26, 1983. _____ SIGNED/*SIGNÉ* _____

PERMANENT ADDRESS/*RÉSIDENCE FIXE*: _____ 1735 Grasmere Cres #2

_____ Ottawa Ont

NL-91 (11-73)

Ripening Processes and Meltwater Movement

in Arctic Snowpacks

By

© Philip Marsh, B.A., M.Sc.

A Thesis

Submitted to the School of Graduate Studies

in Partial Fulfilment of the Requirements

for the Degree

Doctor of Philosophy.

McMaster University

December 1982

SNOWPACK RIPENING PROCESSES AND MELTWATER MOVEMENT

FRONTISPIECE: Top – Aerial view of the Resolute study area.
The McMaster River basin is outlined in black.
Photography was taken in August 1976.

Bottom – Oblique aerial photograph of the Eidsbotn
study area. The Nauyak River basin is outlined by the
dotted line and the numbers refer to individual
tributaries. The photograph was taken in July 1951.

DOCTOR OF PHILOSOPHY (1982)   McMASTER UNIVERSITY
                                        Hamilton, Ontario

TITLE: Ripening Processes and Meltwater Movement
                   in Arctic Snowpacks

AUTHOR: Philip Marsh, B.A.   (York University)
                                M.Sc. (McMaster University)

SUPERVISOR: Dr. M.K. Woo

NUMBER OF PAGES: xviii, .179

ABSTRACT

This is a study of the processes controlling snowpack ripening and the movement of meltwater through wet snowpacks. Measurements made in the Canadian High Arctic during the 1979, 1980, and 1981 snowmelt periods, included premelt stratigraphy, surface energy balance, physical changes in snowpack properties during melt, snow and soil temperatures, and water movement within the pack.

Field observations and computer modelling demonstrated an interdependence of finger flow at the wetting front and ice layer growth at premelt snow horizons. Ice layers grow rapidly in cold snowpacks, slowing the finger wetting front advance and releasing considerable latent heat which warms the underlying snow and soil. Since the ground is frozen when water reaches the ground surface, the meltwater refreezes at the snowpack base. The growth of this basal ice layer limits the amount of water available for daily runoff and extends the melt period, a phenomenon which is typical of cold arctic snowpacks.

A redistribution of flow within the snowpack, concentrating flow in certain areas and diminishing it in others, is due to variations in ice layer properties, and not flow instabilities or vertical flow channels. The result is a spread of the rising limb of the melt wave at depth and a decrease of the peak flow.

Results from a multiple flow path model, suggest that flow variability is similar in snowpacks from different environments. This indicates that the model is applicable to snowpacks in a wide range of environments.

v.

ACKNOWLEDGEMENTS

TABLE OF CONTENTS

LIST OF FIGURES

LIST OF TABLES

NOTATION

a	constant $= 5.47 * 10^{-4}$	$(m\ s)^{-1}$
A_F	fraction of total area covered by fingers	dimensionless
A_s	thermal diffusivity of snow	m^2/s
A_g	thermal diffusivity of the ground	m^2/s
A_w	portion of total area covered by wetting front	dimensionless
C	drag coefficient	dimensionless
C_1	fractional increase in snow density per meter of load per second	$(m\ s)^{-1}$
C_2	snow compaction parameter	m^3/kg
C_i	specific heat of ice $= 2.09 * 10^3$	$J/kg\ C$
C_m	specific heat of mineral fraction $= 1.95 * 10^3$	$J/kg\ C$
C_o	specific heat of organic matter $= 2.50 * 10^3$	$J/kg\ C$
C_p	specific heat of air	$J/kg\ C$
C_s	specific heat of soil	$J/kg\ C$
C_w	specific heat of water	$J/kg\ C$
E	vapour pressure	$Pa=N/m^2$
e	ratio of molecular weights of water and air	dimensionless
F	depth of finger wetting front	m
F_F	fraction of total flow occurring in finger front	dimensionless
F_w	fraction of total flow occurring at general front	dimensionless

g	acceleration due to gravity	m/s²
g$_s$	snow grain diameter	m
H	ice thickness	m
H$_I$	heat released by freezing of infiltrated water	J/m²
H$_{IL}$	heat released by freezing of ice layer	J/m²
H$_{WF}$	heat released by freezing at wetting front	J/m²
H$_T$	total heat released by freezing in snowpack	J/m²
h	distance from node below ice interface to the interface	m
I	soil infiltration	m
K	soil thermal conductivity	W/m C
K$_{DRY}$	dry soil thermal conductivity	W/m C
K$_E$	snow effective thermal conductivity	W/m C
K$_i$	ice thermal conductivity =2.2	W/m C
K$_s$	soil solids thermal conductivity = 8.0	W/m C
K$_{SAT}$	soil saturated thermal conductivity	W/m C
K$_w$	water thermal conductivity = .57	W/m C
k	von Karman's constant =.415	dimensionless
k$_s$	saturated snow permeability	m²
k$_{us}$	non saturated snow permeability	m²
L	section width	m

L_f	latent heat of fusion $= 3.35 * 10^6$	J/kg
L_v	latent heat of vapourization	J/kg
l	section width	m
M	daily snow melt	m
m_i	number of actively growing ice layers	
n	soil porosity	dimensionless
n_f	number of flow paths	
P	atmospheric pressure	$Pa=N/m^2$
p	snow porosity	dimensionless
p_e	effective snow porosity	dimensionless
P_c	capillary pressure	N / m^2
ρ_A	air density	kg/m^3
ρ_b	soil bulk density	kg/m^3
ρ_{bi}	basal ice density	kg/m^3
ρ_m	soil mineral density $= 2700$	kg/m^3
ρ_s	soil density	kg/m^3
ρ_i	density of ice layer	kg/m^3
ρ_m	measured snow density	kg/m^3
ρ_s	snow density	kg/m^3
ρ_w	water density	kg/m^3
$Q*$	net radiation flux density	W/m^2
Q_H	sensible heat flux density	W/m^2
Q_{LE}	latent heat flux density	W/m^2
Q_p	heat flux density due to rain on snow	W/m^2

Q_{TOT}	total heat conduction above and below ice layer	W/m²
R	rainfall	m/s
R_{TL}	ratio between thermal and liquid requirements at the wetting front	dimensionless
r	stability criteria	dimensionless
S	snow water content, by volume	dimensionless
SF	shock front depth	m
siz	flow path size as a fraction of unit area	dimensionless
S^*	effective water content	dimensionless
S_{WE}	total snowpack water equivalent	m
S_{WI}	irreducible water content by pore volume	dimensionless
S_U	water content required to transport flux U	dimensionless
S_R	soil water content by pore volume	dimensionless
T	air temperature	C
T_F	fictious temperature	C
T_G	ground temperature	C
T_M	snow melting point	C
T_R	wet bulb temperature	C
T_S	snow temperature	C
T_{SS}	snow surface temperature	C
T_{SW}	snow temperature below wetting fronts	C
t	time	s

Symbol	Description	Units
t_M	time interval	s
U	mean water flux or melt	m/s
U_F	water flux in finger	m/s
U_{FA}	finger flux over combined width of finger and wetting fronts	m/s
U_{FE}	excess water available to finger front after ice layer growth	m/s
U_{FP}	flux in each flow path	m/s
U_T	sum of flux in all flow paths	m/s
U_W	water flux at general front	m/s
$U+$	larger flux overtaking the shock front	m/s
$U-$	smaller flux overtaken by the shock front	m/s
u	wind speed	m/s
v	dynamic viscosity	m²/s
vol	fraction of total flow occuring in finger	dimensionless
V_s	volume of snow	m³
V_W	volume of water	m³
W	depth of general front	m
W_c	snow cold content	J/m²
W_F	depth of wetting front	m
W_s	change in soil heat storage	J/m²
W_s	weight of snow above a given layer expressed as water equivalent	m
W_T	total finger width across section	mm

W_u	fractional volume of unfrozen water in the soil	dimensionless
$X_{m,o,i}$	fractional volume of mineral, organic, and ice components of soil	dimensionless
Z_{sp}	snowpack depth	m
Z_{il}	ice layer thickness	m
z_s	nodal spacing in snow	m
z_g	nodal spacing in ground	m
z, ss	subscripts denoting height $z = 1.0$ ss = snow surface	m
z_o	surface roughness	m

A listing of the major programs used in this thesis can be obtained from the author. Operation of these programs for conditions other than those used in this thesis cannot be guaranteed.

CHAPTER ONE

INTRODUCTION

1.1 General

Snow is an important component of northern and alpine environments, often controlling runoff during the spring melt period. Techniques for predicting snowmelt runoff have become increasingly more sophisticated since the first empirical attempt at forecasting in North America at Lake Tahoe, Nevada in 1909 (Male and Gray 1981). Empirical techniques generally work well under the environmental conditions for which they were derived, but are prone to large errors when applied to areas with different snowpack conditions. This is a problem because snowpack properties vary from environment to environment, and from year to year. Although hydrological processes operate similarly in different areas their relative importance varies depending on snowpack conditions. To overcome this problem and to make models more general, there has been a gradual shift from deterministic - empirical to deterministic - conceptual type models (Clarke 1973). Anderson(1978) noted that the basic framework of streamflow simulation models is well established, but further research is required to improve our

1

knowledge of certain processes.

The following sections in this chapter offer a brief review of snowmelt runoff and outlines the research objectives of this dissertation. Chapter Two describes the study area as well as methods, and Chapter Three the premelt snow properties of the study sites. Chapter Four describes the snowpack mass balance and the refreezing of meltwater during the entire melt period. A snowpack ripening model is developed in Chapter Five and its predictions compared with measured values. Chapter Six discusses water flux processes in layered snowpacks and Chapter Seven presents the general conclusions of the study.

1.2 Ripening process and meltwater movement

Processes occurring within the snowpack have been of interest to hydrologists and glaciologists for more than 70 years. Initially, hydrologists were concerned with the effects of snowmelt on streamflow and fluvial geomorphology (eg Horton 1915), while glaciologists were interested in the processes transforming snow into firn (eg Ahlmann and Tveten 1923). Since then, research interests of snow hydrologists have followed several avenues such as snowmelt, movement of liquid water into dry snow and the accompanying changes in

snow structure and properties, water movement within the snowcover, and interactions with the soil.

Snowmelt processes have been well understood since the study of Sverdrup (1935b). His energy balance work has been repeated and improved in many studies conducted in a wide range of environments. This work has led to the general conclusion that the energy balance method most accurately predicts melt (Anderson 1976). Yet, the spatial variability of the important parameters makes it difficult to use this type of model at the basin scale and most operational models still use temperature index methods (Male and Gray 1981).

As surface melt begins, water infiltrates into a dry snowpack at a temperature below 0 C. This initial melt may be one of a series of melting events separated by periods of freezing as commonly occur in temperate areas, or it may be the more defined spring melt period characteristic of northern environments. Although this section refers mainly to meltwater, the process of rainwater movement into the snowpack is quite similar. The major difference is that heavy rainfall may occur onto a dry snow cover, while melt more commonly starts slowly and gradually increases over a period of time.

Some of this meltwater infiltrating the sub-zero snowpack must be used to warm the snow through a release of latent heat. It has long been recognized that an isothermal

zone at 0 C, rapidly forms below the snow surface, eliminating the conduction of heat downwards. Sverdrup (1935a) and Ahlmann (1935) conclusively demonstrated that the snow-covered glaciers of Spitsbergen were warmed entirely by a transport of meltwater through this isothermal zone with freezing and subsequent release of latent heat in the cold snow below. Freezing within the pack increased the firn density and produced horizontal ice layers and vertical ice columns. Ice layers and columns have been described in both firn and seasonal snowpacks (Seligman 1941, Gerdel 1945, Gerdel 1948, Sharp 1951, Benson 1962, Wankiewicz 1978a, Berg 1982). The horizontal ice bodies are generally referred to as ice lenses, layers, or sheets, while the vertical columns have been called pillars of ice (Ahlmann and Tveten 1923), ice glands (Ahlmann 1935), pipes (Glen 1941), firn pipes (Sharp 1949, see Sharp 1951), and ice columns (Leighton, see Sharp 1951). Sharp (1951) referred to them as ice glands and that name is still frequently used (Benson 1962). In this thesis "ice layer" will be used for horizontal ice bodies and "ice columns" for the vertical ones.

Yosida (1973) and Colbeck (1976) related the rate of movement of the wetting front into dry snow to a refreezing of sufficient water onto snow grains at the wetting front to warm the snow to 0 C ,and the filling of liquid water storages. The amount of freezing is dependent on the snow

temperature immediately below the wetting front. This temperature, however, is continually changing due to a conduction of heat from the wetting front and ice layers. The wetting front does not move into the dry snow as a horizontal front, but like fluid flow in most porous media (Parlange 1974, Wooding and Morel-Seytoux 1976) it develops flow fingers. Wankiewicz (1978a) provided a theoretical description of the conditions under which fingering should occur in snow, but his ideas have not yet been tested. Fingering is important because it routes some water ahead of the general wetting front (U.S. Army 1956).

Even though ice layers and columns have been frequently described and their importance to warming the snow noted, few studies have dealt with their formation. They are usually assumed to be caused by either burial of surface crusts, or by the freezing within the pack at buried surface crusts. However, it is unclear whether crusts are required or whether changes in snow texture are sufficient for their formation. Most authors believe that some type of surface crust is required, but no evidence is provided. Wankiewicz (1978a) suggests that textural changes result in ice layer growth. Many authors imply that repeated freeze-thaw events are required to account for thick ice layers, but the thermal conditions, rate of growth, or relationship to the wetting front or fingering are unknown.

Once the liquid water reaches the snowpack base it infiltrates the soil or becomes runoff. Interactions between meltwater and soil were first described by Horton (1915), but only lately has their importance been discussed (Dunne and Black 1971, Alexeev et al 1972, Anderson 1978, Guymon 1978) as new data indicate the importance of frozen soils. Once the infiltration capacity of a frozen soil is reached, it is often assumed that all meltwater is available for runoff (Dingman 1975). As the glaciological literature has shown, this is not always true. If the substrate is still below 0 C when the infiltration capacity is reached, ground heat flux is sufficient to freeze water at the snow pack base. This water is not directly available for runoff, but is stored until later in the melt season. This basal ice layer has been observed in seasonal snow (Horton 1915, Work 1948, Dunne and Black 1971, Jordan 1978, Woo and Heron 1981, Woo et al 1982) and glacial environments (Ahlmann and Tveten 1923, Schytt 1949, Baird 1952, Ward and Orvig 1953, Koerner 1970, Holmgren 1971, Wakahama et al 1976). In the glaciological literature this ice layer is referred to as superimposed ice. In this thesis it will be called basal ice. Ward (and Orvig (1953) and Holmgren (1971) used an analytical solution to the heat conduction equation, while Wakahama et al (1976) applied a finite difference approximation to demonstrate that downward heat conduction is sufficient to explain the

formation of this layer. Studies of seasonal snowpack ripening have largely ignored the formation of basal ice.

Because most snow hydrology studies have been concerned with warm snow and unfrozen soil where the thermal ripening of the pack is a minor factor controlling runoff, ripening has been handled in a simplistic manner. Normally all water is assumed to be available for runoff once the cold content of the pack (U.S. Army 1956, Male and Gray 1981) is satisfied and the pack is isothermal. However, very large areas of North America are underlain by either seasonally or permanently frozen ground (Dingman 1975). In these areas the complex feedback processes connecting wetting front advance, fingering, ice layer growth, basal ice growth, and heat conduction below the zones of freezing must be included. At present, there is not sufficient understanding of these processes to allow the ripening of cold snowpacks to be predicted in this fashion.

Several processes behind the wetting front affect the movement of water to the wetting front or to the snowpack base. The most important is a rapid growth of the snow grains. This is often called melt-freeze metamorphism (Sommerfeld and LaChappelle 1970), though Colbeck (1982) noted that grain growth does not require melt-freeze cycles but only the presence of liquid water. Wakahama (1968) and Raymond and Tusima (1979) measured the rate of grain growth

in the laboratory and Colbeck (1974) gave a theoretical discussion on grain growth in the presence of liquid water. There is little field data to determine if the rates of growth in the laboratory are similar to those in a natural pack. Grain growth in the presence of liquid water has two important effects. Firstly, it may result in a decrease in the amount of water held by capillary forces (the irreducible liquid water content) (Gerdel 1948, Linsley et al 1949, Gerdel 1954, de Quervain 1972, Ebough and DeWalle 1977) because fine grained snow may hold more water due to higher capillary forces. Secondly, the liquid permeability of the snow increases rapidly (Kuroiwa 1968, Shimizu 1970) as the grains enlarge. As a result of grain growth, the pack is able to store less water, and water is able to move more quickly.

The rate at which water moves through the snow cover is of interest to hydrologists. A number of empirical studies have been carried out to determine the factors controlling this rate (Horton 1915, Seligman 1936, Gerdel 1954). The most detailed was the U.S. Army(1956) snow hydrology study where simple lag-routing type equations were developed, using a few physically measured parameters and empirically derived constants. These equations produce reasonably good results, but require optimization when transferred to a different environment. The theory of fluid

flow developed for other porous media has not been applied to snow until recently (Colbeck 1972, 1978a). Colbeck adopted Darcy's Law for two phase unsaturated flow in rigid porous media and developed equations for predicting the movement of water in homogeneous snow. Unfortunately, this theory is only directly applicable to homogeneous snow. Many studies have shown that natural snow packs are not homogeneous but that preferential flow paths occur (Ahlmann 1935, Sverdrup 1935a, Gerdel 1954, U.S. Army 1956, Wakahama 1968, Colbeck 1979). Very little is known about these features. It has been suggested that they are related to the initial fingering which occurs at the wetting front. The fingers undergo rapid grain growth and have increased permeability, so that once developed they can survive throughout the melt period. Because of the difficulties imposed by these flow channels, Colbeck's equations predicting water flux in snowpacks have only been used in a few research projects (Dunne et al 1976, Wankiewicz 1976, Ambach et al 1981, Bengtsson 1982). Even the most sophisticated snowmelt runoff models (Anderson 1976) still employ equations similar to those presented in U.S. Army (1956). Before these models may be improved, we must advance our understanding of the number, size, and permeability of ice layers and flow channels, and the effect of these features on water movement in natural snowpacks.

1.3 Research Objectives

In light of the above problems associated with our understanding some of the processes occurring in melting snowpacks, it is the purpose of this thesis to study both the complex feed-back processes controlling the initial movement of liquid water into dry, cold snowpacks underlain by a frozen substrate, and the flow of water in layered heterogeneous snow. Specifically, the objectives are:

(1) to study ice layer and basal ice growth in order to quantify the processes responsible for their growth, and to determine their importance in the ripening process

(2) to monitor wetting front advance and to determine the importance of fingering in moving water ahead of the general wetting front

(3) to develop a physically based snowpack-ripening model which couples the effects of wetting and finger fronts, ice layer growth, basal ice growth, thermal conditions of the pack and soil, with prediction of daily changes in snowpack water equivalent

(6) to measure the variability of flow within a ripening snowpack and to develop a multiple flow path model for the prediction of water movement in a layered snowpack.

CHAPTER TWO

STUDY AREA AND RESEARCH METHOD

2.1 Research sites

During the premelt and the melting periods, snow properties were studied at four locations in the Canadian High Arctic (Figure 2.1). These included Eidsbotn Fiord, Devon Island (76 55 N,94 50 W) and Resolute Bay, Cornwallis Island (74 45 N,94 50 W), for the periods May to August 1979 and 1980, and May to July 1981. Additional premelt observations were made in May 1981 near Eureka, Ellesmere Island (80 00 N,86 00 W) and Mould Bay, Prince Patrick Island (76 20 N,119 15 W). At these locations, measurements were made in the drainage basins listed on Table 2.1 (Figure 2.2).

These locations were chosen to represent a wide range of snowcover conditions found in the Queen Elizabeth Islands. This group of islands corresponds roughly to the region defined as the High Arctic by Bird(1967) and to the rock-desert tundra vegetation zone dominated by lichens, avens, and saxifrages shown in the National Atlas of Canada (1974) (Figure 2.1). It encompasses the Northwestern, Northern, and Eastern (Northern Baffin Bay-Lancaster Sound) climatic regions defined by Maxwell(1980).
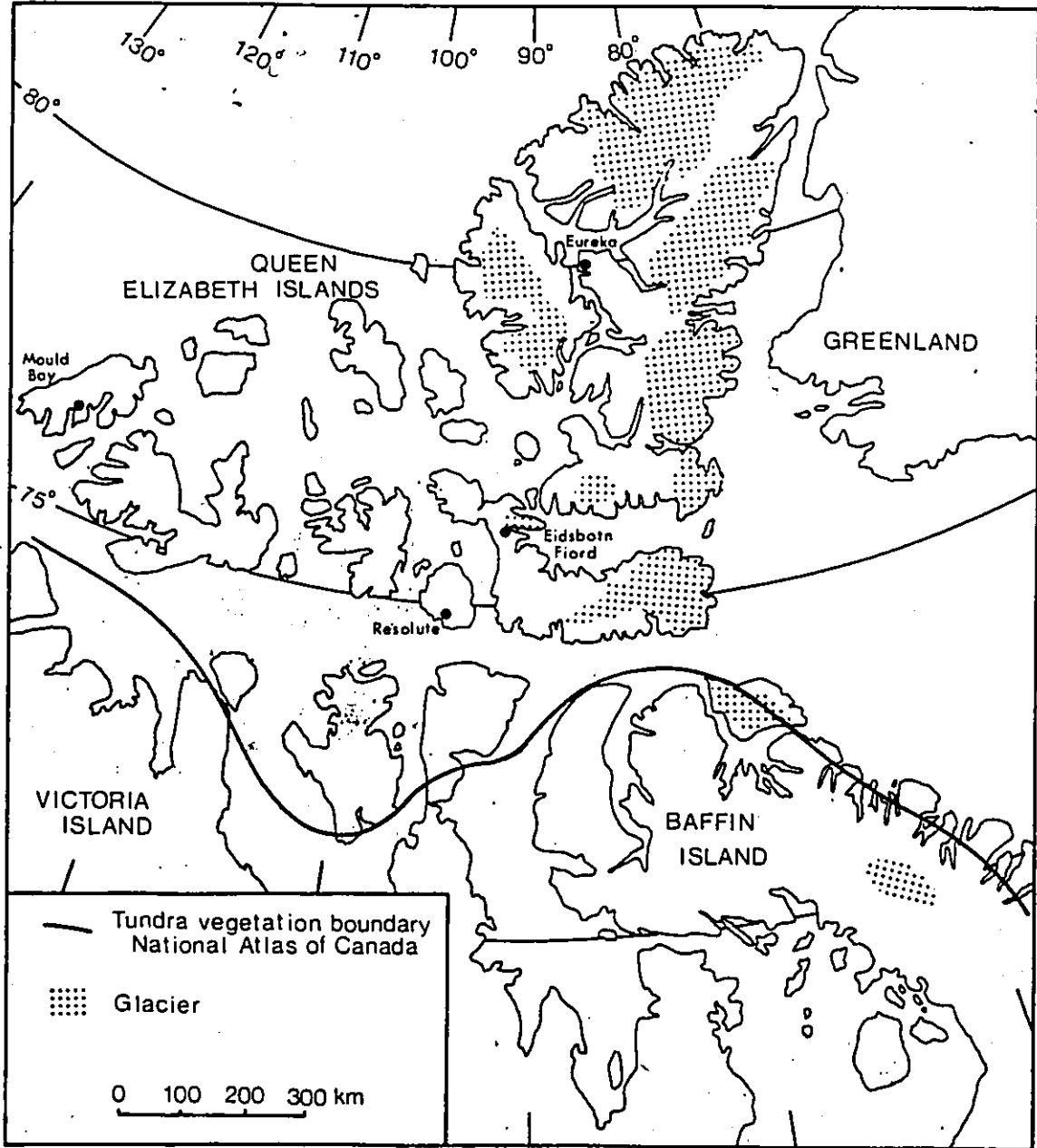
FIGURE 2.1 The Canadian High Arctic and location of the four study areas.
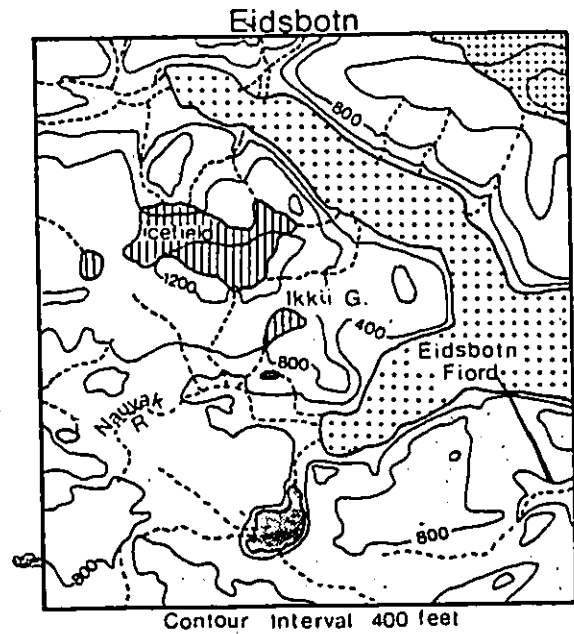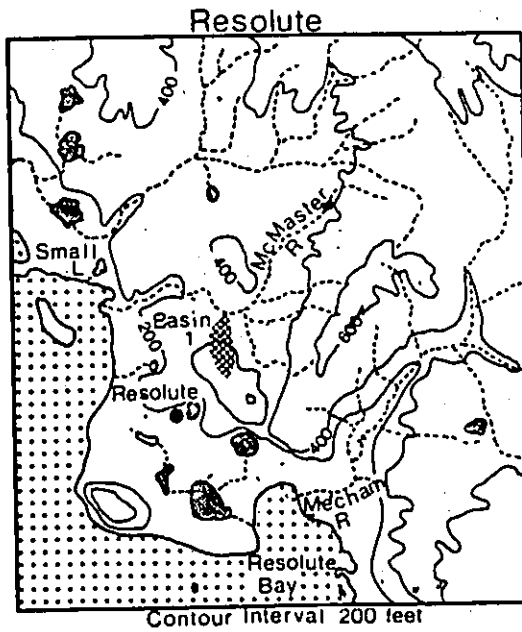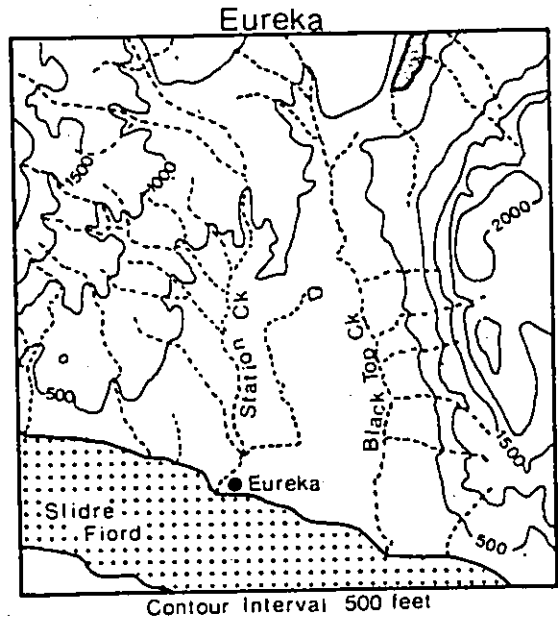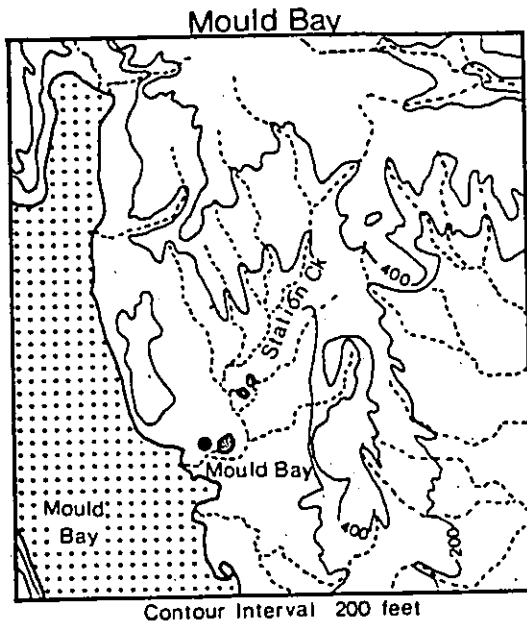
FIGURE 2.2 Topography and basin location of the four study sites.

TABLE 2.1

Size and elevation range of the four study basins

Location	Drainage basin	Area(sq. km)	Elevation(m)
Resolute Bay	Basin #1, McMaster R.	0.5	90 - 170
Eidsbotn Fiord	Nauyak R.	39	30 - 425
Eureka	Station Ck. (lower part)	58	20 - 700
Mould Bay	Station Ck.	44	30 - 150

2.2 Climate and permafrost

Several climatic factors control the amount of snowfall, its redistribution, metamorphism, snowcovered period, and melt. The snowcover characteristics of the High Arctic are dominated by the long duration of sub-zero air temperatures, frequent occurrence of blowing snow, low total precipitation, low net radiation, and cold ground temperatures. Regional variations in these parameters have been described by Maxwell(1980).

In these areas, winter (first day mean temperature less than 0 C) begins between August 20-30 and ends (first day

mean temperature greater than 0 C) between June 10-20. The duration of winter tends to increase from 287 days in the southeast to over 300 days in the northwest. A major exception to this pattern is the Eureka Sound region where winter begins later and ends earlier than other nearby lowlands.

This long winter period is characterized not only by extreme coldness, but also by very persistent low temperatures (Figure 2.3). Above freezing temperatures occur only in early winter and are extremely rare between early October and early May. Mean January temperatures range from -30 C in the southwest to -35 C in the northwest. In many areas, and especially at Eureka, it is common to have extended periods in December and January when temperatures are below -40 C. The radiation regime during late winter is characterized by short daily periods of direct solar radiation, high surface albedo, and negative net radiation. By late May or early June, air temperatures rise considerably and initial snowmelt may begin in sheltered localities. Extensive sublimation may also occur when increased net radiation combines with relatively high temperatures and low humidity. This appears to be quite common in the Eureka Sound region. Intense snowmelt, however, begins when air temperatures rise above 0 C, corresponding with the period between early June and early July. Once spring melt begins,
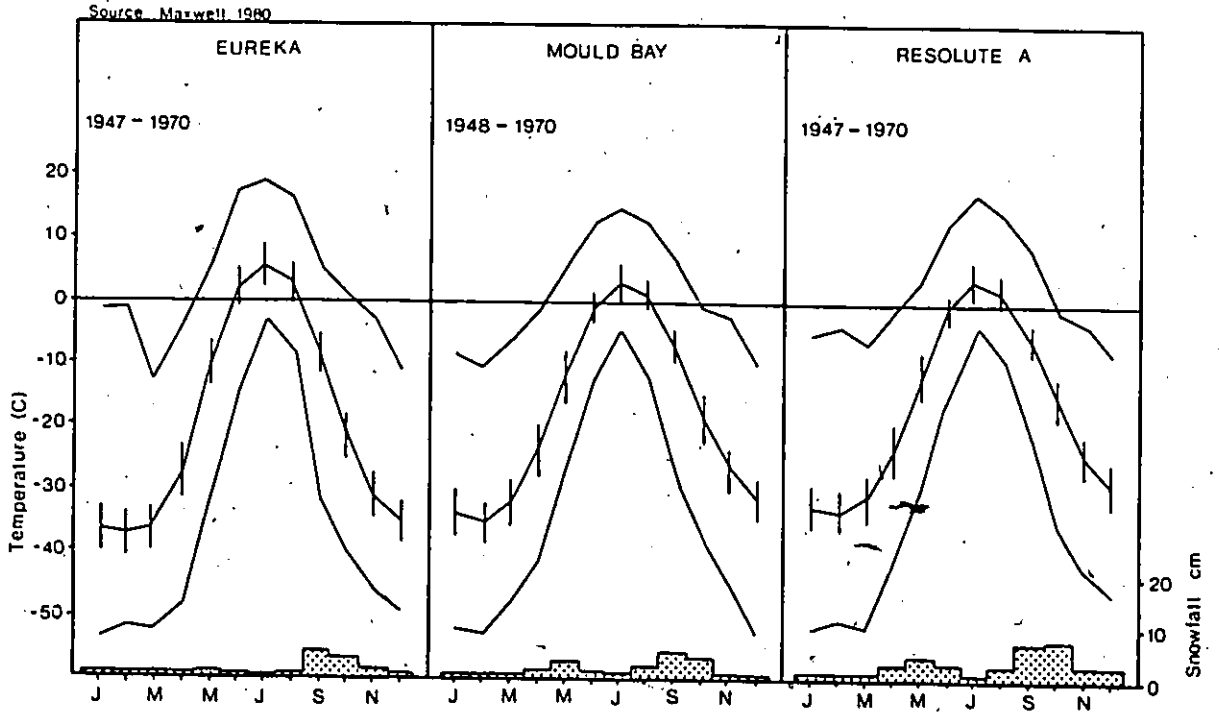
FIGURE 2.3 Daily mean, maximum, and minimum air temperature, extreme maximum and minimum air temperature, and mean monthly snowfall at Eureka, Mould Bay and Resolute Airport.

it progresses rapidly and most snow is melted in 10 to 20 days.

The High Arctic is often classified as a polar desert with mean annual precipitation varying from 100-200 mm in lowland areas to over 300 mm at higher elevations. Snowfall ranges from 0.75 to 1.5 m (Figure 2.4) or some 50 to 90% of total precipitation (Maxwell 1980). Snowfall is concentrated in September and October and is small throughout the remainder of winter (Figure 2.3). Winter rainfall also only occurs in these two months. Numerous water balance studies (Findlay 1969, Hare and Hay 1971, Hare et al 1975, Cogley 1975, Marsh and Woo 1979) have found serious imbalances between inputs and outputs if weather station precipitation is used. Most studies attribute this to an underestimation of true precipitation due to errors in measuring snowfall. True snowfall is difficult to determine due to gauge undercatch in strong winds and the many trace events (Jackson 1960). Snow survey results near Resolute Bay (Woo and Marsh 1977) suggested that actual snowfall is anywhere from 1.7 to 3.1 times that measured by the nearby weather station.

Mean wind speeds (Figure 2.5) in the High Arctic are similar to those of southern areas (Maxwell 1980), but the averages are composed of frequent calm conditions which occur 10 to 25% of the time, alternating with very strong winds

Mean total
precipitation (mm/yr)

for the period
1941 - 1970
Maxwell·1980

Mean total snowfall
(m/yr)

for the period
1941 - 1970
Maxwell 1980
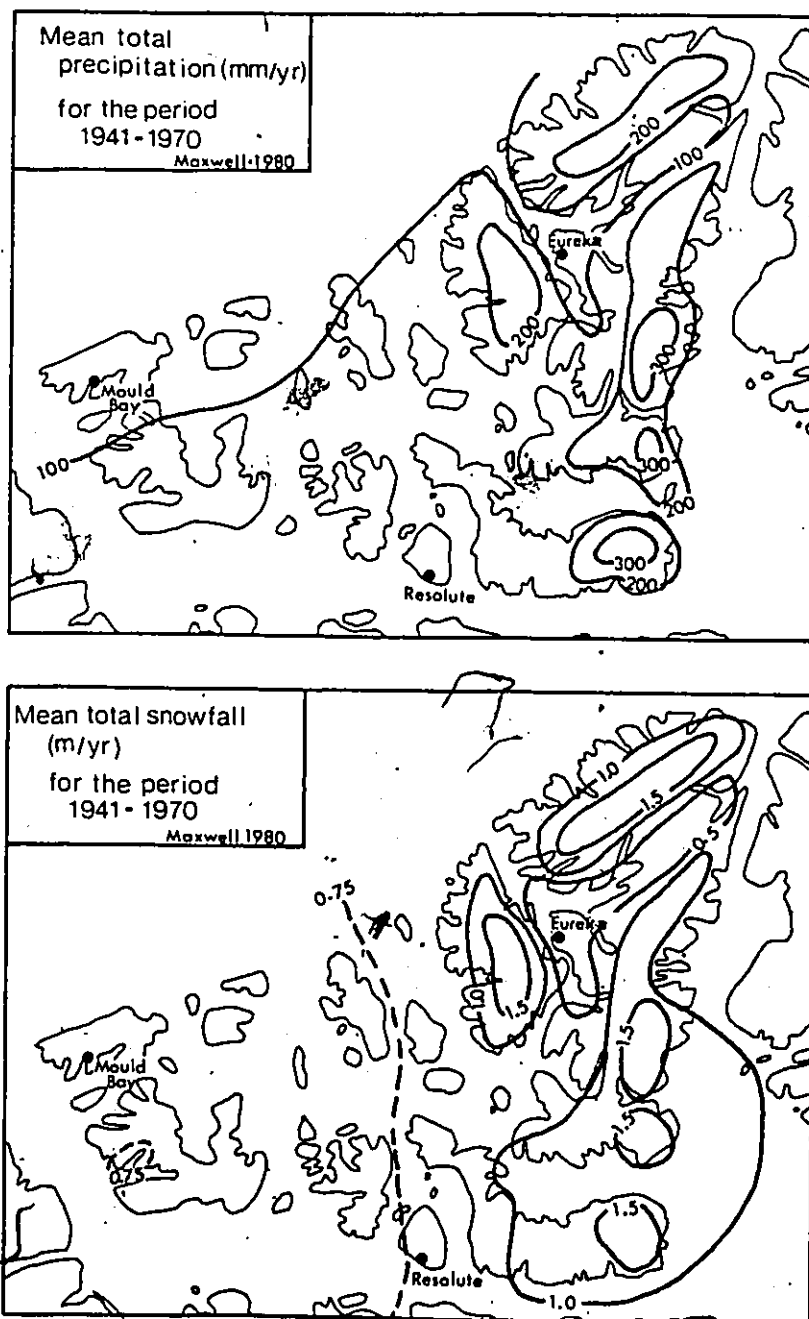
FIGURE 2.4 Mean annual total precipitation and snowfall for
the Queen Elizabeth Islands.

Sept.- Nov.

	mean	ext	calm
Resolute	6 2	39	8
Mould Bay	4 4	23	18
Eureka	2 8	28	20

Values of hourly wind speed
equalled or exceeded
(Maxwell 1980)

.... Resolute

—..— Mould Bay

—— Eureka

period of record   1953-1972

Dec.- Feb.

	mean	ext.	calm
Resolute	5.8	31	13
Mould Bay	4.0	31	3
Eureka	2.8	31	23

Mar.- May

	mean	ext.	calm
Resolute	5.5	32	12
Mould Bay	3.8	21	25
Eureka	3.0	31	19
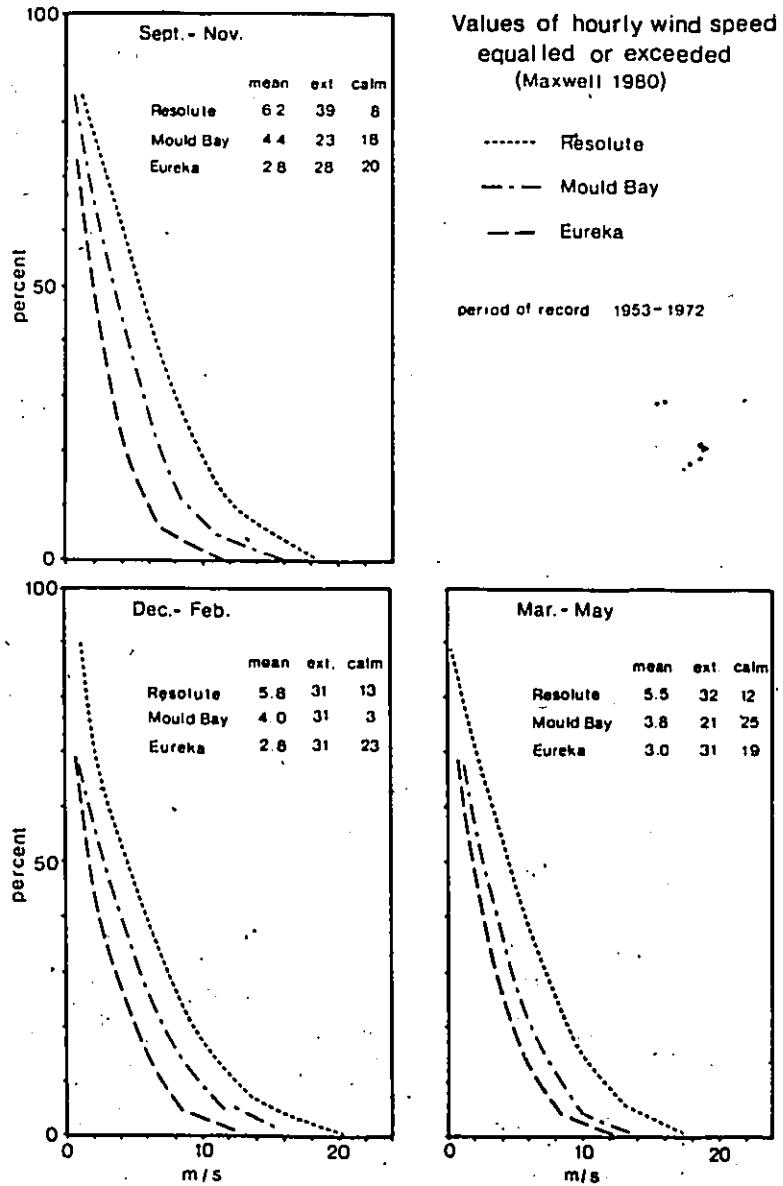
FIGURE 2.5 Values of hourly wind speed equalled or exceeded
at Resolute, Mould Bay, and Eureka. The mean,
extreme, and the percent of time calm are also shown
for each site.

which are frequent in winter. Resolute, for example, experiences a 20% probability of hourly wind speeds of 9.4 m/s or greater during the period December to February. There are regional variations in wind speed, with Resolute being consistently windier than Mould Bay, which is windier than Eureka. Wind exerts a strong control upon the Arctic snowpack, redistributing snow after its initial deposition and increasing its density by wind packing. As a rough estimate, snow drift may commence when wind speeds reach 10 m/s (Mellor 1965). Winds of such magnitude are encountered approximately 5 % (Eureka) and 20 % (Resolute) of the time during the period September to May.

Low air temperatures and a thin but dense snowcover maintain low ground temperatures and a very thick permafrost layer. At Resolute, Miesner(1955) estimated that the permafrost is 390 +/- 3 meters thick, and Cook(1958) determined that the zero annual amplitude occurs at a depth of 19.2 m (Figure 2.6). The temperature at this depth was -12.6 C or 3.3 C higher than the mean annual air temperature. Below this depth the temperature is relatively constant down to 30 m, below which it increases at a rate of 4 C/100 m. Between November and April ground temperatures in the upper meter increase with depth. The associated vapour pressure gradient produces an upward vapour flux from the soil to the snowpack (Woo 1982a). By May, the ground is near its minimum
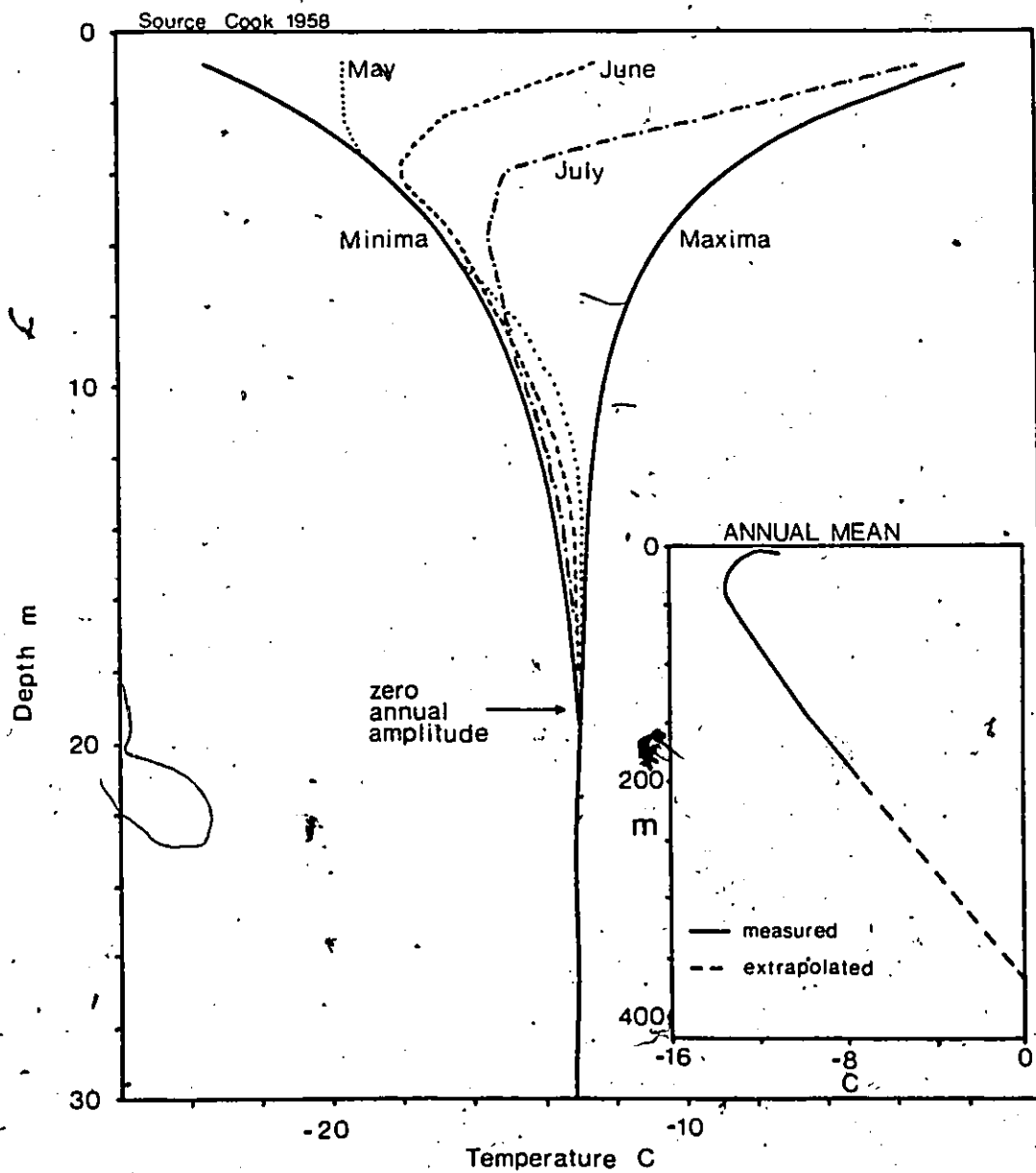
FIGURE 2.6 Mean monthly ground temperature at Resolute for May, June, and July 1955, annual minima and maxima for 1955, and annual mean (Cook 1958).

temperature at all depths. With increasing air temperature and snowmelt, the upper 8 m warms rapidly, but between 8 and 19 m the ground is still cooling in a lagged response to the low winter temperatures. Such a rapid warming of the ground during the snowmelt period has important implications for snowpack metamorphism.

2.3 Snowcover characteristics

Snowcover properties at the beginning of melt, affect the sequence of melt metamorphism events. The thermal and stratigraphic characteristics of the High Arctic snowcover are different from those found in more southerly latitudes and the pack may therefore be expected to ripen differently.

Blowing snow is the dominant factor controlling the High Arctic snowpack properties. It results in the dominance of small grains, less than 1 mm in diameter, due to breakage and high densities caused by wind packing. Billelo (1969) showed that this region has a mean seasonal snow density of over 310 kg/m^3 and that high densities are common throughout winter. Frequent high winds also result in irregular distribution of snow at the end of winter. Young (1969) and Woo and Marsh (1977) found that snow depth could vary from 0

to over 2.5 m within very short distances and that individual terrain units had distinctive snowcovers in terms of depth and density.

Strong temperature gradients (lowest temperature near the snow surface) within the pack induce large vapour pressure gradients. As a result, faceted hoar crystals grow at the expense of rounded grains in the warmer, lower portions of the pack (Colbeck 1982). This temperature gradient metamorphism (Sommerfeld and LaChapelle 1970) or kinetic growth (Colbeck 1982) produces a thick layer of hoar at the base of the snowpack.

A combination of the above processes produces a snowpack that is characterized by high density, small grain size, distinct depth hoar layer, well distinguished layering, and variable snow depth (Gold and Williams 1957). The generalized description of the Alaskan north slope snowcover, presented by Benson et al(1974), also applies to the snowcover of the High Arctic. At the surface there is usually a thin layer of soft, low density snow (150 to 200 kg/m^3) deposited during periods of low wind. Underlying this layer is a sequence of hard, fine grained (0.5 to 1.0 mm) wind slab (350 to 450 kg/m^3), and medium grained (1 to 2 mm) snow (230 to 350 kg/m^3). The properties of each layer are dependent on snow type, temperature, and wind speed during deposition. Finally, at the base of the pack there is always

a layer of coarse (5 to 10 mm), loosely bonded depth hoar crystals (200 to 300 kg/m³). The thickness of this layer is independent of the early winter stratigraphy but is governed by temperature gradient and permeability to vapour diffusion.

Few studies have examined the changing characteristics of the Arctic snowpack during the melt period, although the formation of ice layers within (Benson et al 1974) and at the base of the snowpack (Benson et al 1974, Woo and Heron 1981, Woo et al 1982) have been described.

2.4 METHODS

All major instrumentation sites at Eidsbotn Fiord (1980) and Resolute (1981) are shown in Figure 2.7.

Premelt Snow Properties

The premelt snow properties which affect melt metamorphism are : (1) snow pack depth, (2) layering sequence, (3) layer thickness, horizontal variability and extent, (4) the number of layers, and (5) layer density, grain size and liquid permeability. To examine the spatial variability of these properties within each study basin a stratified sampling procedure based on topographic units was

★ snowpit - melt
• thermistor rod
+ basal ice
::: glacier

N

+IA1
+IA2
IA3 +★5-5
+IA9

Ikkii Glacier

2-11
2-10 ★★

2-7★★2-8
★1-1

Nauyak River

Eidsbotn
Fiord

0   1   2 km

⊙ meteorological station
★ snowpit- melt
• snow-soil thermistor rod
△ recording lysimeters-2
▲ multi-compartment
   lysimeter

McMaster River

Basin 1
boundary

△ •upper
★CC6
▲
★CC7

N

•gravel
★F8

•bog   •F9
★F10   ⊙

0   100   200
            m
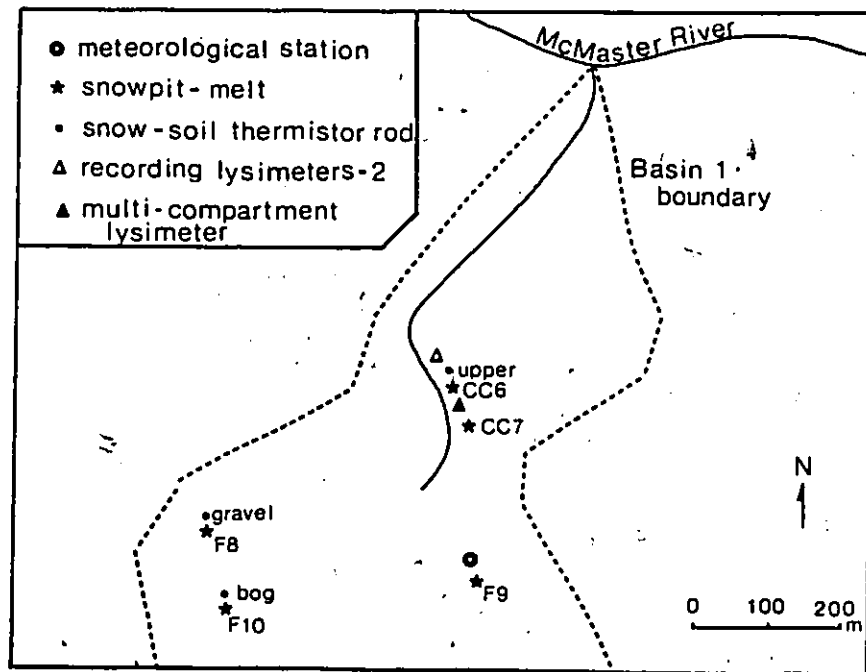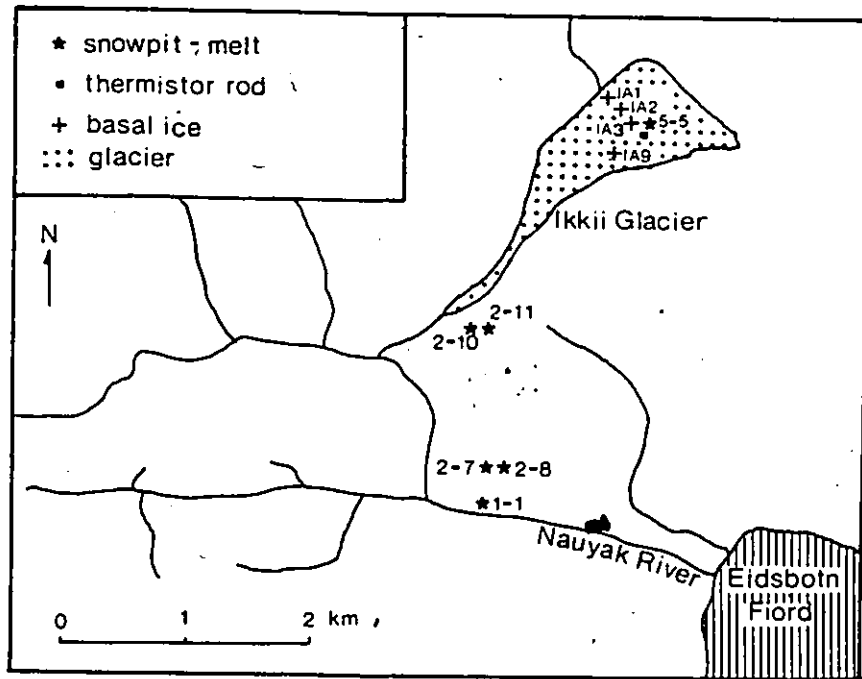
FIGURE 2.7 Instrument and snowpit locations for Eidsbotn
(1979, 1980) and Resolute (1981).

established.

Because drifting dominates the development of Arctic snowpacks, topographic units were chosen on the basis of those factors affecting snow deposition and erosion. As snow accumulates in a topographic area due to drifting, its surface profile and aerodynamic properties gradually change. Eventually, snow storage approaches its maximum value, the surface approaches an equilibrium profile (Tabler 1975), and catch efficiency is reduced. Most snow entering that topographic unit thereafter, is not deposited but transported out of the unit. Based on their relative snow retention capacities, a number of topographic units were selected for each study basin (Table 2.2). Because each drainage basin had different terrain characteristics, each required its own suite of topographic units.

TABLE 2.2

Topographic units and snow survey dates for each study basin

Nauyak R.	Basin 1	Mould Bay.	Eureka
flat	flat	flat	flat
convex slope	convex slope	hilltops	w. slope
concave slope	concave slope	undulating	drainage
valley bottom	gullies	valleys	net
glacier		rolling	rolling
		gullies	gullies
		scarps	valleys
May 1980	May 1981	May 1981	May 1981

In 1980 a preliminary survey was carried out at Eidsbotn Fiord. Snow pits were dug in which detailed stratigraphic measurements were made and sample lines were run across individual topographic units and snow depths sampled. The survey comprised 35 pits and a total of 216 depths measured along seven lines. In May 1981, a similar scheme was employed at Basin 1, McMaster River basin, Resolute. A total of 29 pits were sampled and 272 depths measured along seven profile lines, allowing within and between unit variability to be compared. Figure 2.8 shows the extent and area of each of these topographic units. At the same time a detailed snow survey of McMaster River basin was conducted (Woo 1982b). In addition, seven pits were sampled at both Eureka and Mould Bay. This program did not allow the variation within topographic units to be studied but was used to compare the overall snow properties to those of the other study sites.

One face of each pit was cleaned off with a wire brush or a scraper to highlight individual strata. These strata were usually well defined in terms of snow hardness and were easy to recognize. Within each layer the following measurements were made:

(1) Layer thickness, with a folding carpenter's rule

(2) Snow density, with snow cutters ranging in size from 50
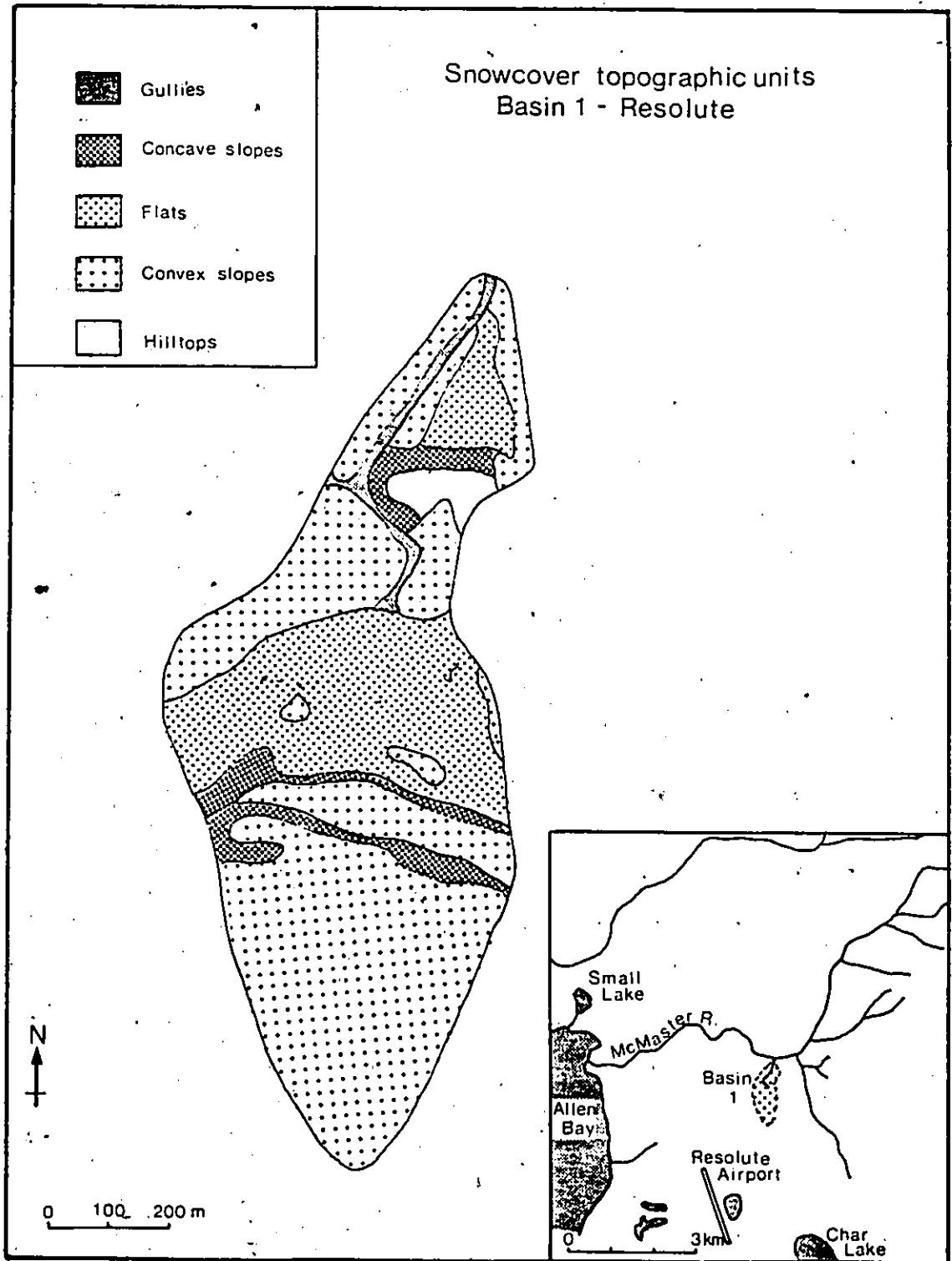
FIGURE 2.8 Snowcover topographic units for Basin 1, Resolute.

to 250 cm³. Samples were weighed in the field on a Geotest temperature compensated snow density scale housed in a case with a plexiglass door to protect it from the wind. Generally, two samples were obtained from each layer, but a few pits were sampled in greater detail to determine the variability within layers

(3) Grain size, determined at representative pits by taking black and white photographs of snow grains placed on a plexiglass plate with 1 mm grid markings, using a transmitted illumination method (LaCapelle 1969). In the laboratory the photographs were projected onto a screen with a 12x magnification. Square grids marked on the screen were picked randomly and all grains within it were measured to an accuracy of 0.1 mm. This procedure was repeated until 100 grains were measured.

(4) Snow temperatures, measured in the snowpit walls using Fenwall disc thermistors.

Snowmelt

During the 1981 field season at Resolute, surface melt
was computed using the energy balance approach (Sverdrup
1935b, Price and Dunne 1976):

(2.1) $U = (Q* + Q_H + Q_{LE} + Q_P)/L_P$

where all fluxes are defined as positive downwards and U is
surface snowmelt, $Q*$ is net radiation, Q_H is sensible heat
flux, Q_{LE} is latent heat flux, Q_P is heat flux due to rain,
and L_P is the latent heat of fusion. When calculating
surface snowmelt, the ground heat flux was ignored. Since
the snow surface temperature is at 0 C and the surface
humidity is close to saturation during melt, the bulk
transfer approach may be used (Heron and Woo 1978) to
calculate the sensible and latent heat fluxes:

(2.2) $Q_H = p_A C_P C u(T_z - T_{ss})$

(2.3) $Q_{LE} = p_A L_v (e/P) C u (E_z - E_{ss})$

where p_A is air density, C_P is the specific heat of air,
u is wind speed, T is air temperature at the surface (SS)
and at 1 m (z), L_v is the latent heat of vapourization, e is
the ratio of molecular weight of water and air, P is
atmospheric pressure, and E is vapour pressure at the surface
(SS) and at height Z. For simplicity it was assumed that the

drag coefficient (C) was the same for both sensible and latent heat fluxes and was calculated from:

(2.4) $C = k^2 / (\ln(z/z_o))^2$

where k is von Karman's constant. The surface roughness (Z_o) was obtained empirically (Heron and Woo 1978).

The drag coefficient was modified with the Richardson number (Price and Dunne 1976) to correct for non-neutral atmospheric conditions. The heat flux due to rain on snow (Q_p) was obtained by:

(2.5) $Q_p = \rho_w C_w R (T_R - T_{ss})$

where ρ_w is water density, C_w is specific heat of water, R is rainfall, T_{ss} is snow surface temperature, and T_R wet bulb temperature.

All instrumentation was installed over a level snow covered site (Figure 2.7) before the beginning of melt. Air temperature and humidity were recorded with a Lambrecht thermohygrograph housed in a Stevenson's screen, and recorder readings were checked at least twice daily with a mercury thermometer and an Assmann psychrometer. Net radiation was measured with a Swisstecco net radiometer, and recorded on a Rustrak recorder. A Cassella sensitive cup anemometer and a Rustrak event recorder continuously monitored wind speed.

The level of all instruments was frequently adjusted to a height of 1 m above the melting snow surface. Air pressure and rainfall measurements were obtained from the Atmospheric Environment Service weather station. Woo et al (1981) estimate that daily melt rates are accurate to +/- 5% using this method.

Snow Ripening

Throughout the 1980 and 1981 field seasons, changes in snowpack properties were monitored at five snow pits at Eidsbotn and Resolute. These were chosen to provide a representative selection of snow depths. Daily measurements of snow depth, layer thickness, density, grain size, position of the wetting front, and ice layer thickness and properties were obtained from the snow pits, and the snow and ground temperatures were measured at the thermistor rods. Between measurements, the snow pits were protected with double layer mylar radiation shields to minimize melting of the pit wall. Immediately before sampling, half of the pit face was cleaned back approximately 0.2 m. This ensured that clean undisturbed snow was sampled and allowed the continuity of the layers to be determined. The techniques for measuring density, snow depth, and grain size were similar to those used during the premelt period. Other observations include the following:

(1) Position of the wetting front was estimated   as   the deepest   point   where   the   snow   grains   were   wet   and rounding of grains had begun

(2) Thickness of ice layers (both within and at the   base   of the snowpack) was measured   to   the   nearest   5   mm   and observations were made on   the   horizontal   extent,   ice type,   and   uniformity   of   these   layers.   Occasional measurements of ice density were obtained   by   immersing preweighed samples in cold diesel oil to determine their volume

(3) Liquid water content of   the   snow   was   calculated   from measured changes in snow density.   After   melt   begins, change in density is due to (1) storage of liquid water, (2) change in density of the snow grains   which   depends on   compaction   and   metamorphic   change   in   structure (Kojima 1967), and the freezing of water   directly   onto the snow grains. As will   be   shown   in   Chapter   Five, little freezing occurs directly onto   the   snow   grains. As a result the increase in snow density is less than 1% and may be ignored.   The increase in snow density due to compaction may be important and can be   expressed   as   a function of time (Anderson 1976):

(2.6) $p_s(n+1) = [1.0 + t_n C_1 W_s \exp(-C_2 p_s(n))$
$\exp(-0.8 (T_n-T_s))] p_s(n)$

where p_s is snow density at time n and n+1, t_M is the time interval, C_1 is the fractional increase in density per meter of load per second, W_s is weight of snow above a given layer, C_2 is a compaction parameter, T_M is the melting point of ice, and T_s is the snow temperature. Anderson (1976) used values of C_1 from $7.2 * 10^{-4}$ to $19.2 * 10^{-4}$ (m s)$^{-1}$ and a constant value for C_2 of 0.021 m^3/kg.   This equation is applicable to wet snow at the normal values of liquid saturation found in freely draining snow.   Then, the difference between predicted and measured density is due to the liquid water content, which may be calculated as:

(2.7) $S = (p_M - p_s)/(p_W)$

where S is liquid water content by volume, p_M is measured snow density, p_s is predicted snow density, and p_W is the density of water .

In order to check the applicability of equation 2.6, it was compared with data from Colbeck et al(1978) who carried out a detailed analysis of the effects of grain growth, liquid saturation, dissolved impurities, and overburden pressure on the densification of wet snow.   Their measured changes in snow density for the conditions shown in Table 2.3 were compared to those

predicted by equation 2.6:

TABLE 2.3

Snow conditions during snow density changes measured by Colbeck et al (1978)
and parameters used in equation 2.6

Snow conditions reported by Colbeck et al (1978)	Parameters for equation 2-6
overburden pressure = 4790 Pa	$C_1 = 13.2 * 10^{-4}$ (m s)$^{-1}$
= .489 m w.e.	$C_2 = .021$ m^3/kg
water pressure = 1014 Pa	$W_0 = .489$ m w.e.
= .1 - .2 by volume	$T_M = 0$ C
solute concentration= 20.5 mg/l	
initial grain size = .5 mm	

These conditions are similar to those found in the
Arctic type of snow. Solute concentrations measured near
Resolute in 1976 varied from 12 to 65 mg/l, grain size
was usually slightly smaller than 0.5 mm, and the water
pressure, and overburden pressure were typical. Results
using equation 2.6 agree well with the data of Colbeck
et al. It tends to underpredict density over the first
two days of compaction and overpredict during the next
10 days. The maximum overestimation was 2 kg/m³. This
could account for an error in estimating liquid water
content of 3%, or approximately 4% of the entire pack
water equivalent, but is sufficiently accurate for the
purposes required in the present study. Profiles of
liquid water content are not used in this study because
they continuously varied as the diurnal melt wave

penetrated the pack and there were large horizontal variations due to flow channels. Instead, the data were only used to estimate the total liquid water storage in the pack.

(4) Snow temperatures in 1981 were obtained from three sites using Fenwall disc thermistors embedded in 0.1 m plexiglass tubes attached to wooden rods. A major problem with measuring snow temperature during melt is the increased melt around the rod, the conduction of heat down the rod and a percolation of melt water along it. An attempt was made to overcome this problem by mounting the thermistors so that they were 0.1 m away from the rod (Figure 2.9). The success of this technique will be discussed later. All thermistors were calibrated in an ice-water bath before and after the study period and have an accuracy of +/- 0.1 C. During the 1979 field season, a 4 m thermistor cable installed on Ikkii glacier in May was monitored during June and July.

Soil Properties

The total volume of water which may infiltrate the frozen soils was measured at two sites in each of the bog and polar desert soil types (Cruickshank 1971) found in the
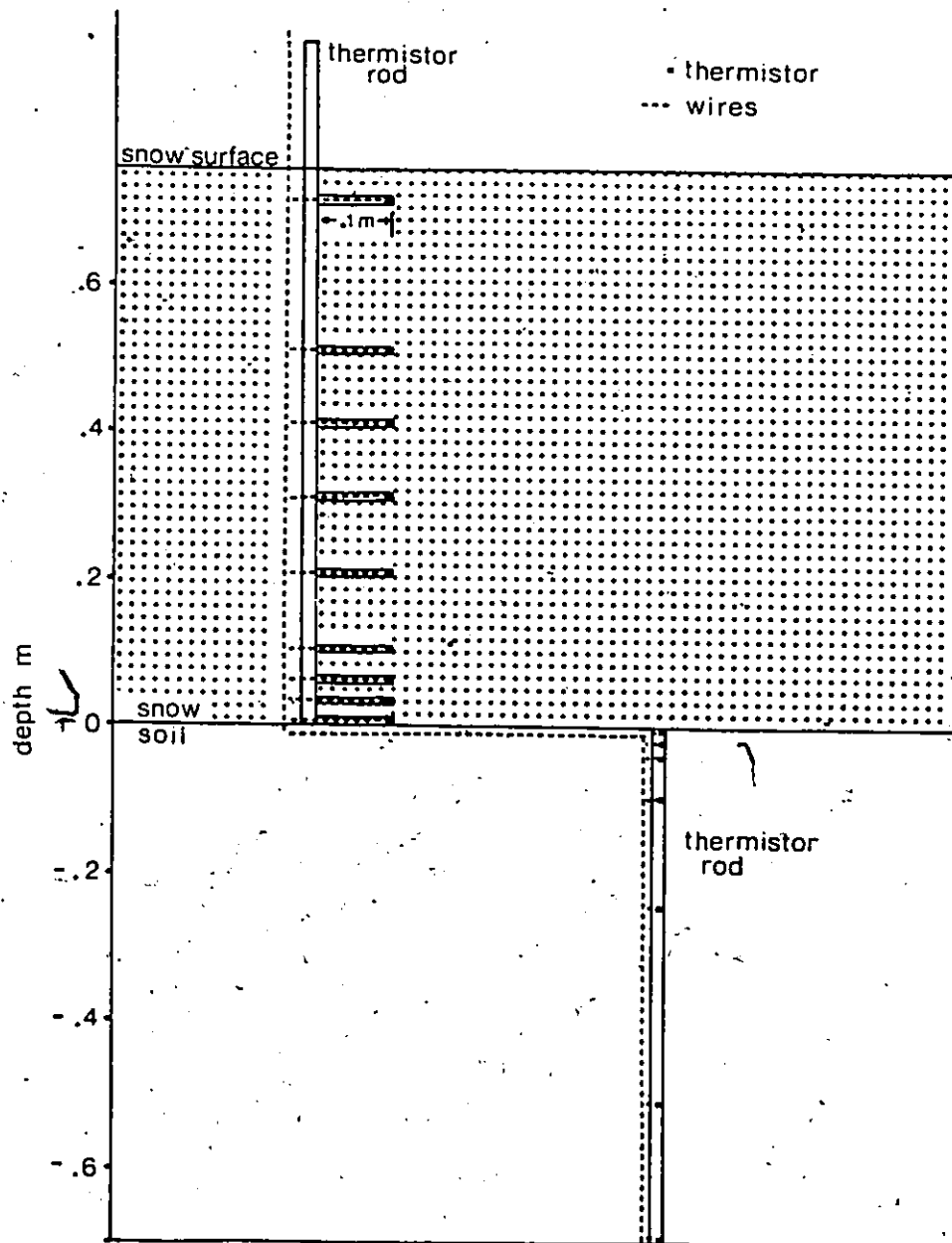
FIGURE 2.9 Combined snow-ground thermistor installation. Snow thermistors project 0.1 m away from the rod to reduce the thermal effects of the rod. Soil rod is cut off at the surface and the wires run up the snow rod to ensure natural conditions. The soil rod was installed prior to snow accumulation, while the snow rod was installed at the end of winter.

Resolute study area. A constant head infiltrometer similar to that described by Hills(1970) was used. Steel cylinders, open at each end and 97 mm in diameter were placed , into the soil in August 1980. In early June 1981, the snow overlying these cylinders was removed, and a known volume of water at 0, C was added until the infiltration rate fell to zero.

Three rods with Fenwall disc thermistors were installed in the ground to a depth of 0.7 m in August 1980 at the Resolute study sites. Two of these were in polar desert soils and one in bog. To ensure that the problems discussed in the snow temperature section were avoided, the thermistor rods were cut off just below the ground surface and the wires run below the ground surface to a pole which carried the wires to the snow surface (Figure 2.9).

The bulk density of each soil type was determined by oven drying samples of known volume. Using an estimated solids density of 2700 kg/m³ (Faurouki 1981) the soil porosity (n) was determined as:

(2.8) $n = 1 - p_b / p_s$

where p_b is the soil bulk density and p_s is the minerals density. The volumetric water content of the soils was measured with a Campbell Pacific Nuclear Model 503 Hydroprobe.

Snow and soil thermal properties

A number of empirical studies have related snow density and snow thermal conductivity. In all cases the measured thermal conductivity combines both the effects of heat conduction through the snow grains and heat transfer by vapour diffusion. The coefficients are therefore termed effective thermal conductivity. Anderson (1976) summarized relationships reported in the literature and suggested the following relationship

(2.9) $K_E = 0.00005 + .006\ p_s^2$

where K_E is the effective thermal conductivity and p_s the snow density.

Farouki (1981) compared four methods for calculating thermal conductivity of frozen soil. He found that the method of Johansen (1975) provided the best predictions for frozen fine soils, sands, or gravels with a water content from 0.10 up to 1.0 by pore volume. Farouki (1981) reported that Johansen determined the dry thermal conductivity (K_{DRY}) as:

(2.10) $K_{DRY} = (.135\ p_s + 64.7) / (2700 - .947\ p_s)$

where p_s is the soil bulk density. The saturated thermal

conductivity (K_{SAT}) was calculated from the geometric mean of the thermal conductivity of the solids (K_s), ice (K_i), and water (K_w):

(2.11) $K_{SAT} = K_s^{(1-n)} K_i^{(n-Wu)} K_w^{Wu}$

where n is the soil porosity, and Wu the fractional volume of the unfrozen water. The soil thermal conductivity (K) was then computed as:

(2.12) $K = (K_{SAT} - K_{DRY}) S_R + K_{DRY}$

where S_R is the water content by pore volume.

The specific heat of the frozen soils (C_s) was computed from (Sellers 1965):

(2.13) $C_s = (X_m C_m + X_o C_o + X_i C_i) / p_s$

where the subscripts m,o,i refer to minerals, organics, and ice, and X is their fractional volume, C their specific heat, and p_s the soil density.

Energy released by the refreezing of meltwater

Considerable amounts of heat are released within the snowpack by a refreezing of meltwater. This energy may be conducted downward from the point of freezing, warming both

the snow and the underlying soil.. Water may freeze onto the snow grains at the wetting front, as ice layers, as basal ice, or within the soil.

The amount of energy released per unit area by the formation of ice layers or basal ice (H_{IL}) was calculated by:

$$(2.14) \quad H_{IL} = L_F \ (p_i - p_s) \ Z_{IL}$$

where L_F is the latent heat of fusion, p_i is the density of the ice mass, p_s is the snow density, and Z_{IL} is the ice thickness measured in the snowpits. Freezing may also occur onto the snow grains at the wetting front where the energy per unit area (H_{WF}) may be calculated from

$$(2.15) \quad H_{WF} = |T_{SW}| \ p_s \ C_i \ Z_{SP}$$

where T_{SW} is the snow temperature immediately below the wetting front, p_s is snow density, C_i the specific heat of ice, and Z_{SP} the snowpack depth at the begining of melt. The heat released by freezing of water infiltrated into the soil (H_i) was calculated as:

$$(2.16) \quad H_i = L_F \ p_w \ I$$

where p_w is water density and I depth of water infiltrated.

In this study, two periods are recognized during melt: (1) the anisothermal period which begins with the start of melt and ends when the main wetting front reaches the snowpack base. During this period the snowpack consists of both wet and dry snow, and (2) the isothermal period which continues until the end of melt, during which the entire snowpack is wet and at 0 C.

During the anisothermal period, the heat released by refreezing is used to warm both the snow and soil. The amount used to warm the snow can be calculated from:

$$(2.17) \quad W_c = |T_s| \cdot \rho_s \cdot C_i \cdot Z_{sp}$$

where W_c is the snow cold content and T_s is the average snowpack temperature for a snowpack of depth Z_{sp}, on the first day of melt. The rest of the energy released by freezing within the pack is used to warm the ground. This energy may be calculated in a way similar to equation 2.17, but such an approach was not used because the soil thermal properties below 0.7 m are unknown. Instead the soil heat flux was calculated as a residual:

$$(2.18) \quad W_s = H_T - W_c$$

and

$$H_T = H_{sL} + H_{uf}$$

where W_s is the heat used to warm the soil, and H_T is the

total heat released by freezing within the snow. Throughout the isothermal period, all heat released by freezing of soil infiltration and the growth of the basal ice layer is used to warm the soil.

Meltwater Movement

To monitor the movement of meltwater within the snow pack, three lysimeters were installed in 1981.

Two of these were large lysimeters (area 1.0 and 0.25 m²) with an impervious base and three walls (Figure 2.10). Three drain-holes were used in each to route the meltwater to a tipping-bucket gauge connected to an event recorder which provided a continuous record of flow. Data were then used to determine hourly mean fluxes. The other lysimeter was also 0.25 m² in area, but was divided into 16 separate compartments (Figure 2.10). Each compartment was drained by a single hole leading to a collection bottle. All bottles were emptied each morning. This multi-compartment lysimeter allowed a direct measurement of daily flow variability within a natural snowcover. All lysimeters were installed on June 15, 1981, the first day the snowpack became isothermal. The installation procedure consisted of digging three snow pits, and inserting the lysimeters into slots cut into the pit wall
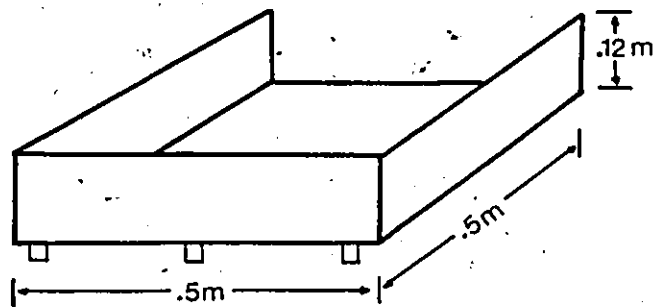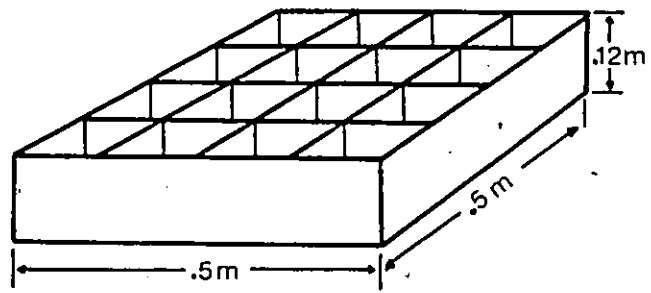
FIGURE 2.10 Top - multi-compartment lysimeter. Each
separate compartment drains into a plastic bottle
which is emptied daily.
Bottom - recording lysimeter. There is no rim along
the upslope edge in order to facilitate installation.
A 1m x 1m lysimeter of the same design was also used.
The three drains at the back of the lysimeter
conducted meltwater to a tipping bucket gauge.

approximatly 0.6 m above the base of a 1.4 m deep snowpack.
The collecting end of the lysimeter was at a minimum distance
of 0.35 m from the pit wall. This notch was then refilled
with snow. These procedures ensured that the lysimeters were
set in undisturbed snow and were well away from the effects
of the pit wall.

A detailed analysis of the hydraulic characteristics of
snow lysimeters was conducted by Wankiewicz (1978b) who
outlined three sources of error associated with their use:
(1) change in surface melt rate due to disturbing the snow
during installation, (2) a transfer error between the surface
and the lysimeter due to changes in storage or diversion of
water due to ice layers, and (3) undercatch of melt water due
to the hydraulic characteristics of the lysimeter. Problems
related to the first type of error were minimal since the
snow surface immediately above the lysimeter was not affected
and effects of the pit wall were eliminated by covering the
pit face with a double-layer mylar radiation shield and also
covering the pit with a mylar-coated plywood sheet. Transfer
errors were minimized by using lysimeters of large surface
area in an attempt to average the flow variations.
Wankiewicz (1978b) showed that problems due to hydraulic
characteristics could be minimized by proper design. He
found that the lysimeter outlet discharge is essentially the
same as the flow at the lysimeter depth when the raised rim

of the lysimeter is equal in height to the pressure gradient zone. This varies in height from 0.07 to 0.18 m depending on flow. The walls of the lysimeters used in this study were 0.12 m in height, a value sufficiently high to maximize catch efficiency. The response time of this type of lysimeter is approximately 15 minutes for a sudden increase in flow rate from 0.05 to $1.0 * 10^{-4}$ m/s (Wankiewicz 1978b). Such a short response time will not seriously affect the determination of hourly flow conditions. A final problem concerns the startup time. Wankiewicz (1978b) found that for flux rates of 1.0 to 0.05 $* 10^{-4}$ m/s this varied from four hours to three days. With melt rates of about $0.1*10^{-4}$ m/s averaged over a daily period, two days were considered to be sufficient to allow the lysimeters to stabilize. Since these response times and starting times were calculated for a horizontal lysimeter (Wankiewicz 1978b), they should represent maximum values for the sloping lysimeters used in this study.

CHAPTER THREE

PREMELT SNOWCOVER CHARACTERISTICS

The snowcover characteristics prior to the melt period play an important role in snowpack ripening. Properties such as snow depth, density, layering, and temperature control the initial movement of water into the pack. This chapter will describe the characteristics of the High Arctic snowpack sampled at Resolute in May 1981. and will demonstrate that the results are applicable to a large part of the Canadian High Arctic.

3.1 Stratigraphy and properties at a pit section

Strata properties

A prominant feature of all snowpits studied over a two year period was the occurence of a number of distinct strata (Figure 3.1). At each snowpit the strata were detected by easily perceptible differences in hardness. Using hardness as the principle criteria, all strata were distinctly different from those above or below, and the boundary between any two strata was very sudden and clear. In many cases, however, the strata could not be differentiated in terms of density or grain size. At pit CC6 for example, a
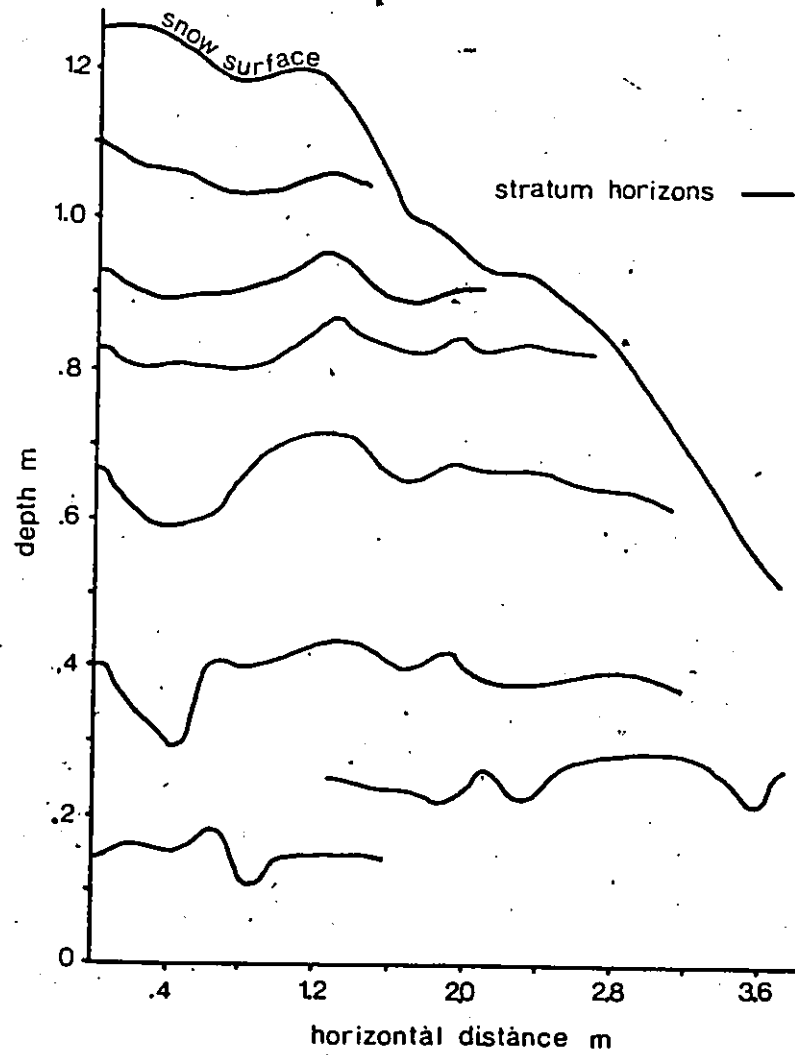
FIGURE 3.1 Layer structure for pit CC6. From daily profiles taken at approximately 0.2 m intervals between June 2 and June 26, 1981.
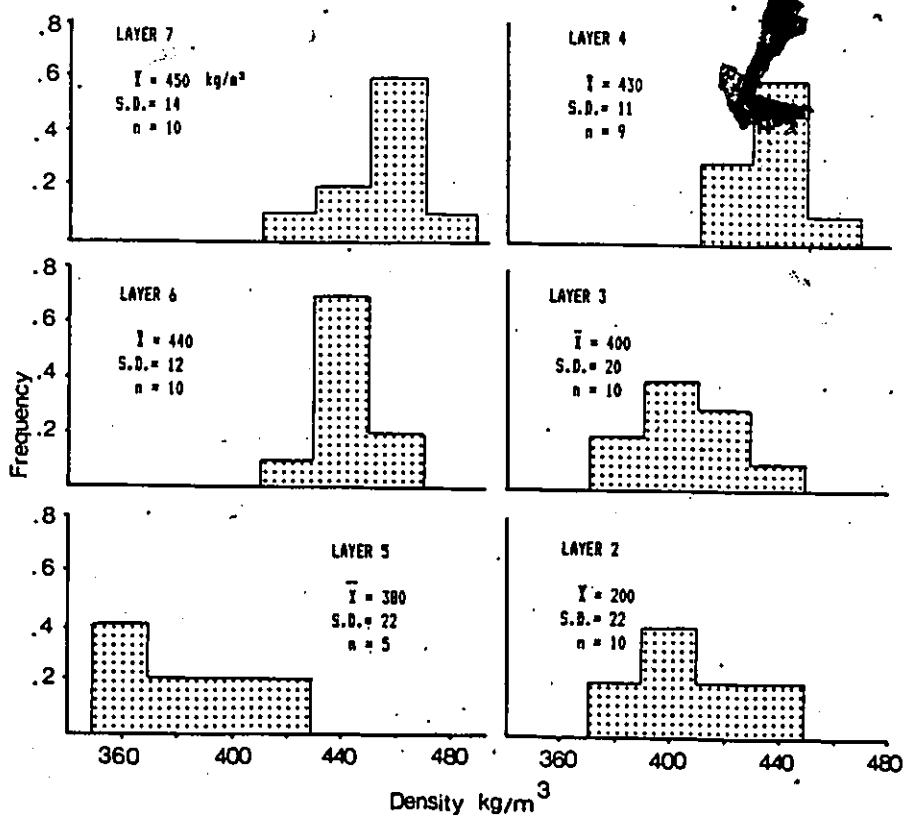
FIGURE 3.2 Freque... distribution of premelt layer densities... Layer 7 is at the top of the snowpack.

Kolmogorov-Smirnov test showed that the density of layers seven - six and three - two (Figure 3.2), and the grain size of layers seven - six, four - three, and three - two (Figure 3.3) were not significantly different at the 5% level. Even though these strata were perceptibly different, and as will be shown in Chapters Four and Five play an important role in snow metamorphism, their differences often could not be quantified.

All strata were characterized by unimodal frequency distributions with a small range of density and grain size. Using the definitions of Greenkorn and Kessler (1969) each stratum is homogeneous and nonuniform. The small range of values within each stratum is demonstrated at pit CC6 for example, where the standard deviation of the density ranged from 10 to 20 kg/m^3 (Figure 3.2) and for the grain size from 0.07 to 0.13 mm (Figure 3.3). This indicates that the conditions occuring during the deposition of each strata were quite uniform. Considering the persistent cold during winter, it is reasonable that conditions do not vary greatly during events, or even from event to event. In addition, any short term changes in snow properties that occur during deposition are overwhelmed by wind action which breaks the snow grains into particles of more uniform size and shape.

These strata may mark either individual depositional events or changes within a depositional event. Variations
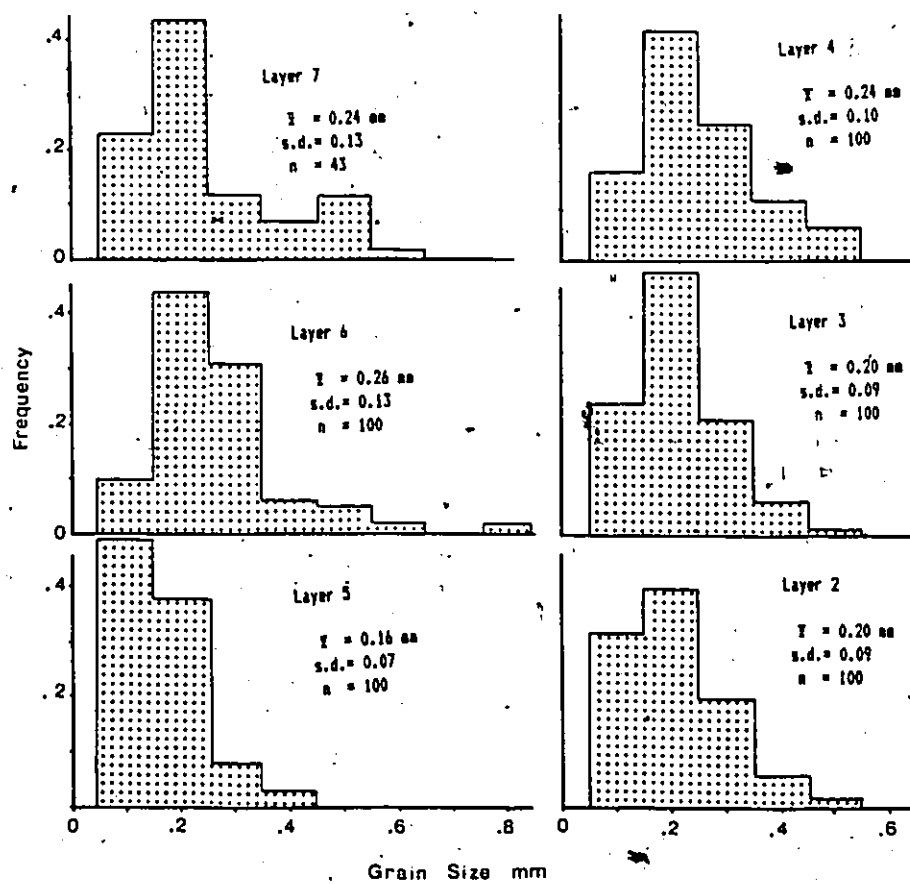
FIGURE 3.3 Grain size distribution for individual strata at pit CC6, June 6 1981, Resolute. Layer 7 is at the top of the snowpack.

within events are due to changes in snowfall rate, crystal type, air temperature, or wind. Mellor (1965) found that constant pulsations in wind speed cause variations in the deposition rate and the particle size deposited, resulting in distinct layers approximately 1 mm thick. Variations between individual deposition events are due to the same factors, but these variations are normally greater than the within-event variations. Seligman (1936) called these major divisions strata.

Horizontal extent of strata

Daily sampling of the snowpits during the melt period demonstrated that most strata were continuous over a horizontal distance of 1.6 to 3.2 m. Figure 3.1 illustrates a case where only one of seven layers was not continuous. Similar horizontal continuity of strata has been observed in other areas where blowing snow dominates. Benson (1971) observed lateral continuity over a 15 m section of pit wall at Byrd station, Antarctica, and Cameron (1971) reported that 49% of the layers in a 1.8 m pit were traceable for at least 14 m, 31% for over 7 m, and only 20% were discontinuous. Other Antarctic studies by Koerner (1964), Rundle (1971), Koerner (1971), and Taylor (1971) have reported similar findings.

Not only are the strata observed in this study

continuous but : (1) they are generally uniform in thickness, (2) the boundaries are very uniform, and (3) they are roughly parallel to the surface. This uniformity may be unexpected considering the existence of dunes, sastrugi, and ripples on the surface. Only rarely do strata boundaries show any indication of these surface features, or dip steeply compared to the surface. Similar conditions are shown in photographs by Seligman (1936), while Shumskii (1964) states that eolian snow covers have more clearly defined stratification than other packs. Benson (1971) observed that although the snow surface is rough, the strata exposed in pit walls tend to be horizontal. He was "impressed by this horizontality of strata in ... Greenland, Antarctica, and in high altitude snow fields of Alaska, and ... (was) convinced that this is generally observed, even in areas of pronounced surface roughness" (Benson 1971, p. 340). The existence of continuous very smooth, horizontal strata boundaries in eolian material has also been noted in the geological literature. Both Bagnold (1941) and Glennie (1970) observed its existence on flat sand areas, even though the surface was covered with small ripples and dunes. Processes resulting in this uniformity of strata boundaries are unclear. Glennie (1970) argued that as wind speed increases, ripples eventually disappear and a plane bed forms. Then as wind speed decreases, sand is deposited on a plane bed. Benson

(1971) proposed that simultaneous erosion and deposition are responsible for horizontal strata in aeolian snow covers. This process implies considerable erosion and redistribution of snow layers after they were initially deposited. The reworked snow may then be mixed and redeposited with new snow.

3.2 Spatial variability of snowcover characteristics

Variability within a basin

Considerable variability in snowpack depth, layer thicknesses, and layer densities occur within each topographic unit. However, it is hypothesized that each terrain unit will have significantly different properties. This hypothesis was tested by using a Kolomogorov — Smirnov test to compare the frequency distributions of snow depth, layer thickness, and layer density at each topographic unit.

Snow depths were significantly different for the four topographic units surveyed (Figure 3.4). Convex slopes had a mean depth of 0.22 m, flat areas 0.45 m, concave slopes 0.88 m, and gullies were the deepest with a mean of 1.44 m. Snow storage on the flat and convex slopes was probably close to the maximum snow retention capacity (Tabler 1975), as was noted by Longley (1960), while the concave slopes and gullies

were not.

The four topographic units (Figure 3.4) also had significantly different strata thicknesses. Convex slopes and flats were characterized by thin layers (mean of 0.05 and 0.08 m), but the flats also had a few thicker layers. Gullies and concave slopes had similar means (0.16 m), but had different distributions. The modal class for the concave slopes was 0.2 m, while only 0.05 m for the gullies. These variations in layer thickness indicate the relative magnitude of catch efficiency during individual accumulation events. Flat and concave slopes had low catch efficiencies while the gullies and concave slopes had high values. In terms of the number of strata (Table 3.1), convex slopes had the fewest(4), followed by flats(5), gullies(7), and concave slopes(8). Generally the topographic areas with deeper packs collect snowfall from a large number of events, each of which deposited more snow than over other terrain types. The small number of strata in all snowpits, certainly much fewer than the number of blowing snow or snowfall events indicated in the Resolute weather station data for the winter of 1980-1981, indicates that considerable erosion and redistribution of snow occurs after it was initially deposited.
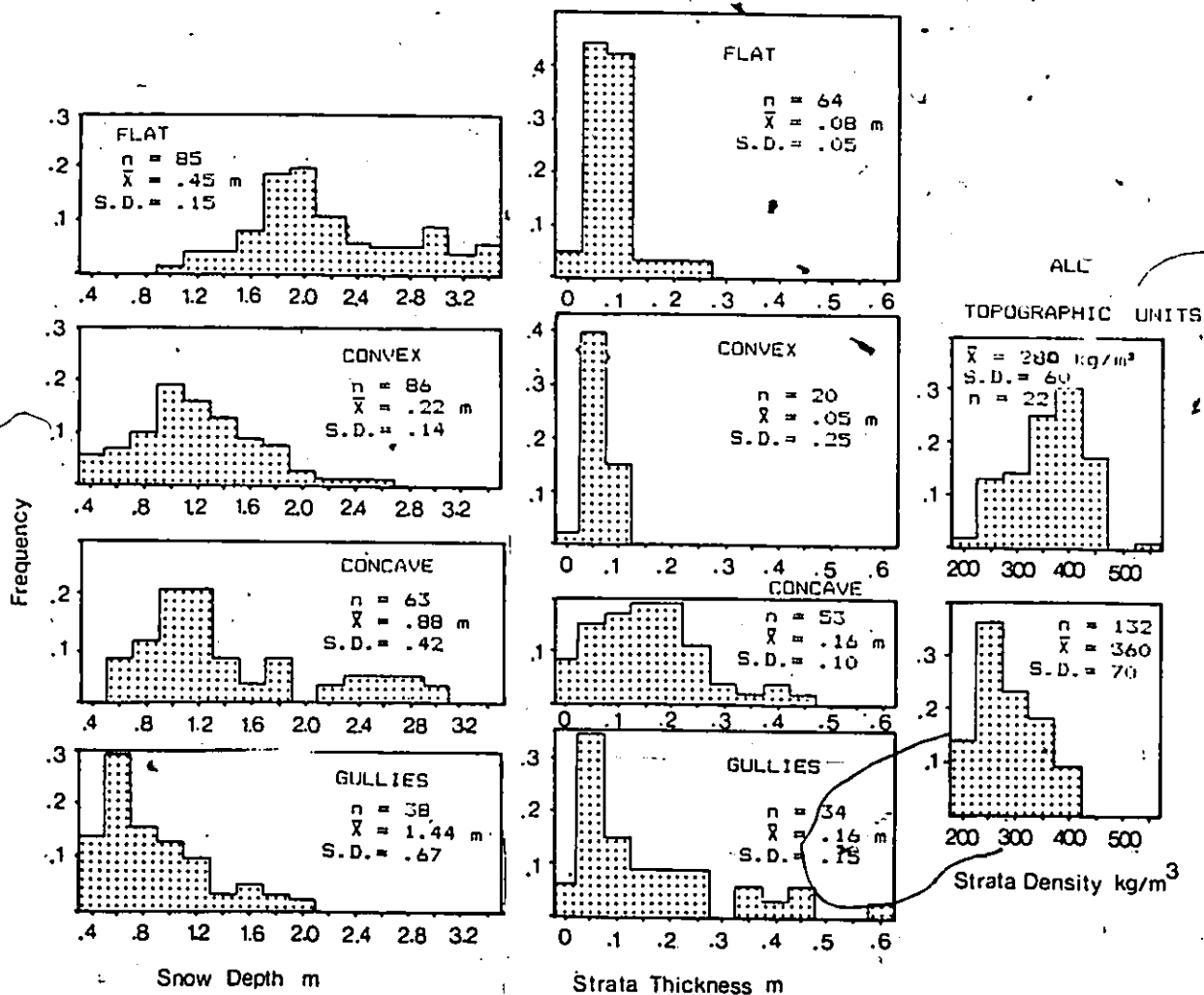
FIGURE 3.4 Frequency distribution of snow depth, layer thickness, and layer density for each terrain type. The layer densities were divided into two groups: depth hoar and all other layers. Since densities of different terrain types were not significantly different, they were all combined,

---

TABLE 3.1

Mean, maximum, and minimum number of strata for each topographic unit (Resolute 1981)

snow topographic unit	number of strata			number of snow pits
	mean	maximum	minimum	
flat	5	7	4	12
convex slopes	4	5	3	5
concave slopes	8	12	4	7
gullies	7	8	4	5

Measurement of stratum density showed no depth-density relationship in any of the snowpits, except for the well defined, low density depth hoar layer at the base of all pits. Because of the extreme difference between the upper layers and the depth hoar layer, the stratum density measurements were separated into two distinct groups. For the upper layers, there were no significant differences between topographic units and all layers were combined into one group. The layer densities of the depth hoar layers were similarly combined. The upper layers had a mean density of 360 kg/m^3 and the depth hoar layer only 280 kg/m^3).

The temperature at the snow-ground interface is a function of snow depth (Figure 3.5) prior to the beginning of snowmelt. The temperature at the snow base decreases from -10 to -14 C as the pack depth increases from 0.2 to 0.6 m, but is nearly constant at -14 to -16 C for all deeper packs.

Representativeness of premelt data

To ensure that the 29 snowpits in Basin 1 were representative of the Resolute area two comparisons were made with a large basin snow survey carried out during the same period (Woo 1982b). A Kolomogorov - Smirnov test of the weighted mean densities for each snowpit (Figure 3.6) compared to the snow survey densities for similar terrain conditions, shows no significant difference between the two samples at the 95% level. Snow storage for Basin 1, calculated from snowpit survey data of depth and density gives a value of 113 mm, compared with the 93 mm determined for McMaster River basin (Woo 1982b). A similar discrepency was found between the results of the McMaster River basin snow survey and a detailed Basin 1 snow mapping procedure in 1976 (Marsh 1978). This difference is probably due to the dominance of a steep north facing slope which accumulates a deep snowpack (Woo and Marsh 1978). These comparisons of snow density and basin storage as determined from the snowpit and snow survey suggest that the snowpit survey provides a representative sample of the snow conditions found in the Resolute study area.
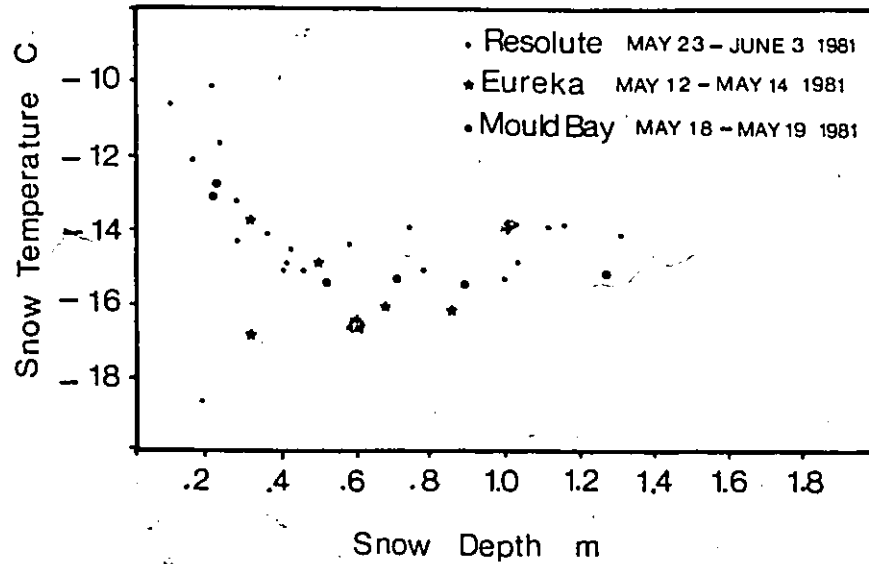
FIGURE 3.5 Temperature at the snow-ground interface versus
        snow depth. Measurements were obtained from the
        premelt snowpits.
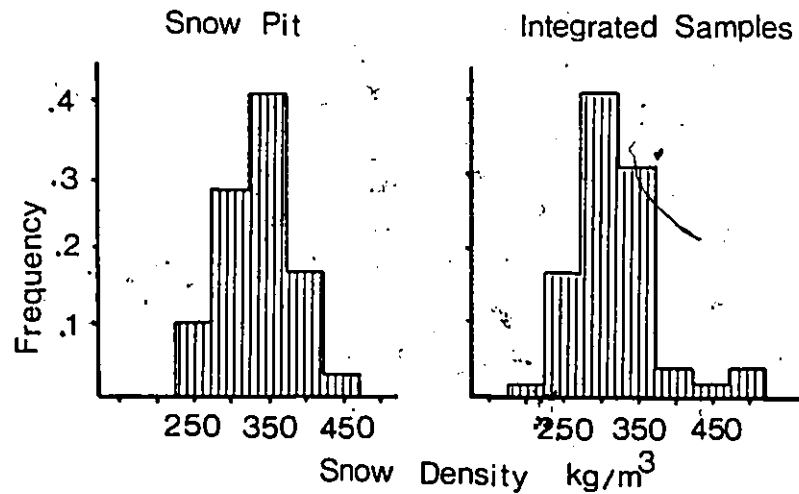
FIGURE 3.6 Comparison of frequency distributions of
        snowpack density estimated from snow pits and
        integrated samples using an MSC snow sampler during
        the basin snow survey. Resolute 1981.

Comparison of Resolute, Eureka, and Mould Bay snowcover

Thickness of individual strata are similar at Resolute, Eureka, and Mould Bay (Figure 3.7). Since snow storage was different at each site (Table 3.2), this suggests that strata thickness is not influenced by snowfall amount but by the catch efficiency of the topographic unit. When layer thickness is expressed as a fraction of the total pack, both Resolute and Mould Bay had mean layer thickness of 17% of total pack depth, and Eureka a mean layer thickness of 24%. This indicates that the snowpack at Eureka was composed of fewer layers.

TABLE 3.2

Comparison of Resolute, Eureka, and Mould Bay hourly wind speeds and basin snow storage for the period September 1980 to May 1981

| Location | % of time with wind | | | | |
	calm	0-10 m/s	over 10 m/s	mean speed (m/s)	snow storage (mm)
Resolute	5	80	15	6.0	93
Mould Bay	14	79	7	4.5	149
Eureka	38	59	3	2.5	67

The mean layer densities are similar for all three sites, but not the distributions. For example, the modal

RESOLUTE

n = 154
X̄ = 350kg/m³
S.D.= 70

RESOLUTE

n = 171
X̄ = .12 m
S.D.= .10

MOULD BAY

n = 40
X̄ = 340
S.D.= 50

MOULD BAY

n = 42
X̄ = .11
S.D.= .09

EUREKA

n = 20
X̄ = 360
S.D.= 80

EUREKA

n = 29
X̄ = .13
S.D.= .10

Frequency

250 350 450 550
Strata Density kg/m³

0 .1 .2 .3 .4 .5
Strata Thickness m
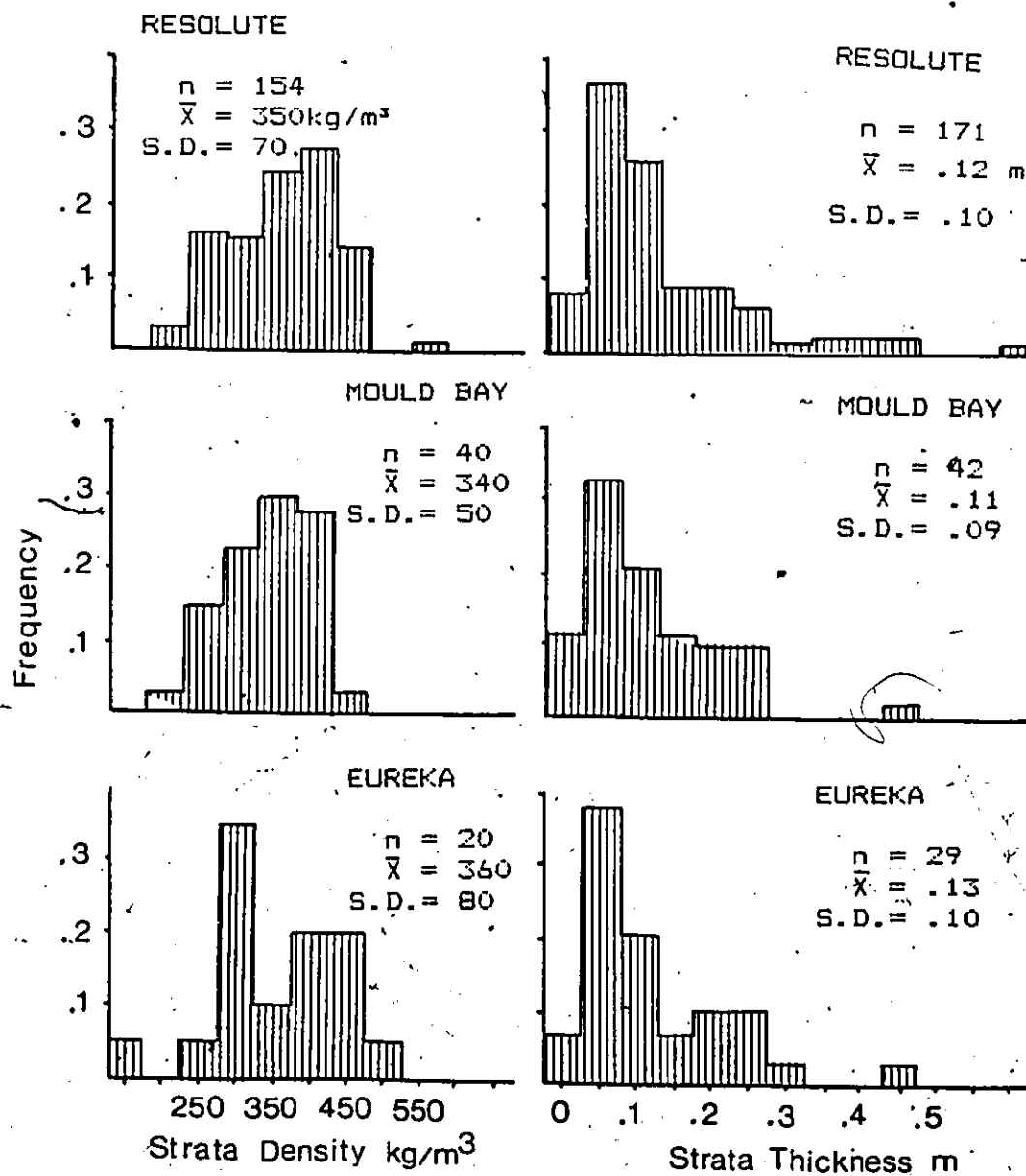
FIGURE 3.7 Comparison of Eureka, Mould Bay, and Resolute
frequency distribution of strata density and strata
thickness.

density for Resolute is 400 kg/m³, Mould Bay 350,
and Eureka only 300. High layer densities occur at each
location due to wind packing during blowing snow events, but
the high frequency of calm conditions (Table 3.2) results in
an increased number of low density layers at both Eureka and
Mould Bay.

Depth hoar development is dependent on both
temperature gradient and snow type. Variations in depth hoar
development between Resolute, Eureka, and Mould Bay (Table
3.3) are probably due to variations in snow density prior to
hoar development, although a different thermal regime might
also be important. As noted earlier, Eureka and Mould Bay
have a higher frequency of low density snow than Resolute.
These layers have a higher permeability and therefore higher
vapour movement under a given temperature gradient. This may
account for the thicker depth hoar layers at Mould Bay and
Eureka.

TABLE 3.3

Comparison of depth hoar thickness and density at Resolute, Mould Bay, and Eureka (May 1981)

Location	Mean thickness (m)	Mean thickness (fraction of snow depth)	Mean density kg/m³
Resolute	.147	.23	300
Mould Bay	.241	.32	330
Eureka	.154	.26	290

CHAPTER FOUR

SNOWPACK MASS BALANCE AND THE REFREEZING OF MELT WATER

Melt water infiltrating the pack surface may: (1) be stored as liquid water within the snowpack, (2) freeze on snow grains at the wetting front, (3) freeze as ice layers, columns, or basal ice, or (4) leave the snowpack as either soil infiltration or lateral saturated flow at the snowpack base. The purpose of this chapter is to illustrate the relative importance of these different storages and to demonstrate the factors controlling the location of freezing within the pack. These observations are then incorporated into a snowpack ripening model in Chapter Five. The first section of the present chapter describes the redistribution of mass throughout the melt period. The second section considers the portion of the melt which freezes within the pack in terms of the amount of energy used to warm the snow and soil. The final section examines the relationship between the wetting front, premelt stratigraphic horizons, and the freezing of water within the pack.

4.1 Snowpack mass balance

During the melt period, the snowpack is composed of three separate components. These are defined as: (1) snow — loose granular ice grains, (2) liquid water — occupies the pores between the loose ice grains, and (3) ice — ice grains which are frozen together and form horizontal ice layers within the snow, vertical ice columns, and basal ice.

Liquid water storage

. Liquid water is stored within the pack as both irreducible and gravitational water. Table 4.1 shows that during the anisothermal period, 50 to 70% of the total melt is used to satisfy the calculated irreducible liquid storage.

For a typical snowpack at Resolute or Eidsbotn, the measured daily total liquid water content (irreducible plus gravitational) gradually increases as the wetting front moves downward but then decreases as the pack depth diminishes (Figure 4.1 a,b). Storage ranges from 0 to 45 mm of water. This represents a range in water content from 1 to 22% by weight, with a mean of 8%. The upper limit corresponds to a water content of approximately 14% by pore volume. All measured values are within the pendular moisture regime characteristic of freely draining snowcovers (Denoth 1980).
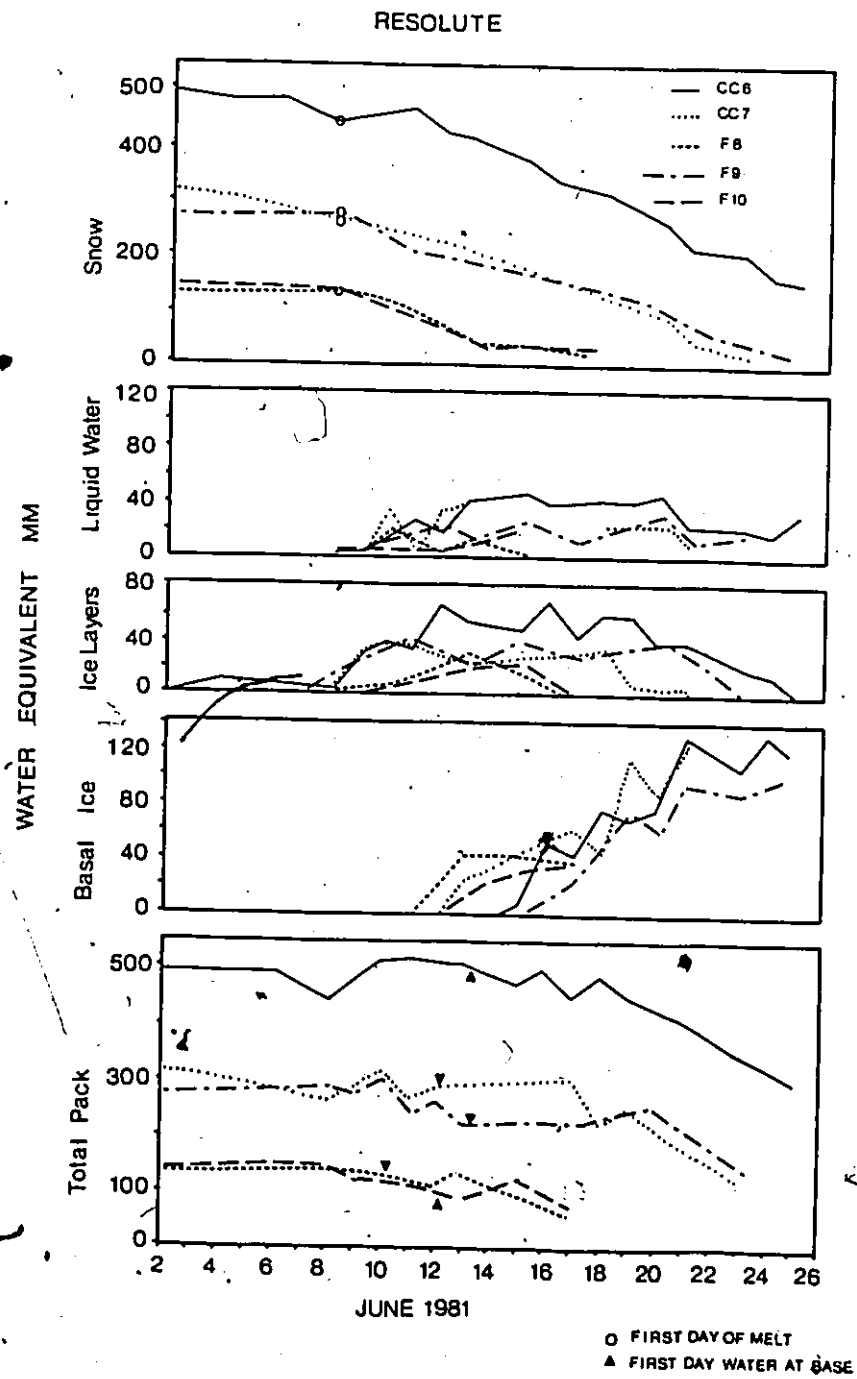
FIGURE 4.1a Daily changes in the individual components of the snowpack at snowpits monitored during the 1981 snowmelt period at Resolute.
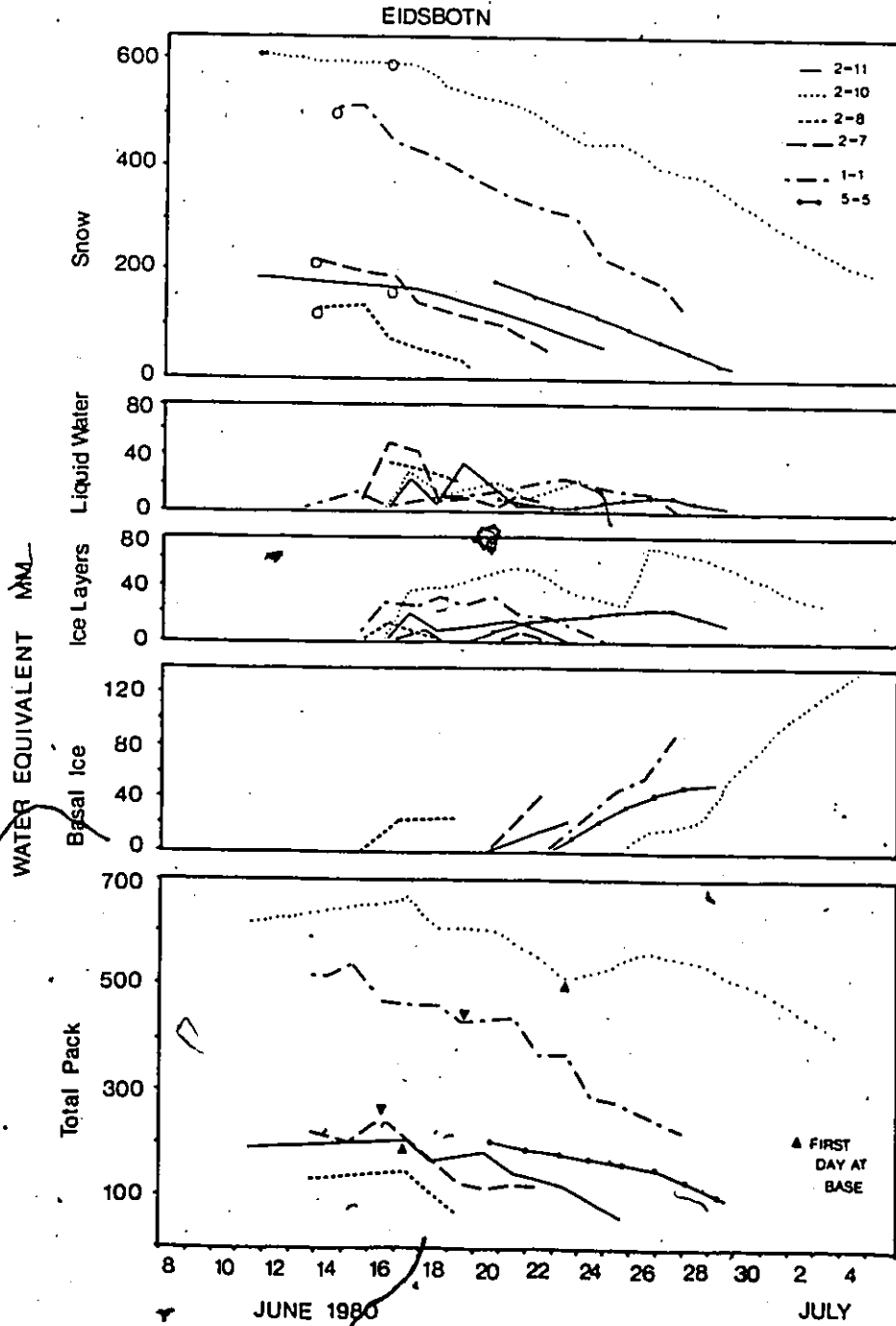
FIGURE 4.1b Daily changes in the individual components of the snowpack at snowpits monitored during the 1980 snowmelt period at Eidsbotn Fiord.

TABLE 4.1

The amount of water (as water equivalent) which fills the irreducible liquid storage, freezes and is available for runoff during both the anisothermal and isothermal periods, Resolute 1981

Site	snow[1] depth (m)	melt[2]	irreducible[3] water storage	freezing[4]				change in[5] pack W.E.	total measured water storage, freezing and change in W.E.
				wetting front	ice layer	soil inf.	basal ice		
(1) Anisothermal period									
CC6	1.20	63.4	46.8	3.0	15.3	0	0	0	65.1
CC7	.75	36.7	31.5	1.7	10.6	0	0	0	43.8
F8	.40	24.9	16.8	.9	7.2	0	0	0	24.9
F9	.75	45.9	31.0	1.8	13.9	0	0	0	46.7
F10	.40	41.6	16.8	.9	13.7	0	0	0	31.4
(2) Isothermal period									
CC6	1.20	274.2	0	0	0	20.0	73.5	169.0	262.5
CC7	.75	149.5	0	0	0	20.0	62.4	113.0	195.4
F8	.40	60.7	0	0	0	20.0	26.0	10.0	56.0
F9	.75	195.7	0	0	0	7.0	56.1	128.0	191.1
F10	.40	37.4	0	0	0	7.0	20.8	19.0	46.8

1 - snow depth at each pit at the beginning of melt
2 - melt determined from the surface energy balance
3 - calculated irreducible water storage for the snowpack depth , density, and assuming an irreducible water content of .07
4 - freezing - at the wetting front is calculated for a temperature immediately below the front of -1 C.
       - ice layers were observed from the snowpits.
       - the soil infiltration was measured
       - basal ice was observed from the snowpits.
5 - change in pack water equivalent was observed from snowpits.

Freezing within and beneath the pack

Even though the snowpack is very cold at the begining of melt, the wetting front propagates into snow with a temperature between 0 and -1 C and only 3 to 5% of melt during the anisothermal period freezes at the wetting front (Table 4.1). Since such freezing adds only a small amount of mass to the snow portion of the pack, the snow water equivalent gradually decreases (Figure 4.1a,b) from the onset of melt.

Freezing may be concentrated at certain areas to produce two types of ice layers:

(1) Discontinuous ice layers are thin (1 mm) and extend horizontally for only 0.1 to 0.2 m. They are not related to any observable premelt boundaries, and are probably caused by micro-scale variations of snow properties within a stratigraphic unit. They are not common in any of the snowpits studied and do not contribute significantly to the snowpack mass.

(2) Continuous ice layers are much thicker (1 to 40 mm) and may be traced for at least 2 or 3 m. The thickest layers are usually found near the snowpack base. Continuous ice layers range from solid ice to frozen granular ice. The solid ice layers appeared to have a low permeability and had measured

densities ranging from 630 to 950 kg/m³ and a mean of 800 kg/m³. The frozen granular layers were more permeable and were composed of loosely frozen ice grains. Only these continous ice layers will be considered in the rest of this thesis.

The total water equivalent of these continuous ice layers increases as new layers form below the advancing wetting front, and then decreases as layers near the surface decay (Figure 4.1a,b). At maximum growth they account for 10 to 15% of the total pack water equivalent. During the entire anisothermal period, 24 to 44% of all melt freezes into continuous ice layers (Table 4.1).

Ice columns may also form during the anisothermal period. These columns are roughly cylindrical, have a density, similar to that of ice layers, and are generally located in the deeper, colder sections of the pack. They range in size from 0.02 m in diameter and 0.1 m in length, to 0.1 m by 0.6 m. Bumps on exposed basal ice (Woo et al 1982) suggest that ice columns are common, but they were observed at only 10 of the approximately 115 snowpit profiles observed over a two year period. They occur infrequently because, as will be shown later, meltwater is seldom able to penetrate very far below the 0 C isotherm. The bumps may represent the locations of flow channels which are formed during increased water flux. They do not contribute significantly to the snowpack mass.

Upon reaching the ground surface, some water may infiltrate the soil and freeze. The measured total soil infiltration at Resolute ranged from 20 mm for polar desert soils to only 7 mm for bog soils. Infiltration at the polar desert sites accounted for 8 to 36% (Table 4.1) of the melt during the isothermal period, while for bog sites 4 to 15% of the melt infiltrated the soil.

Once infiltration ceases, basal ice forms immediately above the snow-ground interface and continues to grow throughout the melt period (Figure 4.1a,b). It is denser than the ice layers, ranging from 850 to 950 kg/m^3 and has a mean of 880 kg/m^3. Values higher than the density of ice are within the range of experimental error. Maximum thickness ranges from 50 to 150 mm and accounts for 20 to 30% of the initial snowpack water equivalent. During the isothermal period, 28 to 44% of all melt is used to form a basal ice layer (Table 4.1). As a result of both the freezing of soil infiltration and basal ice formation only 18 to 67% of the melt was available to runoff. This is unlike warm snowpacks where once meltwater reaches the ground surface it is available for runoff either as overland flow or subsurface flow. In the High Arctic, basal ice growth may consume a significant portion of the surface melt. As a result, the decrease in snowpack water equivalent is always less than the rate of melt.

During the anisothermal period, the total water equivalent of the snowpack stays constant. Small day to day variations (Figure 4.1a) are possibly related to the sampling technique rather than to actual changes in water equivalent.

4.2 Energy released by refreezing of meltwater

During the first day of melt an isothermal zone forms at the top of the snowpack, effectively eliminating the conduction of heat from the snow surface. Instead heat is transferred into the pack by infiltrating melt water which freezes and releases latent heat. This heat may then be conducted downwards from the freezing location, warming both the snow below the wetting front and the underlying soil (Figure 4.2).

The proportion of the latent heat used to warm the snow to 0 C compared to that used to warm the soil varies considerably. In all cases a significant portion of the heat is conducted into the soil during the anisothermal period.
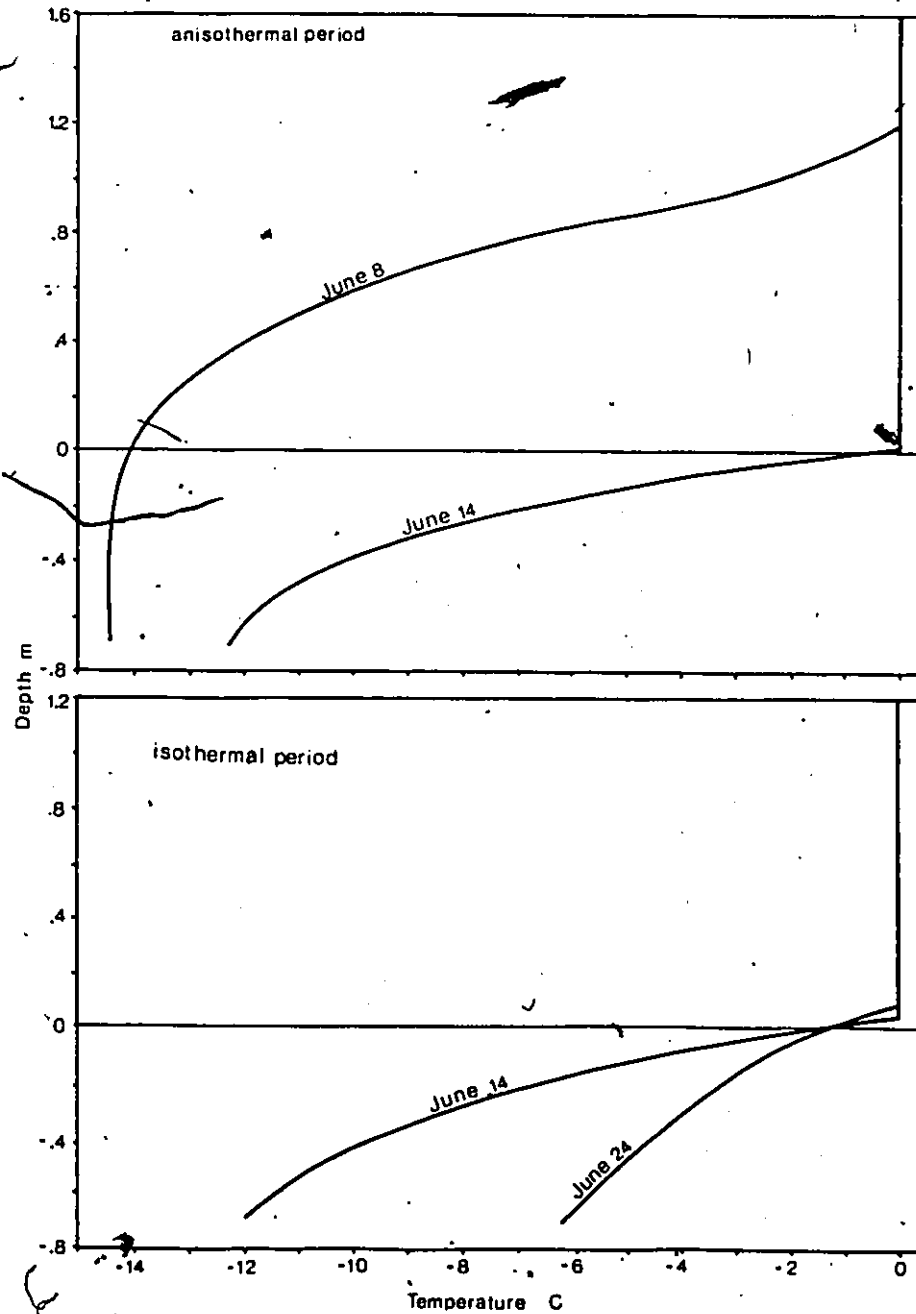
FIGURE 4.2 Warming of the snow and soil as a result of freezing within the pack during the snow anisothermal and isothermal periods at the upper thermistor rod, June 1981. Zero depth marks the snow-soil interface.

For pits CC6, F8, and F10 (Table 4.2) the proportion used to eliminate the snow cold-content varied from 20 to 90%. From the limited sample it appears that more of the heat is conducted into the soil at the shallow sites. This large soil heat flux results in an extension of the anisothermal period. In fact, both the snow and soil must "ripen" before the pack becomes isothermal.

TABLE 4.2

Amount of heat (MJ/m²) released by freezing within the pack compared to changes in snow and soil heat storage

Site	melt	latent heat sources				sensible heat sinks	
		wetting front	ice layer	soil inf.	basal ice	snow cold content	change in soil heat
(1) Anisothermal period							
CC6	21.2	1.0	5.1	0	0	5.5	.6
F8	8.3	.3	2.4	0	0	.9	1.8
F10	13.9	.3	4.6	0	0	1.0	3.9
(2) Isothermal period							
CC6	91.6	0	0	6.7	24.5	0	31.2
F8	20.3	0	0	6.7	8.7	0	15.4
F10	12.5	0	0	2.3	7.0	0	9.3

During the isothermal period, all of the heat released by freezing of soil infiltration and the formation of basal ice is conducted downwards to warm the soil. This accounts

for approximately 34 to 76% of the total melt energy released during the first few days of the isothermal period (Table 4.2). It is this downwards conduction of heat which limits daily runoff, and extends the melt period.

4.3 The wetting front, stratigraphic horizons, and ice layers

The effect of stratigraphic horizons on the wetting front advance was determined by conducting dye infiltraton tests and observing ice layers and columns within the ripening snowpack. In the case of the dye infiltration tests, the dye marks the path of water movement within the snow, whereas in the ripening snowpack, the path is marked by the location of the layers and columns. These studies indicate the following sequence of events as melt water moves into a dry snowpack. The wetting front quickly divides into two distinct portions; a general wetting front above which there is no dry snow, and a number of relatively thin fingers which transmit water below the wetting front (Figure 4.3). The deepest penetration of these fingers is referred to as the finger wetting front (Figure 4.4). For simplicity, these two wetting fronts will be referred to as the general front and the finger front. When these fingers reach a stratigraphic horizon, their downward movement is arrested,

FIGURE 4.3 Development of a wet layer at premelt horrizons
and flow fingers after dye injection into dry, cold
snowpack, June 7,1981.
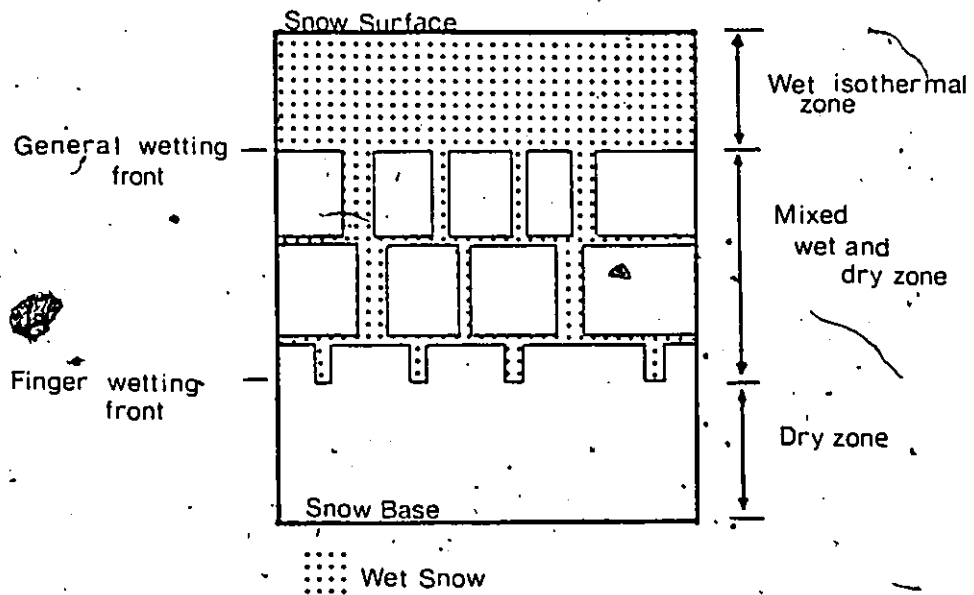
FIGURE 4.4 The zonation of a ripening snowpack and the
definition of the general wetting front and finger
wetting front.

and water spreads horizontally, to form a thin wet layer.
Conduction of heat into the sub-zero snow above and below
this layer results in the formation of an ice layer. As
water is continually added, the wet layer thickens until a
number of fingers form below the horizon. If the snow is
cold enough, incremental freezing of non-saturated water in
the flow fingers results in the growth of ice columns.

The snowpack may be divided into three distinct zones
during the ripening period (Figure 4.4):

(1) wet-isothermal zone - all snow is wet and isothermal at 0
C. The base of this layer is well defined by the general
front.

(2) mixed zone - composed of a mixture of wet and dry snow.
Ice layers grow only in this area. The base is defined by
the finger front.

(3) dry zone - snow is sub-zero and no liquid water is
present.

During the dye infiltration tests, thin wet layers and
fingers developed at all the stratigraphic horizons, and
there was a strong relationship between the pre-melt horizons
and continuous ice layers. Figure 4.5 shows five snowpits
from Resolute in 1981 as an example. The 11 snowpits studied
over a two year period had a total of 47 premelt
stratigraphic horizons. Of these, 38 or 81%
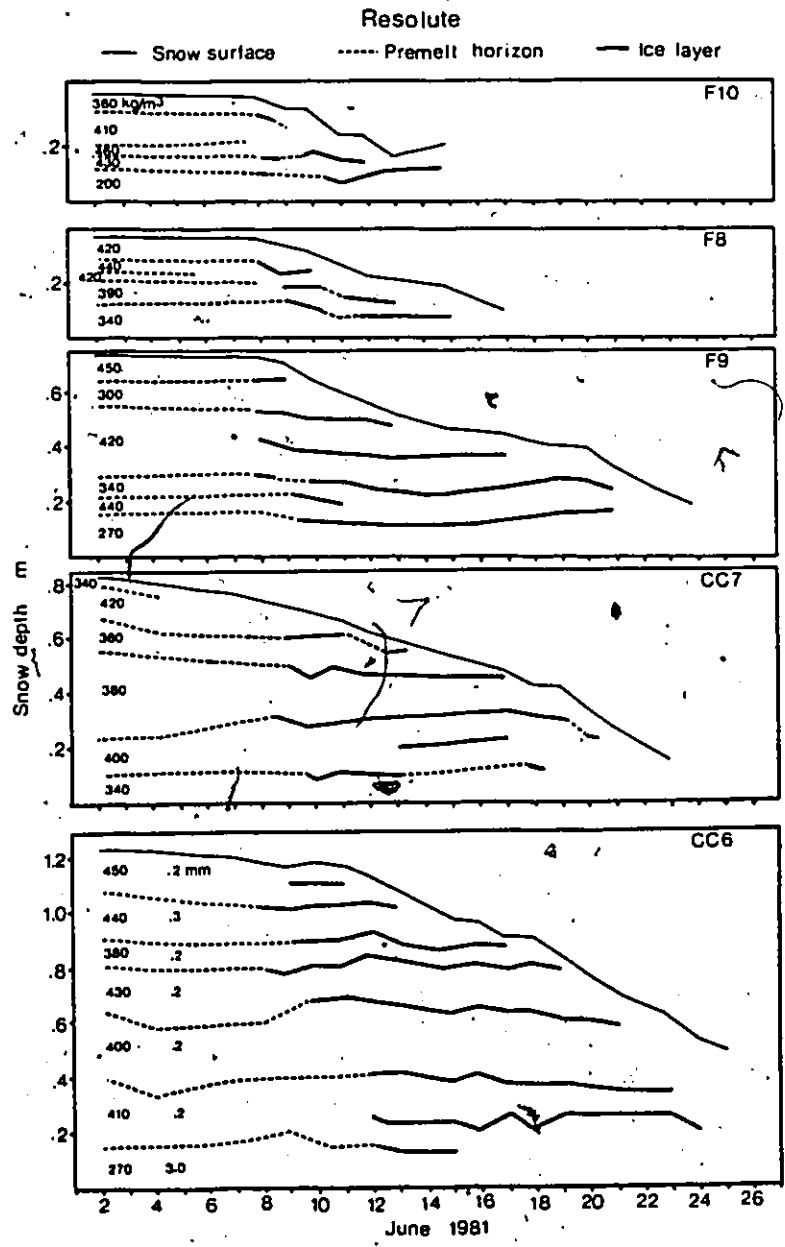
FIGURE 4.5 Relationship between premelt strata horizons and the development of continuous ice layers, Resolute 1981. Strata densities were obtained on June 2 and grain sizes on June 6.

developed continuous ice layers, and only 9 or 19% of all ice layers were not related to observed premelt horizons. It must be remembered that the sampling technique requires the pit wall to be cut back about 0.2 m daily to reveal a new stratigraphic profile. Occasionally a stratigraphic horizon disappears, but is replaced by a new one at a different level. If measurements could be made at the same location each day, it is probable that all horizons would develop continuous ice layers, and that continuous ice layers would form only at premelt horizons.

A relationship between premelt horizons and development of ice layers allows the use of premelt stratigraphy to predict the location of ice layers at a given site and the mean, maximum, and minimum number of ice layers for the snowpack of different topographic units (Table 4.3). In these arctic areas, the number of continuous ice layers at a vertical section does not vary greatly, ranging from one to eleven. The deeper packs tend to have more ice layers.

The average width and spacing of flow fingers penetrating dry snow was determined from the dye tests and from measurments of ice columns. Results from seven dye tests show that the flow fingers are fairly uniform in size averaging 33 mm in width. The spacing between their edges is also quite uniform, averaging 121 mm (Table 4.3). The ice columns had a mean width of 46 mm and a spacing of 148 mm. A

t-test of both finger width and spacing reveals no significant difference between the mean of the two sets of results at the 95% confidence level. These two sample sets were therefore combined to determine an overall mean finger width of 36 mm and a spacing of 131 mm (Table 4.4).

TABLE 4.3

Predicted mean, maximum, and minimum number of continuous ice layers for each snow topographic unit, from presmelt stratigraphy, Resolute 1981 and Eidsbotn 1980

Snow topographic unit		Number of continuous ice layers			number of pits
		mean	maximum	minimum	
Resolute	flat	4	6	3	12
	convex	3	4	2	5
	concave	7	11	3	7
	gullies	6	7	3	5
Eidsbotn	flat	1	2	1	5
	concave	5	8	2	18
	valley	5	5	5	2
	glacier	4	6	2	10

Measurements of flow finger widths from dye tests may be used to determine the portion of the total horizontal cross sectional area covered by the fingers. From six dye tests, each approximately one meter in width, the total finger width over the entire test width will be representative of any random profile. Therefore, the horizontal area covered by the fingers may be determined as

$$(4.1) \qquad A_F = [\sum_{j=1}^{B} ((W_T, j, 1,) / (L, 1,)] / B$$

where A_F is the proportion of the total area covered by fingers. L is the width of each section, 1 is the length of each section, B is the number of sections, and W_T is the total width of all fingers across a section of width L. The portion of the area covered by the general wetting front (A_W) is then

$$(4.2) \qquad A_W = 1 - A_F$$

Results from the dye tests indicated that the fingers covered 22% of the cross sectional area and the background front 78%.

TABLE 4.4

Finger width as determined by dye tests and measurements of ice columns (1980 and 1981)

Sample type		mean (mm)	Std. deviation	sample size
dye	width	33	19	26
	spacing	121	54	32
ice columns	width	46	28	8
	spacing	148	39	17
all samples	width	36	22	34
	spacing	131	69	49
	Af	.22		
	Aw	.78		

Wankiewicz(1978a) postulated that a simple horizon
(either a textural or density change) could impede,
accelerate or have no effect on the flow. The observations
outlined above suggest that for High Arctic type snow covers,
all snow horizons. impede flow regardless of whether the
boundary marks a fine/coarse, coarse/fine, dense/less dense,
or less dense/dense transition (Figure 4.5). Fingering may
be caused by either flow instabilities (Hill and Parlange
1972), or they could be triggered by a horizontal variation
in snow properties. These two types of flow fingers appear
similar and cannot be distinguished visually. For the
purposes of this study, it is not important to distinguish
between the two. Since all horizons appear to be of the
impeding type, the flow fingers and ice columns observed in
the Arctic are probably caused by variations in the horizon
but not flow instabilities (Wankiewicz 1978a).

CHAPTER FIVE

THE WETTING FRONT AND ICE LAYER GROWTH

5.1 Snowpack ripening model

Based on snowpit observations discussed in the previous chapter and existing literature, a mathematical model was developed to predict when liquid water would reach the snowpack base, the change in snowpack water equivalent, and the warming of the snow and soil. This model combines a two component wetting front, ice layer growth at premelt stratigraphic horizons and at the snowpack base, soil infiltration, and heat conduction. Previous studies have considered some of these individual processes, but none have combined them in order to investigate the snow ripening phenomena.

The following model describes the organization provided by the simplified flow chart shown in Figure 5.1 and presents the basic equations governing its operation.
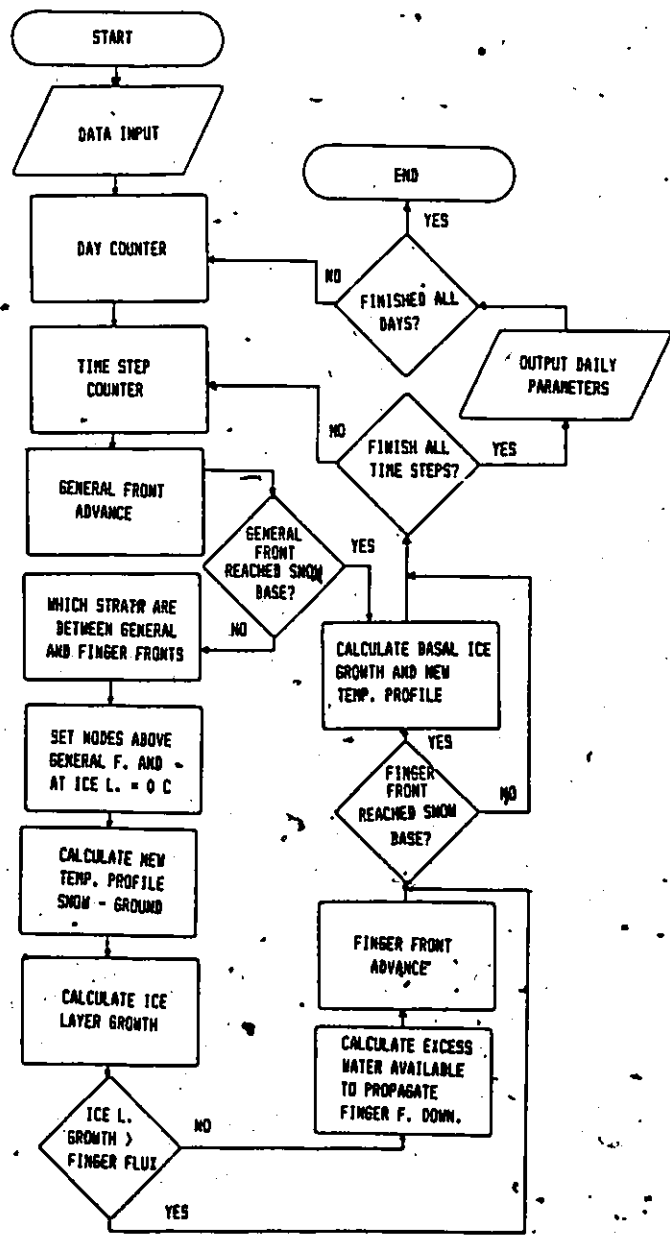
FIGURE 5.1 Simplified flow chart of snowpack ripening model.

Model description

The rate at which the wetting front advances into dry snow is controlled by (1) the water supply to the front, (2) the irreducible liquid water storage to be satisfied and (3) the need to raise the snow directly below the front to 0 C. In order to satisfy the liquid and thermal requirements, the rate of movement of the front is always less than the rate at which water is supplied to the front.

The requirement for liquid water per unit volume of snow (V_w/V_s) at the wetting front is given by (Colbeck 1976)

$$(5.1) \quad V_w/V_s = (p\ S_{wi}) + (T_{sw}\ p_s) / ((L_f/C_i)\ p_w)$$

where p is the porosity after freezing of water onto the snow grains, S_{wi} the irreducible water saturation, T_{sw} the snow temperature immediately below the wetting front, p_s the snow density, L_f the latent heat of fusion, C_i the specific heat of ice, and p_w the water density. In the calculations, the porosity prior to melt was used since the decrease in porosity due to freezing was negligible. In fact, the liquid water content at the front must be raised to $S_w > S_{wi}$, where S_w is the water content required to transport the flux U just above the front. On a daily basis however, it is assumed that all gravitational water will reach the wetting front.

The daily rate of propagation of the front, dW_F/dt,
is then (Colbeck 1975)

(5.2) $dW_F/dt = U /[(p\ S_{wi}) + (T_{su}\ p_a)\ /\ ((L_F/C_i)\ p_w)]$

Equation 5.2 assumes that the front advances
uniformly. As was shown in the previous chapter this does
not occur. Instead there is a rapid movement of flow fingers
ahead of the wetting front due to a local concentration of
water, increasing the flux at the fingers and reducing it at
the general wetting front. In this model, therefore, the
wetting front is assumed to have two components: a general
wetting front and a finger wetting front. The general front
defines the bottom of the completely wet zone, while the
finger front marks the deepest penetration of liquid water.
Using measurements of proportion of total area covered by the
fingers and proportion of flow occurring in the fingers, the
fluxes at the finger front and general front were calculated
as

(5.3) $U_F = U\ (F_F/A_F)$

(5.4) $U_w = U\ (F_w/A_w)$

where U_F and U_w are water flux along the finger and the
general wetting front, F_F and F_w are proportion of total flow
carried by the finger and general front, A_F and A_w are their

respective portion of total area, and U is the mean melt rate. U_F and U_W may then be substituted for U in equation 5.2 to calculate the separate general wetting (W) and finger front (F) advances as

(5.5) $dW/dt = U_W / [(p\ S_{WI}) + (T_{SW}\ p_s) / ((L_F/C_i)\ p_W)]$

(5.6) $dF/dt = U_F / [(p\ S_{WI}) + (T_{SW}\ p_s) / ((L_F/C_i)\ p_W)]$

Continuous ice layers are allowed to form at all premelt stratigraphic layers between the two fronts. At each horizon the water spreads laterally to form a thin wet layer across the combined width of the finger and the wetting fronts. This thin layer is assumed to be at 0 C. The rate of freezing of each saturated layer will depend on the rate of heat conduction into the cold dry snow above and below it. As long as water is not limiting, the rate of heat released by freezing equals the rate of heat conduction, or

(5.7) $dH/dt\ L_F\ (p_i - p_s) = Q_{TOT}$
and
(5.8) $Q_{TOT} = (-K_E\ dT_s/dz)_{UP} + (-K_E\ dT_s/dz)_{DOWN}$

Where dH/dt is the rate of ice growth, L_F is the latent heat of fusion, p_i and p_s the ice layer and snow density, Q_{TOT} the total heat conduction above and below the ice layer, K_E the effective snow thermal conductivity, dT_s/dz the temperature gradient above and below the layer, and the negative sign is

required to make the heat flow positive and away from the growing ice layer. Rearranging equation 5.7 gives the rate of ice growth

$$(5.9) \quad dH/dt = Q_{TOT} / (L_F (p_i - p_s))$$

The change in temperature gradient above and below the ice layer is determined by

$$(5.10) \quad dT/dt = (K_s/(p_s C_i)) d^2T/dz^2$$

where dT/dt is the change in temperature with time, K_s is the thermal conductivity, p_s is snow density, C_i is the specific heat of ice, T is temperature and z is the vertical coordinate. This equation was solved using an explicit finite difference approximation (Ozisik 1980). This technique has the advantage that the temperature at a given time can be determined directly from a knowledge of the temperature profile at the previous time step. Its disadvantage is that for a given thermal diffusivity and nodal spacing, there is a maximum possible time step which cannot be exceeded because of instability considerations. The temperature profile at each time step is calculated by

$$(5.11) \quad T(m,n+1)=(r\ T(m-1,n))+[(1 - 2r)T(m,n)]+(r\ T(m+1,n)]$$

where T is temperature, m the number of depth increments of

size z, n the number of time increments of length t, the
temperature at all nodes above the wetting front and at
actively growing ice layers is set to 0 C, and the
temperature at the depth of zero annual amplitude is held
constant. The parameter r is calculated as

$$(5.12) \quad r = [(A_s) \; t] \; / \; z_s^2$$

The thermal diffusivity (A_s) is given by

$$(5.13) \quad A_s = K_g / (p_s \; C_i)$$

where K_g is the snow effective thermal conductivity, p_s is
snow density and C_i is the specific heat of ice. The
appropriate nodal spacing (z_s) and time step (t) must be
chosen such that

$$(5.14) \quad 0 < r < 0.5$$

The time step was set to 30 minutes and a nodal spacing of
0.05 m was used in the snow. For compatibility with the
nodal spacing in the snow, the nodal space in the ground is
(Fertuk et al 1971)

$$(5.15) \quad z_g = [(z_s^2 \; A_g) / A_s]^{1/2}$$

Where z refers to the nodal spacing, A the thermal

diffusivity, and g and s refer to the ground and snow respectively. For commonly observed thermal conditions, and for the given time step and nodal spacing in the snow, the ground nodal spacing varied from 0.075 to 0.095 m.

Advancement of the wetting fronts and ice layer growth are interdependent. The temperature at the node immediately ahead of the wetting fronts is used in the calculation of the general and finger front advance. The general wetting front is allowed to advance continuously, while the finger front may only advance if the finger flux is greater than the rate of ice layer growth or

$$(5.16) \qquad U_{FA} > \sum_{j=1}^{mi} [(dH/dt), (p_i - p_s)]$$

where mi is the number of actively growing ice layers between the two fronts, dH/dt is the rate of growth of ice layer j, and where U_{FA}, the finger flux averaged over the entire finger plus general front, is calculated from

$$(5.17) \qquad U_{FA} = U_F (A_F / (A_F + A_W))$$

where U_F is the finger flux, and A_F the finger area and A_W the general front area are expressed as a portion of total area. If the relationship in equation 5.16 is not true, then all water is assumed to freeze at a rate equal to the rate of

water supply. An ice layer ceases to grow when either the temperature gradient above and below it reaches zero due to heat conduction, or the general wetting front advances past the ice layer. The excess water available (U_{FE}) to propagate the finger downward is the finger flux over the total area (U_{FA}) minus the total ice layer growth times a concentration factor

$$(5.18) \quad U_{FE} = [U_{FA} - \sum_{j=1}^{mi}(dH/dt), (p_i - p_s)]] (F_F/A_F)$$

Water reaching the snowpack base from the finger or the general front is assumed to enter the soil until the infiltration ceases. This water will freeze within the soil, but the depth where this freezing occurs is unknown. For simplicity, the freezing depth is assumed to be near the ground surface. For soils with low total infiltration, this probably does not cause large errors.

When infiltration ceases, a saturated layer forms at the base of the snowpack. The process of basal ice growth is the same as for ice layer growth. Since observations indicated that basal ice growth did not begin until the snowpack was isothermal it was assumed that heat was only conducted downwards. Substituting the ground thermal conductivity (K) and the basal ice density (p_{bi}) into equations 5.7 and 5.8 allows the rate of basal ice growth to be determined. As the basal ice grows, the

interface is generally not located at a node. To estimate the temperature gradient through the ice layer, a fictious temperature was calculated for the node immediately above the interface (Fertuk et al 1971), assuming a linear temperature profile between nodes and a temperature of 0 C at the ice interface

(5.19) $T_F(k+1) = - T(k-1) (z_s - h)/(z_s + h)$ if $h < z_s/2$

(5.20) $T_F(k+1) = - T(k) (z_s - h)/h$ if $h > z_s/2$

where T_F is the fictious temperature at the node above the interface, T is the temperature at k the first node below the basal ice-snow interface, h is the distance from node k to the interface, and z $_s$ the nodal separation in the snow.

The assumption that the basal ice-snow interface is always at 0 C assumes that water supply is not limiting. Except for the first day of basal ice growth this is correct on a daily basis.

The total snowpack water equivalent stays constant until melt water reaches the snowpack base. Once meltwater reaches the base it is assumed to infiltrate the soil until the infiltration ceases. Once this occurs, basal ice growth limits the amount of melt available to runoff and the total pack water equivalent may be calculated as

(5.21) $S_{WE}(n+1) = S_{WE}(n) - M(n) + H(n) (\rho_{si} - \rho_s)$

where S_{wn} is the total snowpack water equivalent on days n

and n+1, and M is daily snowmelt, H daily basal ice growth,

ρ_{bi} the basal ice density, and ρ_s the snow density.

5.2 Data requirements

The snowpack ripening model described in the previous

section requires the following data:

(1) snowpack properties at the beginning of melt
    (a) snow-soil temperature profile
    (b) snow stratigraphy
    (c) snowpack density and depth

(2) daily snowmelt rate

(3) snow and substrate thermal properties
    (a) thermal conductivity
    (b) specific heat

(4) properties of the wetting front
    (a) proportion of area covered by fingers
    (b) proportion of total flow along fingers
    (c) irreducible liquid water content

(5) soil infiltration capacity

Results computed by the model were tested against

observations from five snowpits monitored during the 1981

melt period at Resolute. All pits had detailed snow property

measurments while two (F8 and F10) also had snow-soil

temperature profiles. A third snow-soil temperature rod was

near pit CC6 but since the snow depth at the pit was 0.4 m

shallower than at the temperature rod, the two were treated

separately. The other two pits (CC7 and F10) did not have detailed temperature data.

. The snow-soil temperature profiles immediately before the beginning of melt are shown on Figure 5.2. These were measured from temperature rods at sites F10, F8, and Upper. At the other sites (F9, CC7, CC6), snow temperatures were measured in the snowpit walls, and soil temperatures were estimated from (1) temperature measured at the snow-soil interface, and (2) the observation that the temperature at -0.7 m in the soil was approximately -14.5 C regardless of the overlying snow depth. The soil temperature profile from 0.7 to 20.0 m (depth of zero annual amplitude) was estimated from Cook (1958) (Figure 5.3).

To simplify calculations, the mean weighted snowpack density at the beginning of melt was used for each site (Table 5.1). The location of premelt horizons was determined (Figure 5.2) and rounded off to the nearest 0.05 m interval to coincide with the nodes used in the temperature calculations. A mean ice layer density of 600 kg/m^3 was assumed and the measured mean basal ice density of 890 kg/m^3 was used.
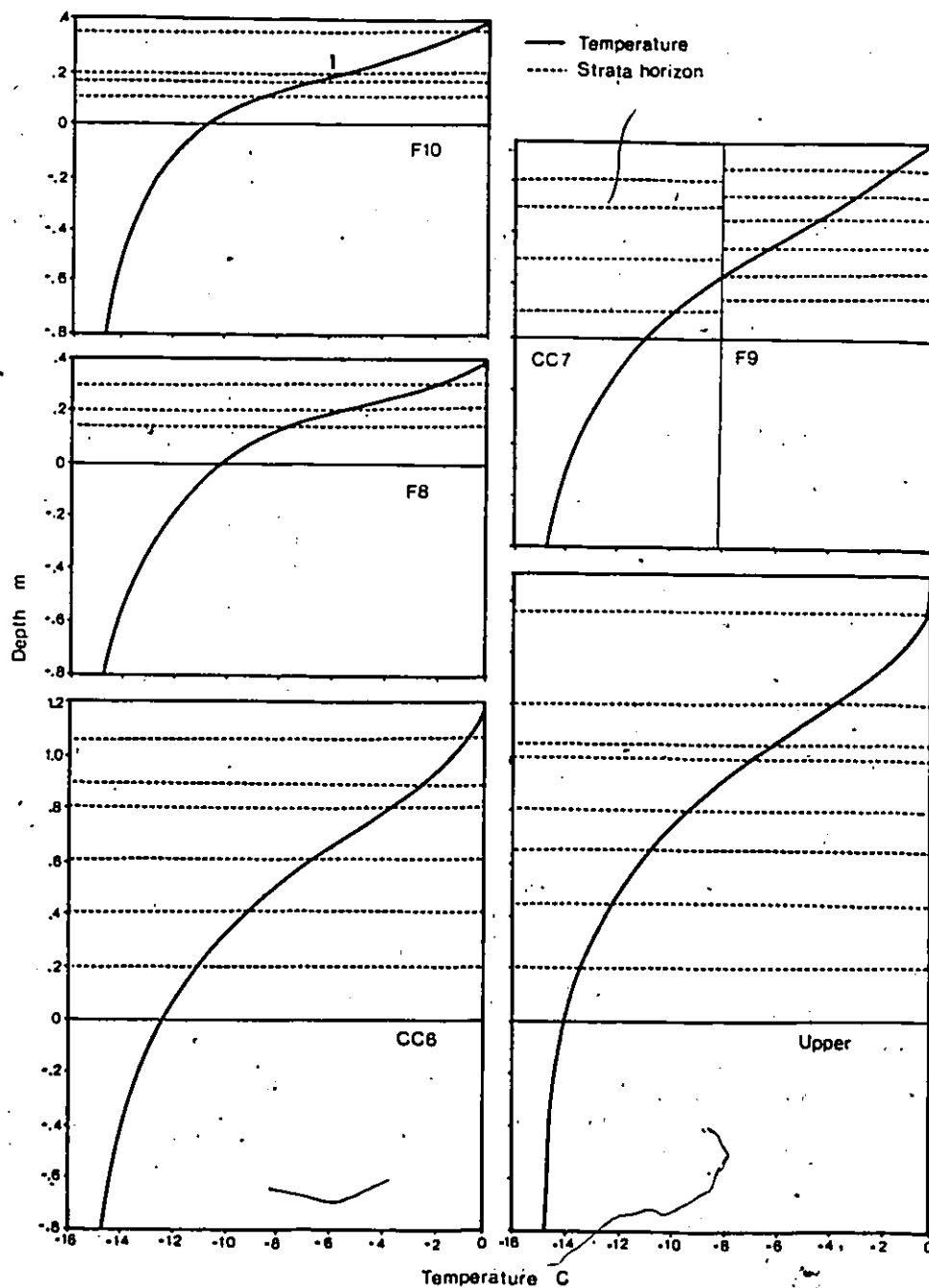
FIGURE 5.2 Snow stratigraphy and temperature profile on
June 7,1981 for the six locations used to test the
snowpack ripening model, Resolute. The zero depth
marks the snow-ground interface, and the top of each
graph marks the initial snow surface.

FIGURE 5.3 Substrate temperature profiles on the first day of melt at Resolute, June 8 1981, and on the first day of basal ice growth at Ikkii Glacier, Eidsbotn, July 6, 1979. The Resolute temperature was estimated from Cook(1958) and the Eidsbotn temperature was measured.

TABLE 5.1

Snow and substrate thermal properties

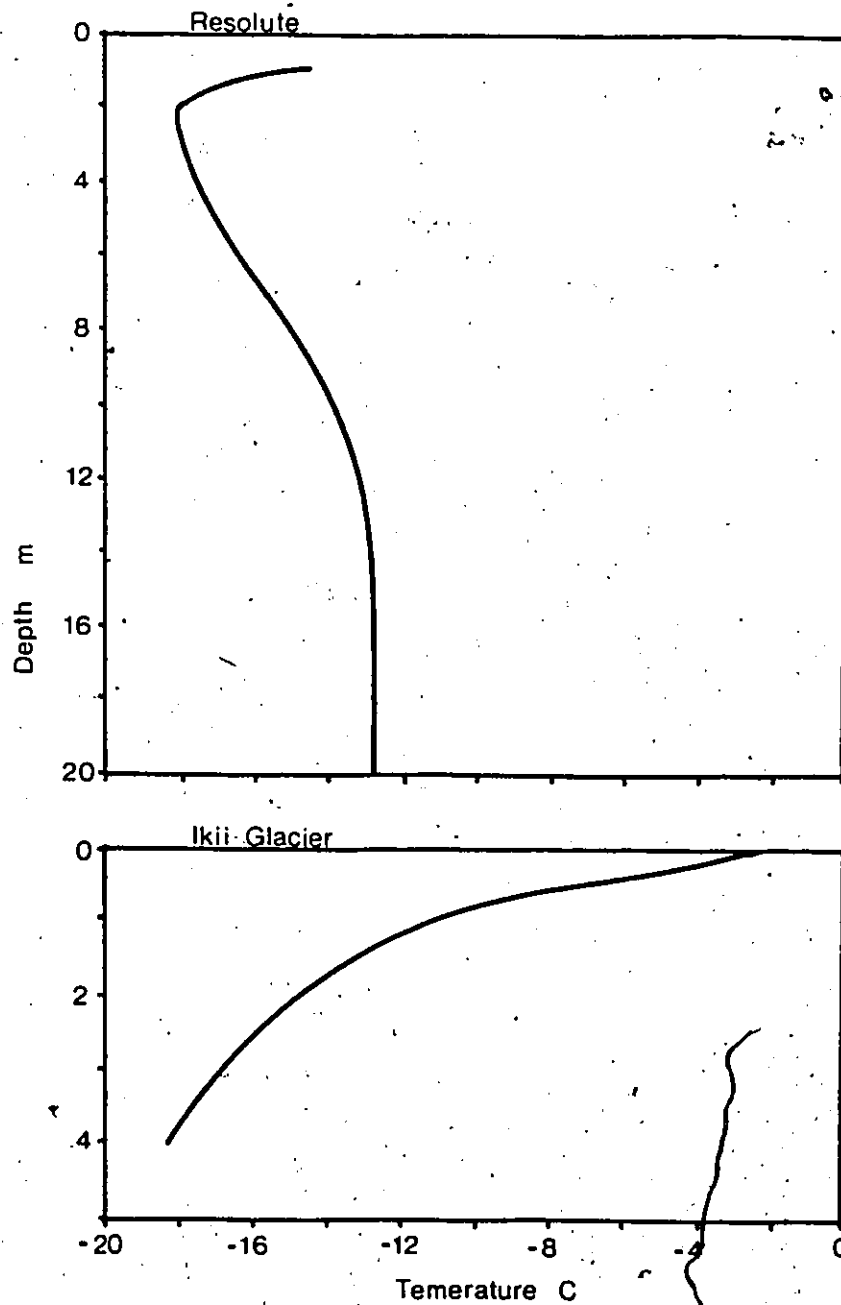| | Resolute | | | | | | Eidsbotn | | | |
	CC6	CC7	F8	F9	F10	Upper	2-11 2-7 1-1	2-10	glacier ice	
snow properties										
density	380	350	350	390	360	400	-	-	-	kg/m³
thermal cond.	.38	.34	.34	.42	.34	.42	-	-	-	W/m C
substrate properties										
thermal cond.	3.01	3.01	3.01	2.33	2.33	3.01	3.11	3.11	2.20	W/m C
specific heat	916.9	916.9	916.9	996.5	996.5	916.9	896.0	896.0	2,139.5	J/kg C
infiltration	20	20	20	7	7	20	40	20	0	mm
wetting fronts										
finger area(A_f)		.22								
fraction of flux in finger		.48								
S_{ui}		.07								

Snow thermal conductivity (Table 5.1) was determined from equation 2.9 using the listed snow densities. Substrate thermal conductivity was calculated from equations 2.10, 2.11, and 2.12 using the data listed in Table 5.2. The fractional volume of unfrozen water was estimated from Penner (1970), who showed that for clay soils its value was nearly constant at 0.1 for temperatures less than -2 C. For coarse grained soils it is negligable (Penner 1970). Specific heat for the soils was determined from equations 2.13.

TABLE 5.2

Substrate properties used to calculate thermal properties

	Gravel soils (CC6,CC7,F8,Upper)	Bog soils (F9,F10)	Eidsbotn (gravel)	
bulk density	.1709	1683	1800	kg/m^3
porosity	.37	.38	.33	
fractional vol. unfrozen water	0	.1	0	
volumetric water content	.30	.38	.26	
degree of saturation	.8	1.0	.8	
vol. fraction of solids	.63	.62	.67	
vol. fraction of organics	0	.1	0	
vol. fraction of ice	.30	.38	.26	
soil density	2009	2063	2060	kg/m^3

Daily snowmelt during the 1981 study period was determined from the surface energy balance (Figure 5.4). Measurement of flow variability from the multi-compartment lysimeter (Figure 5.5) on the first measurement day after the passing of the wetting front indicates that 48% of the total daily flow (F_r) occurred through an area equal in size to the proportion of total area covered by flow fingers (A_r=.22). The area covered by the background wetting front carried the rest of the total flow. Using these values the flux at the finger front was concentrated by a factor (F_r/A_r) of 2.18 times that of the uniform surface melt flux, while at the wetting front it was diminished (F_w/A_w) by 0.67 times.
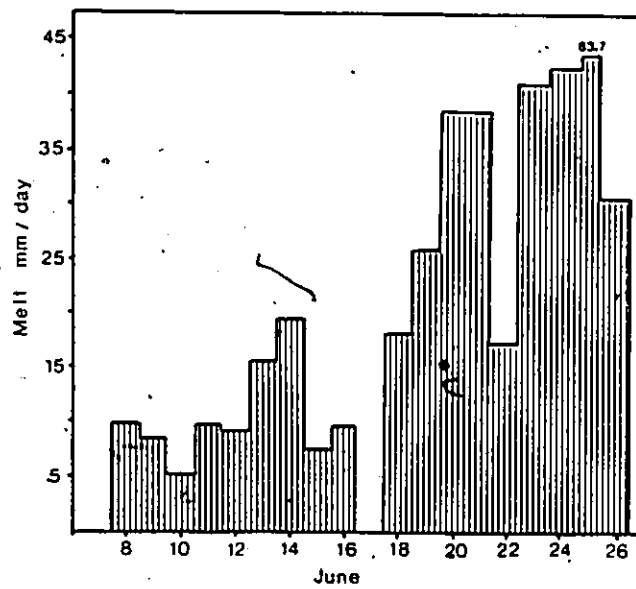
FIGURE 5.4 Daily snowmelt as determined from the surface energy balance at Resolute, June 8-26 1981.
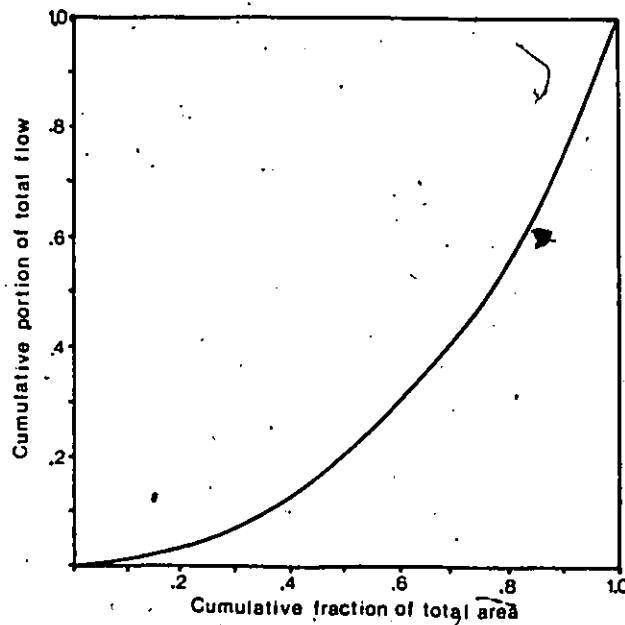

FIGURE 5.5 Measured flow variability soon after the wetting front passed the multi-compartment lysimeter level, June 15 1981.

The infiltration capacities for each substrate are summarized in Table 5.1.

In addition, predicted basal ice growth was compared with measured values for sites at Eidsbotn Fiord in 1979 and 1980. In 1979 temperature measurements were obtained from Ikkii glacier (Figure 5.3), but no ground temperature measurements were available for 1980. Instead, the measured temperatures at Resolute (1981) were substituted (Figure 5.2 and 5.3). The thermal properties for the glacier ice and soil and flow properties are listed in Table 5.1 and 5.2.

5.3 Snowpack ripening - results

Results from the snow pack ripening model were compared with measurements of: (1) general wetting front advance, (2) ice layer development, (3) basal ice growth, (4) snow-soil temperature profile, and (5) changes in snowpack water equivalent for the five snowpits at Resolute in 1981. Additional basal ice and ice layer data were used from Eidsbotn in 1979 and 1980. To determine the importance of various input parameters on the snowpack ripening processes, a sensitivity analysis was carried out. Sensitivity, defined as the change in one factor with respect to change in another factor (McCuen 1973), was determined by the method of parameter perturbation.

General wetting and finger wetting fronts

The predicted daily position of the general front generally agrees with that observed at the five Resolute study sites in 1981 (Figure 5:6). For sites F8, F9, CC7 the predicted general front was within 0.1 m of the measured value. However, at CC6 the predicted was up to 0.2 m too deep on June 9 and 10, too shallow on June 12, and comparable to the measured values on the other days. The calculated general front was consistently too deep at site F10. This error can be attributed to the development of a thick, impermeable ice layer which blocked all water movement and delayed progression of the general front for a few days. This type of ice layer is very infrequent. That the predicted general wetting front was generally too deep at most sites for the first two or three days of melt may be due to an overestimation of snow melt. The lag time between the beginning of melt and the general front reaching the snowpack base ranged from three to seven days. In every case, except for site F10, the model accurately predicted the time of the general front reaching the snowpack base to within 24 hours.

The model results demonstrate that the finger front never extends further than 0.1 to 0.15 m below the general wetting front. This compares favourably with field observations that the deepest ice layer, which is an
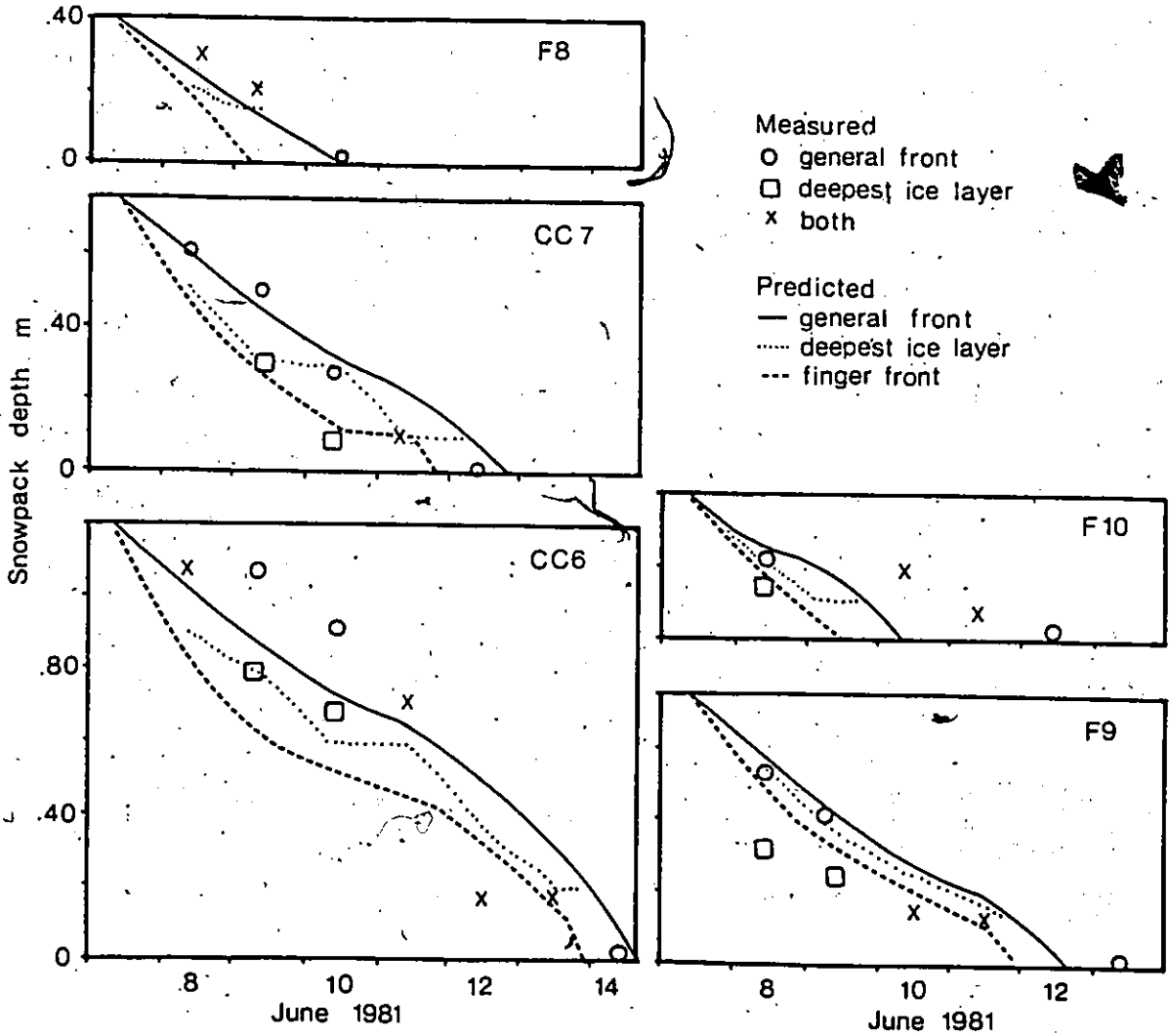
FIGURE 5.6 Predicted versus measured daily general wetting and finger wetting front advance, and deepest measured ice layer, Resolute 1981. Zero depth marks the snowpack base.

indication of the maximum penetration of liquid water, was never more than 0.2 m below the wetting front, and was usually much closer. The predicted finger front reached the snowpack base between 12 and 24 hours before the wetting front. A similar result was indicated by daily snowpit observations where water was seldom observed at the snowpack base prior to the arrival of the general wetting front.

The close proximity of the general and finger fronts is related to the strong feedback relationship between the rate of finger front advance, ice layer growth, and snow-soil temperatures. If the snow is sufficiently cold, ice layer formation consumes all of the finger flow and the finger front remains stationary. The continuously advancing general front gradually catches up to the finger front. As the snow warms around the ice layer, its rate of growth declines, and excess water is available to propagate the finger front downwards. The general pattern, therefore, is for the general front to progress downward steadily, while the finger front is characterized by alternating advances and halts (Figure 5.7). The predicted ice layer growth rates ranged from 3.3 to 3.6 mm water equivalent per day averaged over the entire individual ice layer growth period, to a high of 21.0 mm water equivalent per day for the first half hour of ice layer growth. This contrasts with water flux along the fingers which ranged from 2.5 to 9.6 mm water equivalent per
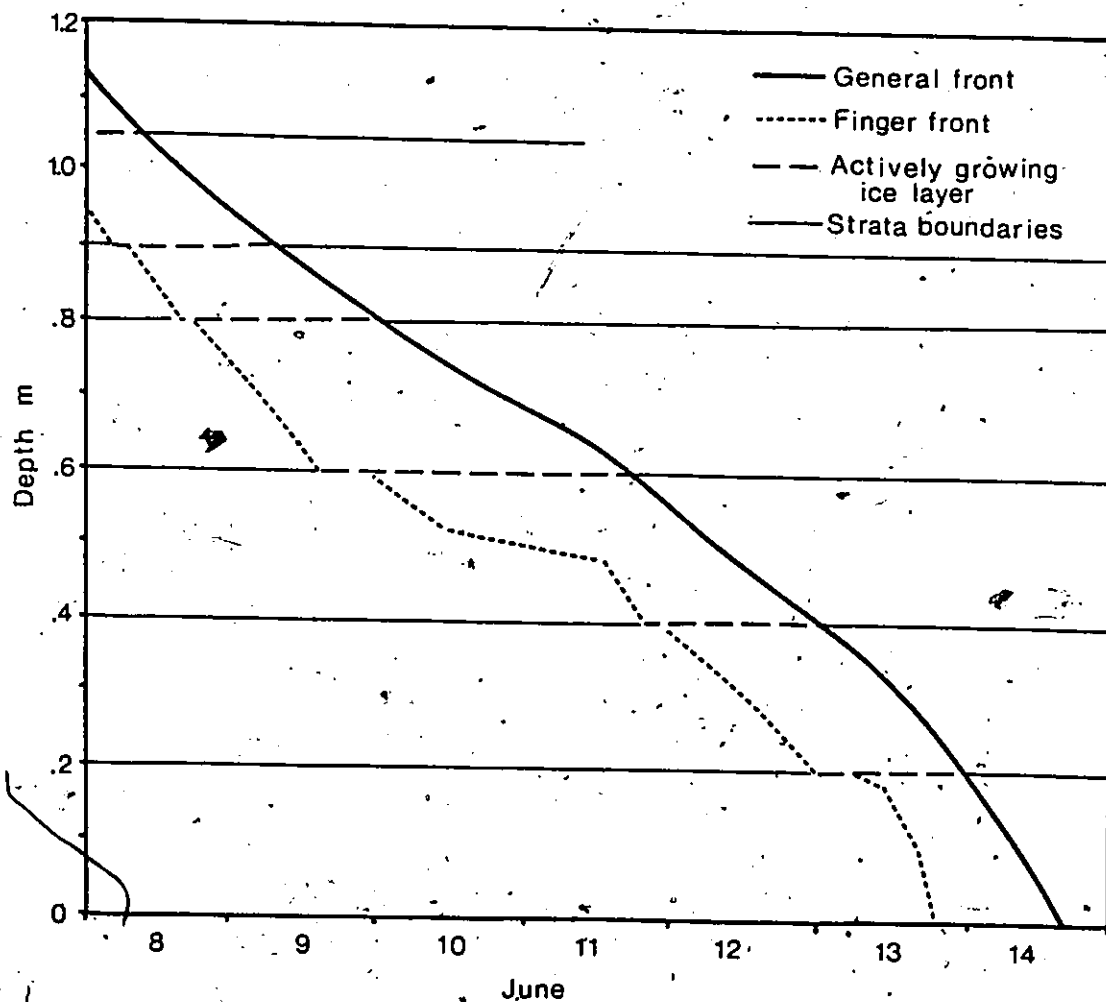
FIGURE 5.7 Predicted, hourly general wetting and finger wetting front advances, demonstrating continuous advance for the general wetting front, and periods of no advance for the finger wetting front due to ice layer growth at strata horizons. Snowpit CC6.

day, with a mean of 5.3 mm.

Figure 5.8 compares two snowpacks which are identical except that one is initially isothermal at 0 C and the other has a temperature typical of High Arctic snowcovers. In the isothermal case, the finger front proceeds quickly, reaching the snowpack base four days before the general front. However, in the cold snowpack, it reaches the ground surface only 12 hours before the general front. The wet-isothermal zone extends downward at the same rate in both warm and cold snowpacks, but the mixed zone behaves differently. In cold packs this mixed zone is thin due to a rapid growth of ice layers. Decreased ice layer growth in warmer snowpacks allows the finger front to advance rapidly and this mixed zone may be quite large. Under these conditions water may reach the ground surface before the liquid water and thermal requirements of the pack are filled. This type of zone has been described by studies of mid-latitude snowpacks (U.S. Army 1956), but is not signifacant in High Arctic snowpacks.

Because the general front lags the finger front by only 12 to 36 hours in cold snowpacks, individual fingers are short lived. As a result, large differences in grain size cannot develop. In warm snowpacks, however, fingers may last for several days before being caught up by the advancing general front (Figure 5.8). As a result, their grains may grow considerably larger than those in the surrounding snow,

Initial
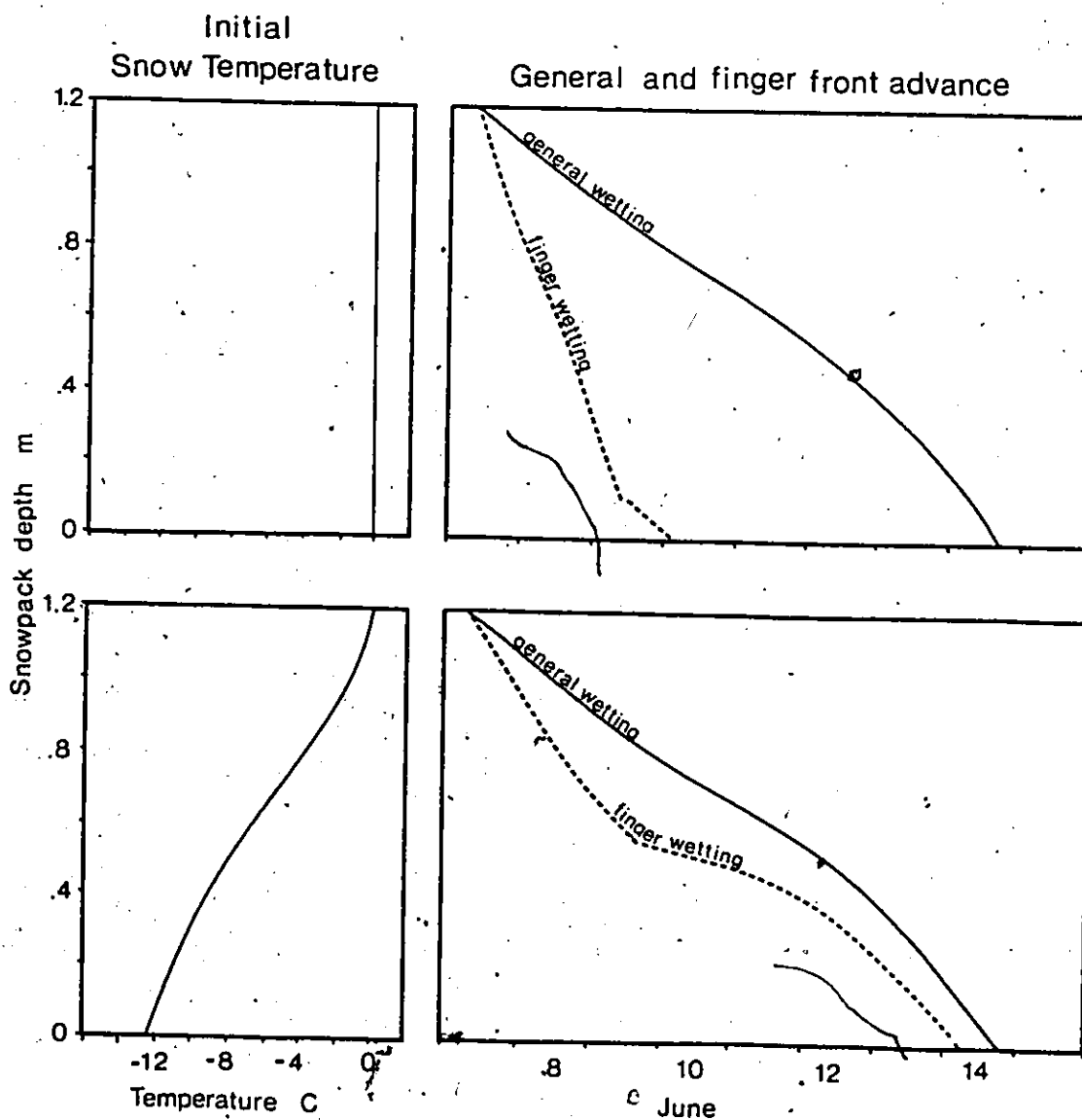Snow Temperature

General and finger front advance

FIGURE 5.8 Comparison of general wetting and finger wetting
front development in warm and cold snowpacks.

thus increasing their permeability. This may concentrate more flow within the fingers, thus inducing an accelerated advancement of the finger front and a greater lag between the finger front and the general wetting front.

Even though the High Arctic snowpack is initially very cold, the conduction of heat from developing ice layers warms the snow temperature immediately below both the general and finger fronts. The model showed that this temperature ranged from 0.0 to -3.0 C with a mean of -0.5 C below the general front; and -0.1 to -6.0 C with a mean of -2.6 C below the finger front. Weighting these temperatures against the ratio of the width of the general and finger fronts gives a mean of -1.0 C for the snow into which liquid water enters. The volume of water required to raise the snow to 0 C and that required to fill the irreducible water storage at the wetting front may be compared as the ratio of the thermal to liquid requirements (R_{TL}) (Colbeck 1975):

$$(5.22) \quad R_{TL} = [(|T_{sn}| \, p_s) / (L_F / C_i \, p_w)] \, / \, p \, S_{wi}$$

For an irreducible water saturation of 0.07 and a snow density of 380 kg/m³, R_{TL} varies from 0 to 0.17 for the general front, from 0 to 0.35 for the finger front, and averages 0.06 for both fronts combined. In other words, the thermal portion of the total liquid water requirement to advance the wetting fronts is only 6% of the

irreducible water storage, even though the snowpack was· very cold. For this reason, the rate of the general wetting front movement is practically the same in both cold and warm packs (Figure 5.8). The thermal requirements of the snow and soil in cold packs are not filled by freezing at the fronts, but by a release of latent heat at the growing ice layers.

Ice layer growth

Several ice layer conditions play an important role in snowpack ripening, including

(1) ice layer growing period

(2) the number of ice layers growing at any one time

(3) rate of growth, and

(4) total water frozen.

These conditions are interrelated and they control the rate of latent heat release and warming of the snowcover. They also affect the amount of water abstracted from finger flow and the time at which liquid water first reaches the ground.

The predicted beginning of ice layer growth at each horizon corresponds with observations (Figure 5.9). At pit CC6, for example, the predicted and observed starting times are within one day for all six ice layers. The ice layers grow sequentially, starting with the uppermost horizon, but more than one layer may be growing simultaneously.

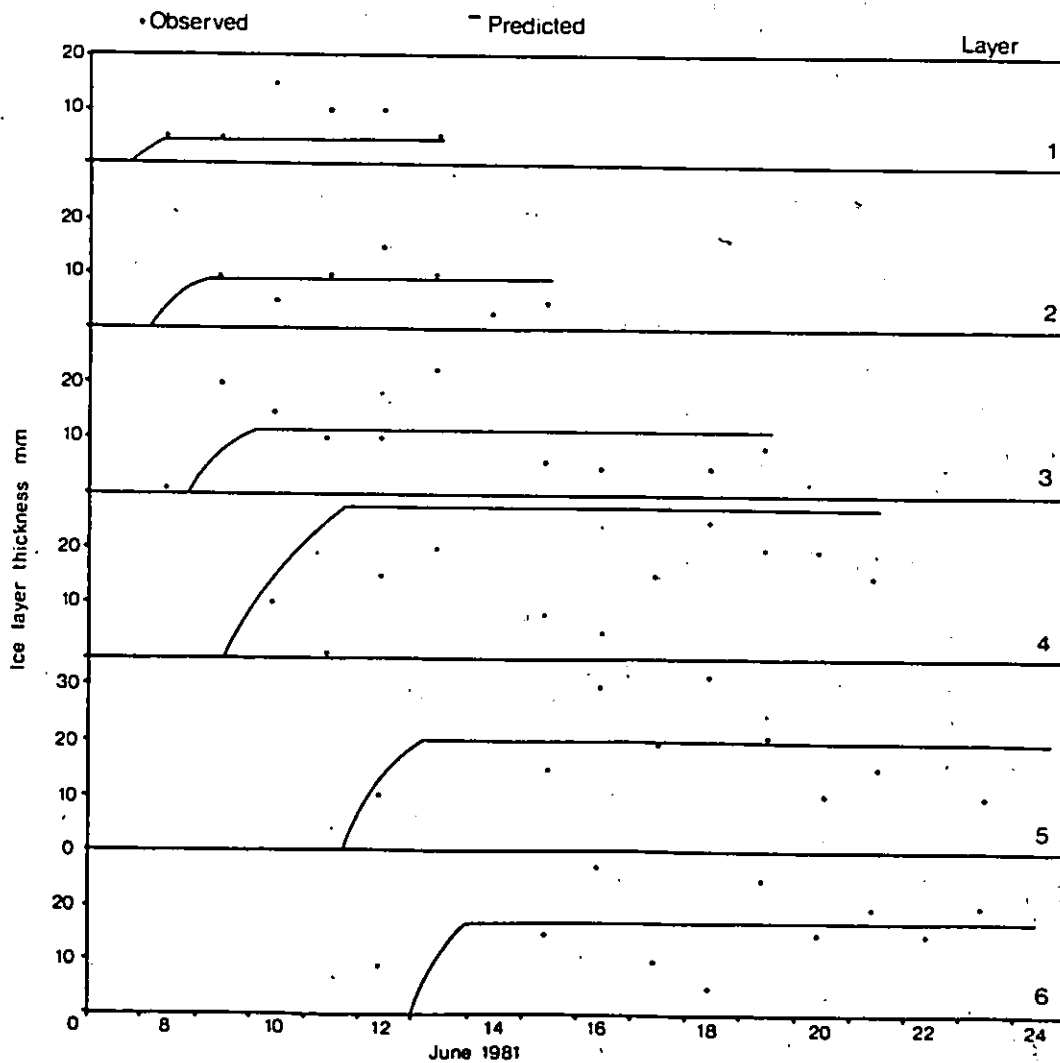These thick ice layers are able to grow during a short

FIGURE 5.9 Predicted ice layer growth and measured daily
ice layer thickness for each horizon in pit CC6,
Resolute. Layer one is closest to the snow surface.

24 to 36 hour period. The length of the growing period is controlled by the lag between the finger and general fronts. In warmer snowpacks, the greater separation between the general and finger fronts could result in a longer growing period for each ice layer, but the growth rate would be slower.

Averaged over the entire ice layer growth period, predicted growth rates varied from 3.3 to 3.6 mm water equivalent per day. For short periods, the predicted rate attains a maximum of 21.0 mm water equivalent per day. The temperature surrounding these actively growing ice layers decreases with increasing depth below the snow surface. At pit CC6, for example, the uppermost layer formed in snow with a predicted temperature between -2.4 and 0 C, while the bottom layer developed in snow with a temperature between -6.9 and 0 C. These colder temperatures are responsible for the thicker ice layers deeper within the pack (Figure 5.9). Measurements from pit 2-10 at Eidsbotn Fiord, on June 16, 17, and 18 1980 provide one opportunity to compare predicted and measured growth rates. Between the morning of June 16 and the morning of June 17, a 20 mm ice layer grew at a horizon 0.9 m below the snow surface. Between June 17 and 18 the water supply to this layer had apparently been cut off and ice growth ceased. The snow temperature above and below this ice layer on June 18 was still below 0 C. The ice layer

growth model was tested for this ice layer, assuming ice layer growth began on the morning of June 16, continued for 24 hours, at which time ice layer growth ceased. The predicted ice layer water equivalent of 5.1 mm for the morning of June 17, is similar to the measured value of 6.4 mm, and the predicted temperature profile above and below the ice layer on June 18 is close to the measured value (Figure 5.10).

The predicted total water equivalent frozen at the ice layers (Figure 5.11a) for pits CC6, CC7, and F9 are all within 10% of the 1:1 line. For the two shallowest pits (F8, F10), the model seriously underpredicts total ice layer growth. This is related to the general wetting front problem at both locations (Figure 5.6). Since the predicted general front advances too quickly, the predicted ice layer growth period is too short, and therefore the predicted total water equivalent frozen at all ice layers is too small.

The prediction of individual ice layer thickness is not required for snowpack ripening. However, it does illustrate some features of the hydraulic properties of strata boundaries and is important to water movement through the snowpack.

There are considerable differences between the predicted and observed individual mean ice layer thickness (Figure 5.11b), though the general patterns agree in most
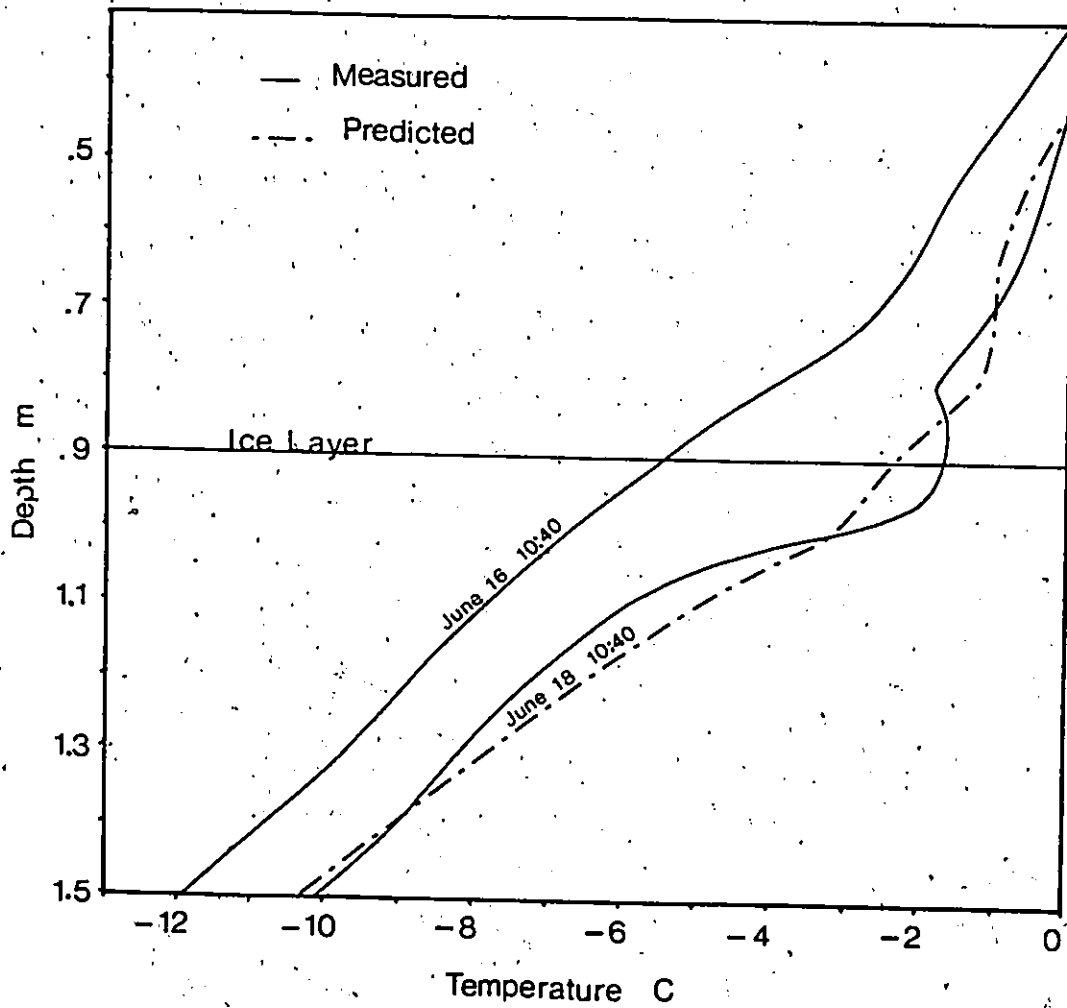
FIGURE 5.10 Measured versus predicted temperature above and below an ice layer in snowpit 2-10, Eidsbotn, 1980.
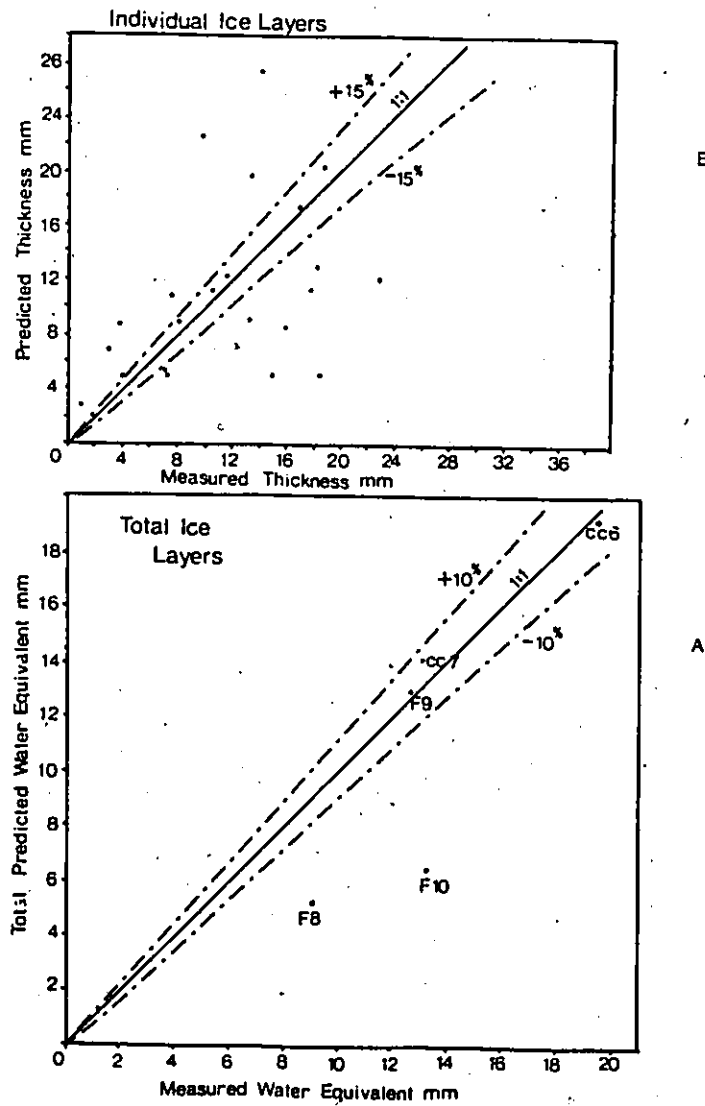
FIGURE 5.11 Top — predicted versus observed individual ice layer thickness (maximum) for all pits, Resolute 1981.
Bottom — predicted versus observed total ice layer water equivalent for all ice layers at each snowpit, Resolute 1981.

cases (Figure 5.11b, Table 5.3). Variations between measured and predicted values are due to both the use of a mean ice layer density of 600 kg/m³ for all predicted layers, and errors in the ice layer growing period. When the growing period is accurately predicted, as for layers two, three, five and six at pit CC6, the predicted and measured ice layer thicknesses are within +/- 15% (Table 5.4). These errors are likely due to using an incorrect ice density. Errors in predicting the general and/or finger front advance lead to either over- or under-estimating the length of the ice layer growing period. Since most ice layers grow to their maximum thickness in only 24 hours, small errors in the growing period may be resposible for significant errors in ice layer thickness. At pit CC6 for example (Table 5.4), this problem was responsible for very large errors at layers one and four.

Ice layer density is dependent on the water content immediately above the stratum boundary, which in turn depends on the hydraulic properties of the stratum interface. Although most horizons within the High Arctic pack are impeding, impedance varies from horizon to horizon, and laterally along a single horizon. Given the present state of our knowledge, it is not possible to incorporate these variabilities in the model. In general, dense ice layers will form where a completely saturated layer develops above a

highly impeding horizon, and less dense ice layers above horizons with little impedance. However, the total amount of water freezing at an interface will be controlled by thermal conditions, and not by the water content. Thus, the effects of ice layer growth in relationship to ripening may be predicted by thermal conditions alone.

Table 5.3

Comparison of predicted and observed ice layer growth of six ice layers in pit CC6

Layer number	depth below surface (m)	maximum ice layer thickness (mm)		difference between
		measured	predicted	measured and predicted(%)
1	.15	7.3	5.0	-27
2	.30	8.0	9.2	15
3	.40	10.7	11.5	7
4	.60	14.3	27.5	92
5	.80	18.8	20.3	8
6	1.0	17.2	17.1	0.6

Relationship between frontal movement and ice layer growth

The previous sections demonstrated that the advance of the general and finger wetting fronts, and ice layer growth are interdependent. In order to study this interdependence, the sensitivity of the two principle output parameters of the model (the time required for the general and finger fronts

to reach the snowpack base, and the total ice layer thickness) to changes in four important physical properties of the snowpack (fraction of flow in the fingers, thermal conductivity, snow density, and the irreducible water content) was carried out using snowpit CC6 and an example. The snow at this site was 1.256 deep at the beginning of melt, and the finger front covered 22% of the total horizontal area and the general front the remaining 78%. Figure 5.12 illustrates the relationship between the important inputs and outputs, and in addition gives the temperature of the snow immediately below the finger and general fronts. This is a parameter calculated by the model, and is not an important output parameter, but is presented here because it illustrates the changing thermal conditions affecting wetting front advance and the ice layer growth rate. This sensitivity analysis also allows an estimate of which input parameters need to be accurately measured in order to ensure accurate predictions of snowpack ripening.

(i) proportion of flow occuring in the fingers

The example in Figure 5.12(i) shows that with a low proportion of total flow occurring in the finger and a high proportion at the general front, the finger front takes about 6.1 days to reach the snowpack base, and the general front 6.5 days. Under these flow conditions only 40 mm of ice
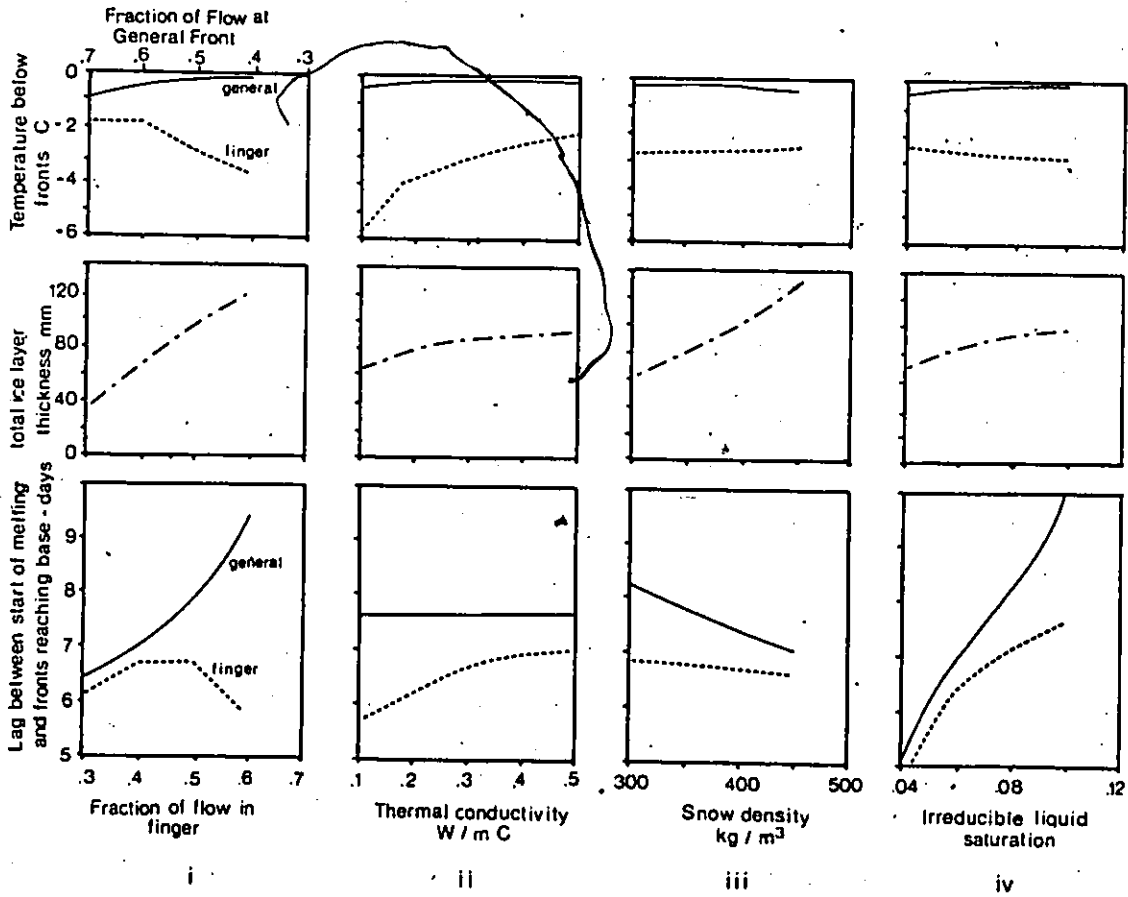
FIGURE 5.12 Effect of model parameters on general wetting and finger wetting front advance and ice layer growth using snowpit CC6 as an example, Resolute 1981.

layers grow within the snowpack. The low total ice layer growth is due to a short growing period and insufficient water to satisfy the maximum potential ice growth. As water is diverted away from the general front to the finger front, it takes a longer time for both fronts to reach the snowpack base. The slower general front advance is due to a decreased water supply, not increased thermal requirements. Note that the temperature below the general front (Figure 5.12i) actually increases with increasing finger flow. This is due to increased heat release by ice layers below the general wetting front. The slower finger front advance is caused by increased ice layer growth as water supply is no longer limiting the growth rate. When the proportion of flow in the finger is between 0.4 and 0.5 of the total, the finger front lag time reaches a maximum of 6.5 days, and the general front lag time continues to increase to 7.5 days. Under these flow conditions the ice layers are growing at their maximum rate, which is controlled by the rate of heat conduction away from the ice layers, not water supply. The increase in total ice layer thickness to 80 mm is due to the greater separation between the two fronts and therefore the increased growing period for individual ice layers, and a decreased temperature immediately below the finger front from −2 to −3 C (Figure 5.12i). This decrease in temperature occurs because the flow fingers are extending further below the general front. Since

the ice layer growth rate is at a maximum, the extra water carried by a further increase in finger flow to 0.6 of the total is used to decrease the finger front lag time to 6 days. The increasing separation between the two fronts is responsible for ice layer growth reaching a maximum of 120 mm. Over the range of flow conditions discussed, the general front lag time increases by 3 days, but the finger front lag time never changes more than 12 hours. In these cold Arctic snowpacks therefore, increased finger flow is used to grow thicker ice layers, not to rapidly advance water to the snowpack base.

The above discussion indicates that finger flow has a significant effect on snowpack ripening. Unfortunately this parameter is difficult to measure, and further work is required to determine the range of values it normally covers, and its dependence on snow properties.

(ii) snow thermal conductivity

Changes in the snow thermal conductivity have no effect on the general front advance (Figure 5.12ii). This is because the temperature immediately below the general front is always very close to 0 C, and therefore the frontal advance is controlled primarily by liquid requirements, not thermal requirements. An increase in thermal conductivity, from 0.1 W/m C (low density snow 100 kg/m³) to 0.5 W/m C

(high density snow 450 kg/m³) results in an increased lag
time between the beginning of melt and the finger front
reaching the snow base from 5.7 to 7 days, and the gap
between the two fronts decreases. This increase in the
finger front lag time is primarily due to an increase in ice
layer growth from 64 to 94 mm. This increased thickness is
caused by a higher heat flux caused by the increased thermal
conductivity. However, increases in ice growth are limited
by the decreased growing time since the fronts are closer
together, and increased snow temperature below the finger
front (Figure 5.12ii), due to the greater heat conduction.

For the range of snow densities commonly observed at
the beginning of melt in the high Arctic, thermal
conductivity ranges from 0.2 to 0.4 W/m C (Anderson 1976).
Over this range, thermal conductivity has little or no
influence on the total ice layer growth or wetting front
advance, and changes the finger front advance by less than
one day (Figure 5.12ii). This evidence suggests that present
methods using snow density alone to estimate thermal
conductivity (equation 2.9) are sufficiently accurate for
predicting snow ripening.

(iii) snow density

Increasing the snow density from 300 to 450 kg/m³ results in a decrease in the general front lag time from 8.2 to 7.2 days, and a negligible decrease from 6.8 to 6.6 days for the finger front (Figure 5.12iii). The primary reason for the decreased lag time of the general front is that an increase in density results in decreased porosity, and therefore less water is required to fill the irreducible water storage. As Figure 5.12(iii) shows, the temperature below the general front is nearly constant, and close to 0 C. As a result, the thermal requirements are small. The effect on the finger front is minor because its advance is dominated by ice layer growth, not liquid requirements. The amount of water frozen at the ice layers remains relatively unchanged since the temperature between the fronts is nearly constant (Figure 5.12iii). However, the ice layer thickness does increase (Figure 5.12iii) due to the decreased snow porosity, not the freezing of more water.

This analysis suggests that in terms of snowpack ripening, snow density is not very important. Considering that snowpack density may be measured to within 6% (Goodison et al 1981) or 12 to 27 kg/m³, for commonly observed densities at the begining of melt, the corresponding error in estimating snowpack ripening will be minimal.

(iv)irreducible water content

A change in the irreducible liquid saturation from 0.04 to 0.10 increases the wetting front lag time from 5.2 to 10 days and the finger front from 5 to 7.5 days (Figure 5.12iv), due to the increased liquid requirements at both fronts. Its effect is not as important on the finger front advance, because of the dominant effect of ice layer growth. With increasing irreducible water storage, the finger front can advance further ahead of the wetting front, increasing the ice layer growth period. The result is to increase total ice layer thickness from 63 to 104 mm (Figure 5.12iv). The small increase in temperature below the finger front plays a minor role in this increase in ice growth.

This analysis suggests that the irreducible water storage may play a significant role in snowpack ripening. Previous work has suggested that its value covers a narrow range in coarse grained, wet snow, but there is conflicting evidence concerning its value in freshly wetted snow. The agreement between predicted and measured wetting front advance in the present study, suggests that an irreducible water content of 0.07 is reasonable. But considering the magnitude of the possible error, more work is required to relate the irreducible water content to snowpack properties.

Basal ice growth

Calculations using three years of data, and four different substrates showed that the predicted and observed growth rates and maximum ice thicknesses agree for all 13 sites shown on Figure 5.13. The maximum growth rate varied from 2.8 mm/hour for the gravel sites to 1.5 mm/hour at Ikkii glacier to only 1.0 mm/hour for the bog sites. The larger growth rates at the gravel sites were primarily due to their higher thermal conductivity (Table 5.1). After 10 days of growth, growth rates declined to approximately 0.4 mm/hour at all sites. The lag between water reaching the snowpack base and the initiation of basal ice, ranged from zero over the impermeable ice surface of Ikkii glacier, to approximately 8 hours for the bog soils of Resolute, to 24 hours for the Resolute polar desert soils, to a maximum of 3 days for the coarse, high infiltration gravels of Eidsbotn Fiord (Figure 5.13). The predicted lag agrees with the observed values for most cases. The maximum basal ice thickness at each site ranged from 50 to 140 mm of ice.

A sensitivity analysis was conducted in order to illustrate the relative importance of (1) soil infiltration, (2) soil temperature, (3) soil thermal conductivity, and (4) the melt rate and length of the basal ice growing period.
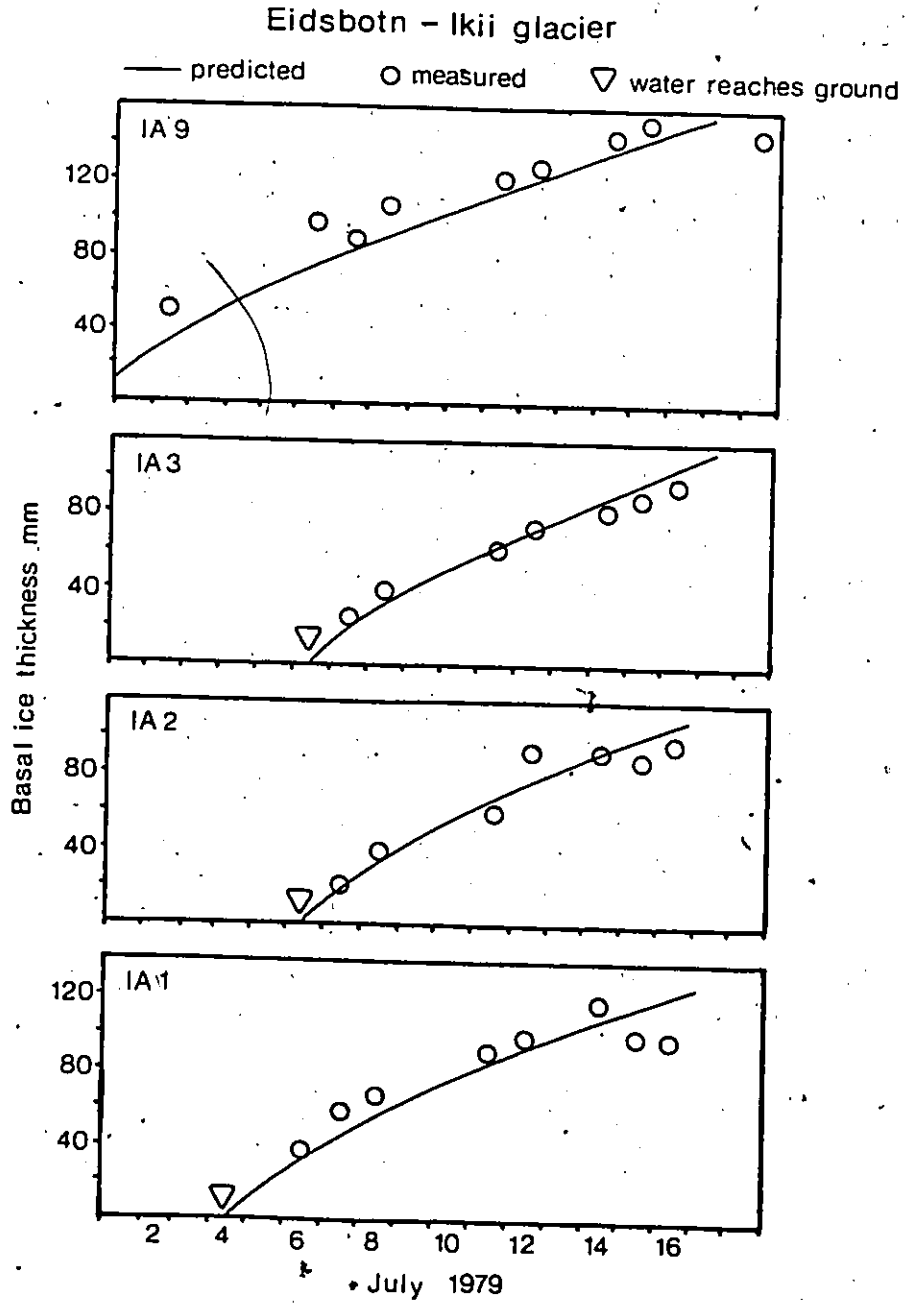
FIGURE 5.13a Precicted versus observed basal ice growth at
Ikkii Glacier, Eidsbotn 1979.

Eidsbotn

—— predicted   O measured   ▽ water reaches ground

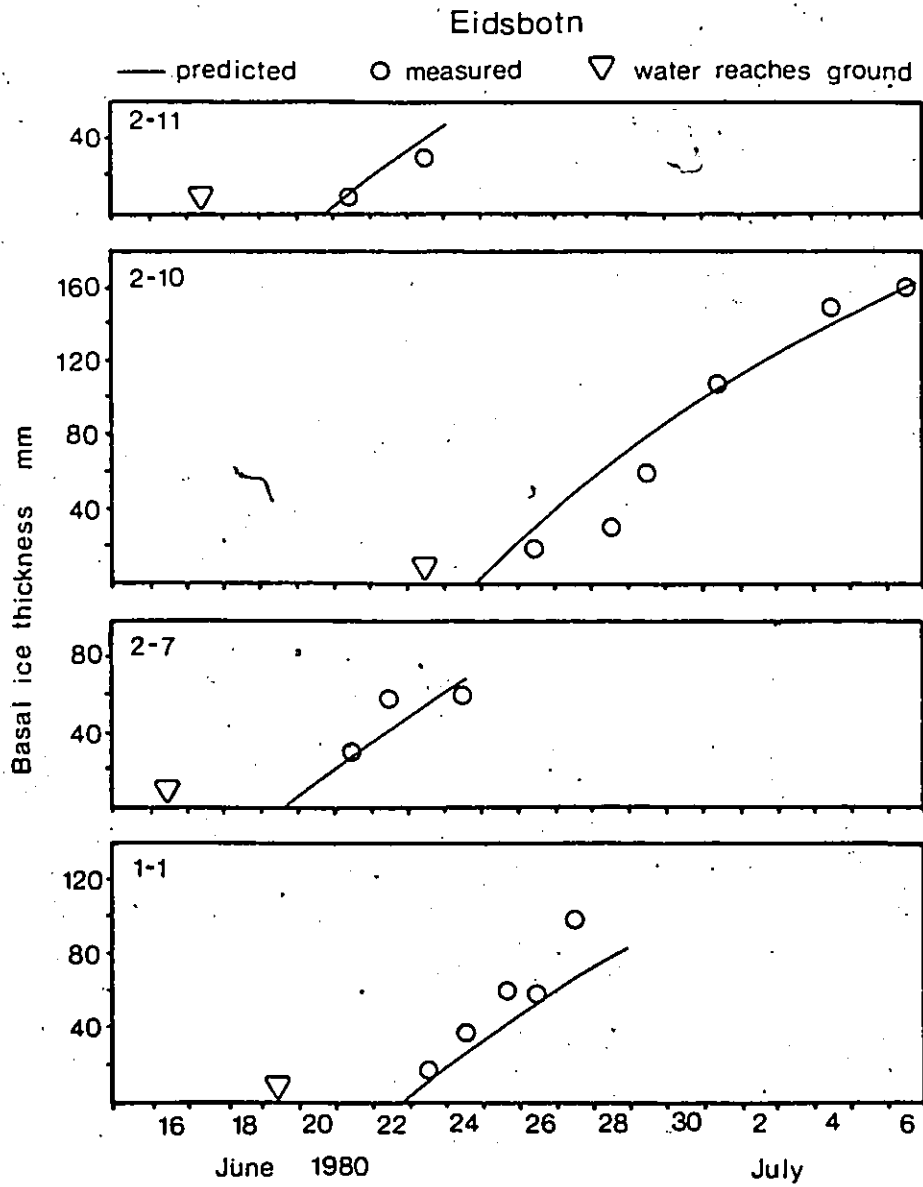FIGURE 5.13b Predicted versus observed basal ice growth at Eidsbotn 1980. All sites were underlain by gravel soils.

Resolute

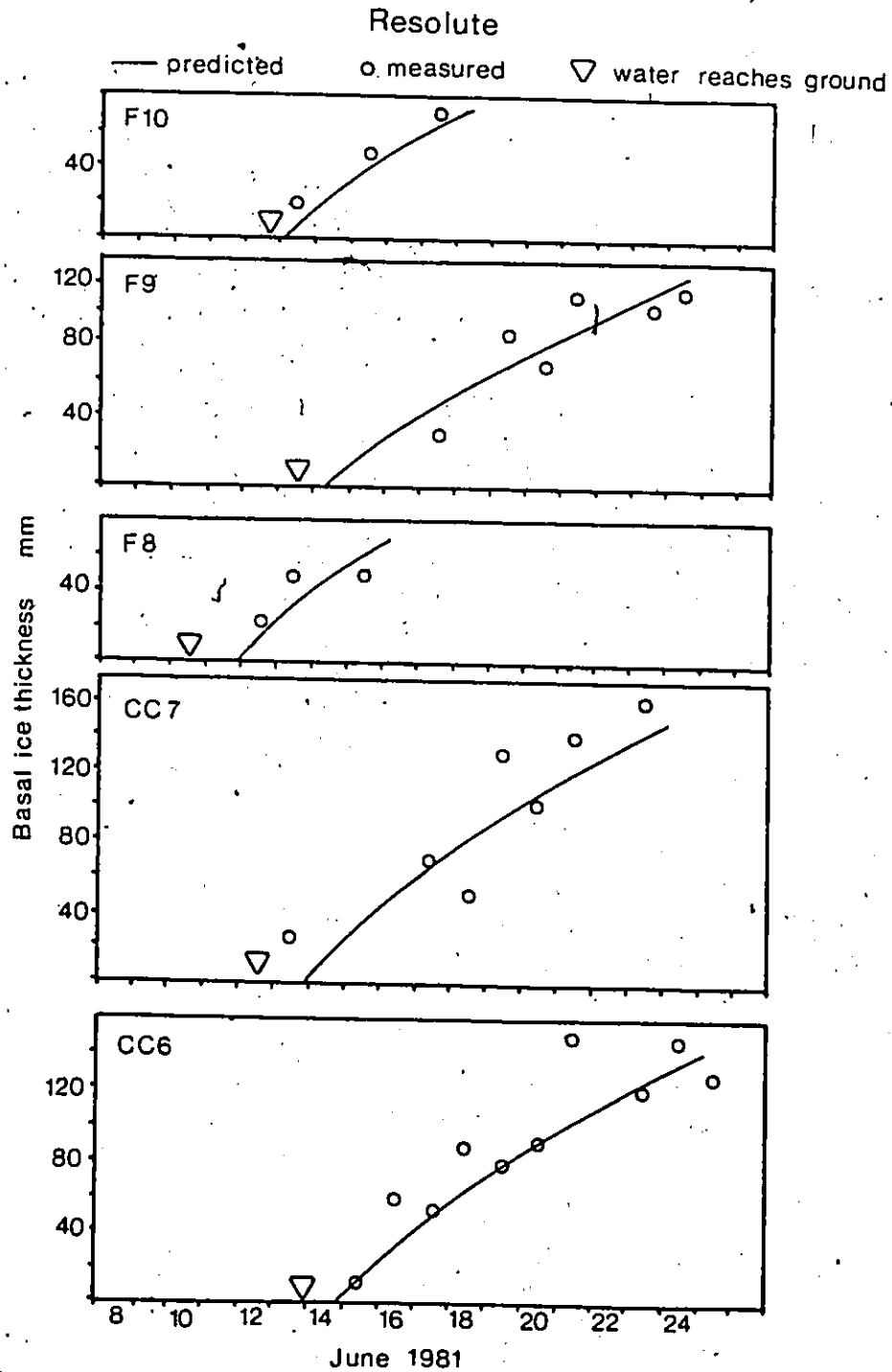— predicted   o. measured   ▽ water reaches ground

FIGURE 5.13c Predicted versus observed basal ice growth at
Resolute 1981. Sites F9 and F10 were underlain by
bog soils and F8, CC6, and CC7 gravel soils.

This analysis allows an estimate of which parameters need to be accurately measured in order to predict basal ice growth.

(i) soil infiltration

Soil infiltration results in a lag between water reaching the snow base and the start of basal ice growth and it limits the maximum basal ice thickness. Using CC6 as an example (Figure 5.14), varying the soil infiltration from 0 to 50 mm causes a decrease in total basal ice thickness from 186 to 84 mm. If the infiltration is large enough, no basal ice forms. This is unlikely for deep snowcovers, but quite likely for shallow packs overlying soils with a high infiltration capacity. Since soil infiltration may vary over small areas, and it has a very large influence on basal ice growth, it is necessary to include accurate estimates of soil infiltration when calculating basal ice growth.

(ii) soil temperature

The temperature gradient just below the snow-ice interface is the major factor controlling the growth rate. Figure 5.15 is an example of basal ice growth under different temperature regimes. Decreasing the temperature from -1 to -14 C at the 1 m depth, and holding the temperature gradient constant from 1 to 10 m (Figure 5.15a), increases the basal ice growth over a 15 day period from 20 to 175 mm. The
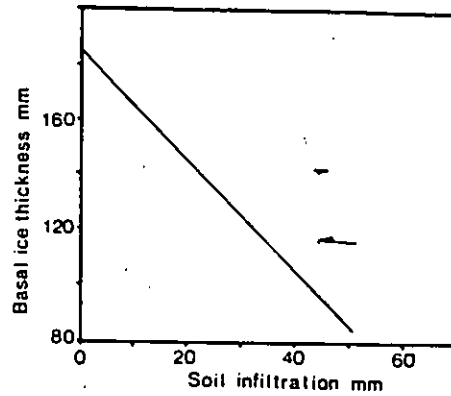
FIGURE 5.14 Effect of soil infiltration capacity on total
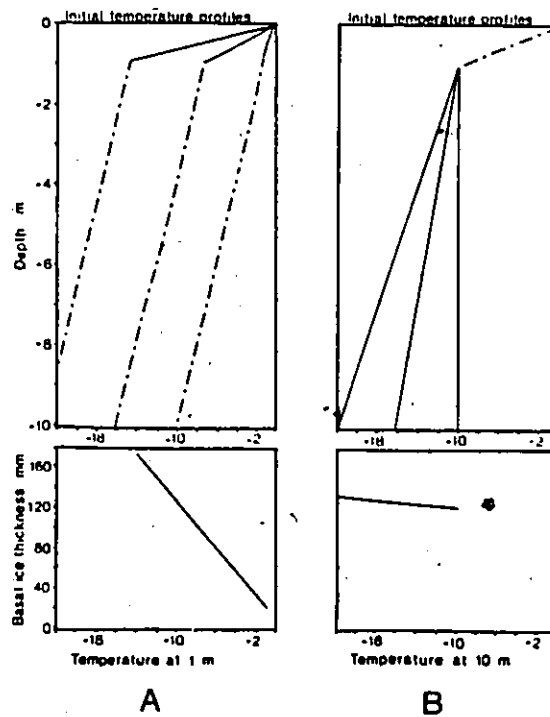basal ice thickness after 12 days of growth.

FIGURE 5.15 Effect of initial temperature profiles on total
basal ice thickness after 15 days of growth.

temperature gradient at depth, however, is of minor importance. Decreasing the temperature at 10 m from -10 to -22 C while keeping a constant gradient from the surface to 1 m only increases basal ice growth from 122 to 136 mm (Figure 5.15b). In modelling ice growth, therefore, accurate estimates of the temperature gradient immediately below the soil surface are required, but not the temperature profile below 1 m depth.

(iii) soil thermal conductivity

The rate of heat conduction below the interface is also dependent on the soil thermal conductivity, which can range from 0.5 W/m C to near 4 W/m C. For a given temperature gradient, doubling the thermal conductivity results in a doubling of the basal ice growth rate (Figure 5.16). Since thermal conductivity is dependent on soil type and moisture content basal ice growth will vary greatly between soil types and between years depending on the moisture content at freeze-up. Obviously an accurate estimate of the soil thermal conductivity immediately below the ground surface is required.
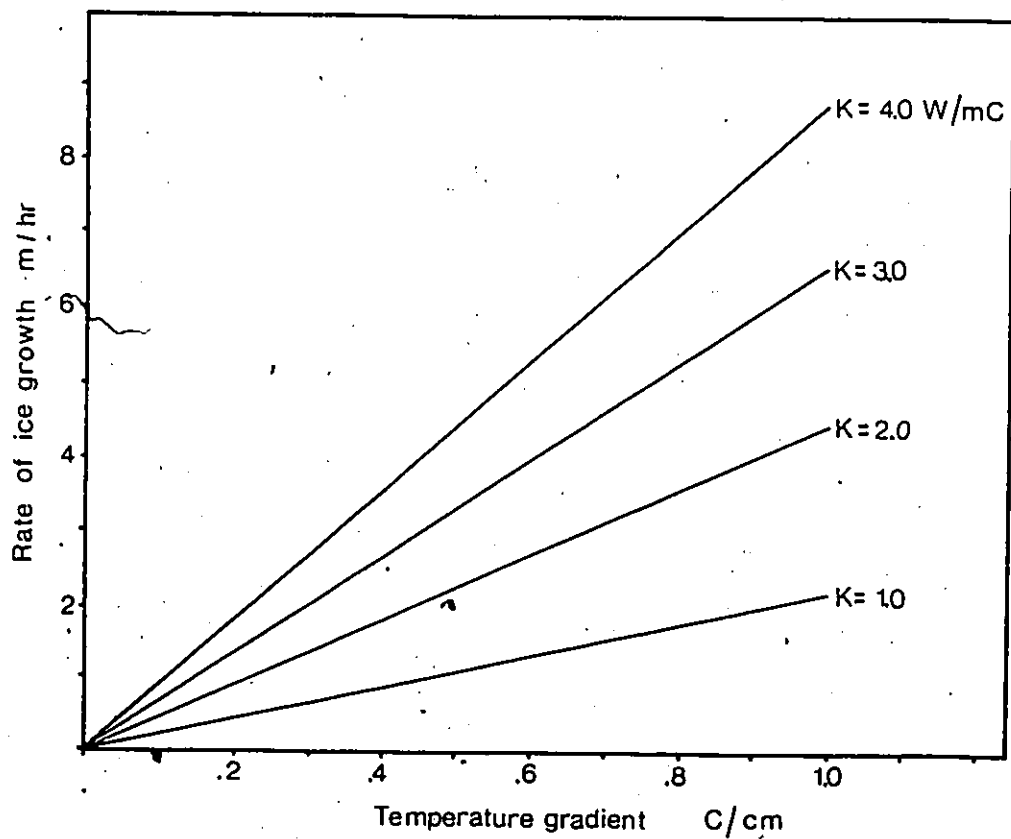
FIGURE 5.16 Effect of thermal conductivity on rate of basal ice growth for different initial temperature gradients.
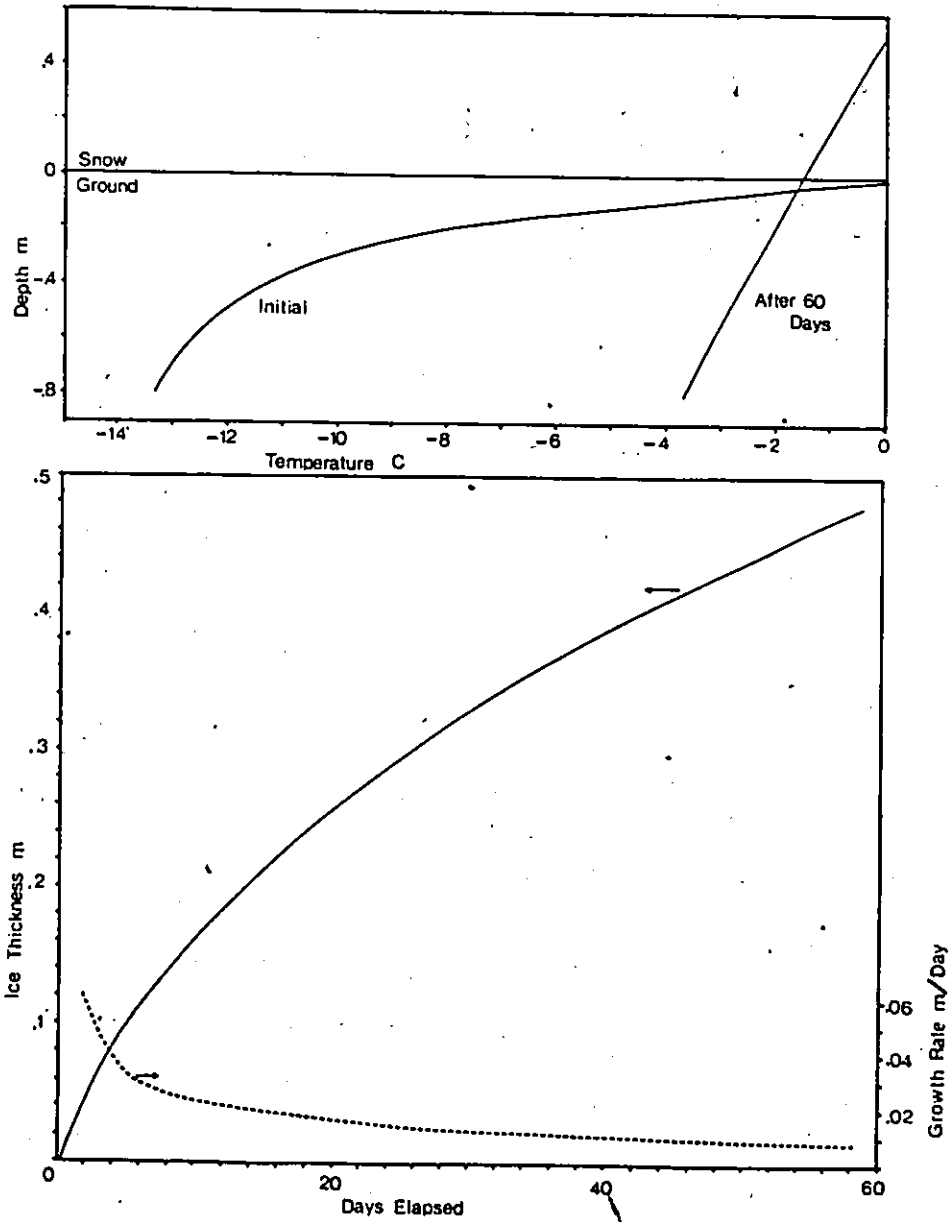
FIGURE 5.17 Total basal ice thickness, rate of growth, and temperature gradient at the start and after 60 days of basal ice growth.

(iv)ice growth period

The duration of the basal ice growth also effects maximum basal ice thickness. Figure 5.17 shows a hypothetical example where the snow depth is great enough to sustain basal ice growth over a 60 day period. The growth rate decreased from an initial rate of over 0.06 m per day to a final value of less than 0.01 m per day, with total thickness reaching 0.488 m. Even after 60 days of growth, the soil temperature was still below 0 C (Figure 5.17), indicating that under very deep snowpacks basal ice could continue to grow for long periods of time. All other factors being equal, deeper snowpacks tend to form thicker basal ice layers.

Since melt rates are usually greater than the rate of basal ice growth, the ice growth rate is generally not affected by the melt rate. This may not be correct for the first day of basal ice growth when all meltwater may freeze (Table 5.4), or occasional days with little melt, but over the entire melt period the rate of ice growth is mainly controlled by the rate of downward heat conduction. However, the total ice thickness at the end of melt is dependent on the melt rate. For example, slow melt rates will extend the basal ice growth period, and increase the maximum ice thickness. The magnitude of such an effect is shown in
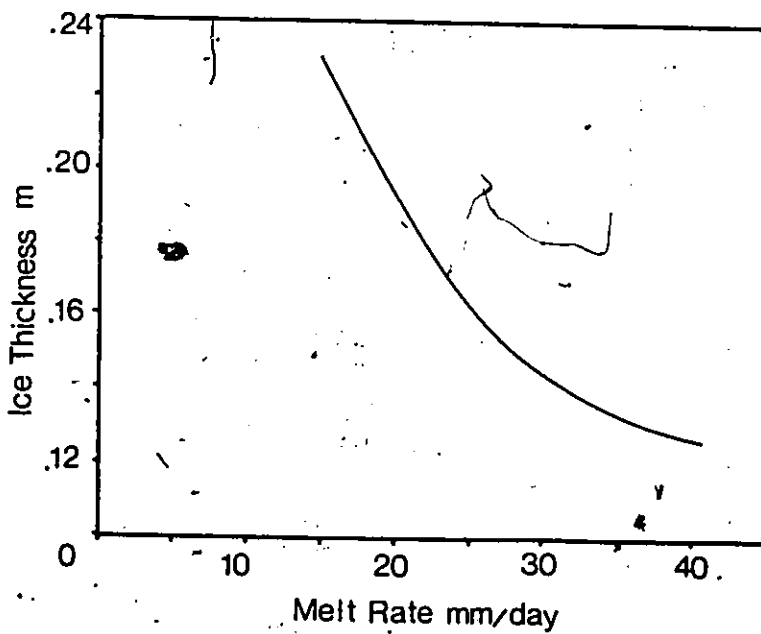
FIGURE 5.18 Effect of melt rate on total ice thickness for an initial snowpack of 250 mm water equivalent.

Figure 5.18, where the total ice growth is calculated assuming different melt rates. For a mean melt rate of 15 mm per day, basal ice would grow to a maximum thickness of 0.23 m over a 17 day period. Increasing the mean melt rate to 35 mm per day decreases the ice thickness to 0.13 m during a 7 day growing period. Maximum basal ice thickness is found when the daily surface melt equals the rate of daily ice growth. In this case the entire water equivalent of the snowpack would be transformed into basal ice. The rate of melt is important in determining both the basal ice thickness, and the amount of melt water available to runoff during basal ice growth.

TABLE 5.4

Daily basal ice growth as a percentage of daily snow melt

| June | Snow melt (MJ/m²) | Basal ice growth | | |
		CC6 %	FB %	F10 %
12	3.0		100	
13	6.1		54	48
14	6.6		42	42
15	2.7	100	90	90
16	3.3	100		68
17	-	-		-
18	6.1	46		
19	8.7	24		
20	13.3	20		
21	13.3	16		
22	5.8	30		
23	13.7	15		
24	14.2	12		

Snow and soil temperature

Observed snow temperature at the upper thermistor site (Figure 5.19) increases considerably faster than was predicted for the period June 9 to 16, but the observed and predicted soil temperatures were in agreement. The rapid warming of the snow was probably due to a preferential conduction of both water and heat along the thermistor rod. Since the soil thermistor rod was situated below undisturbed snow, it was not affected.

On June 13 and 14 there was a discrepancy between observed and predicted soil temperature values at the upper thermistor. Most of this warming occurred between 16:20 June 12, and 09:15 on June 13. The discrepancy is unlikely to be due to heating of the thermistor rod, and the predicted finger and wetting fronts were still 0.64 and 0.80 m above the ground surface. Since the model shows that heat conduction cannot explain this rapid warming, it is most likely that an unusual flow finger was able to penetrate deeply, releasing latent heat and causing a rapid increase in temperature. Field data indicated that some fingers occasionally extend quite far ahead of the general wetting front. After June 14, the predicted temperature converged on the measured value, and during the June 17 to 24 basal ice growth period it accurately predicts the temperature profile

FIGURE 5.19a Predicted versus observed snow and ground temperatures at the upper thermistor during the snowmelt period, Resolute 1981. Snow depths are shown for each days.

Predicted —   · Measured

F 10 BOG

F 8 GRAVEL

Temperature C
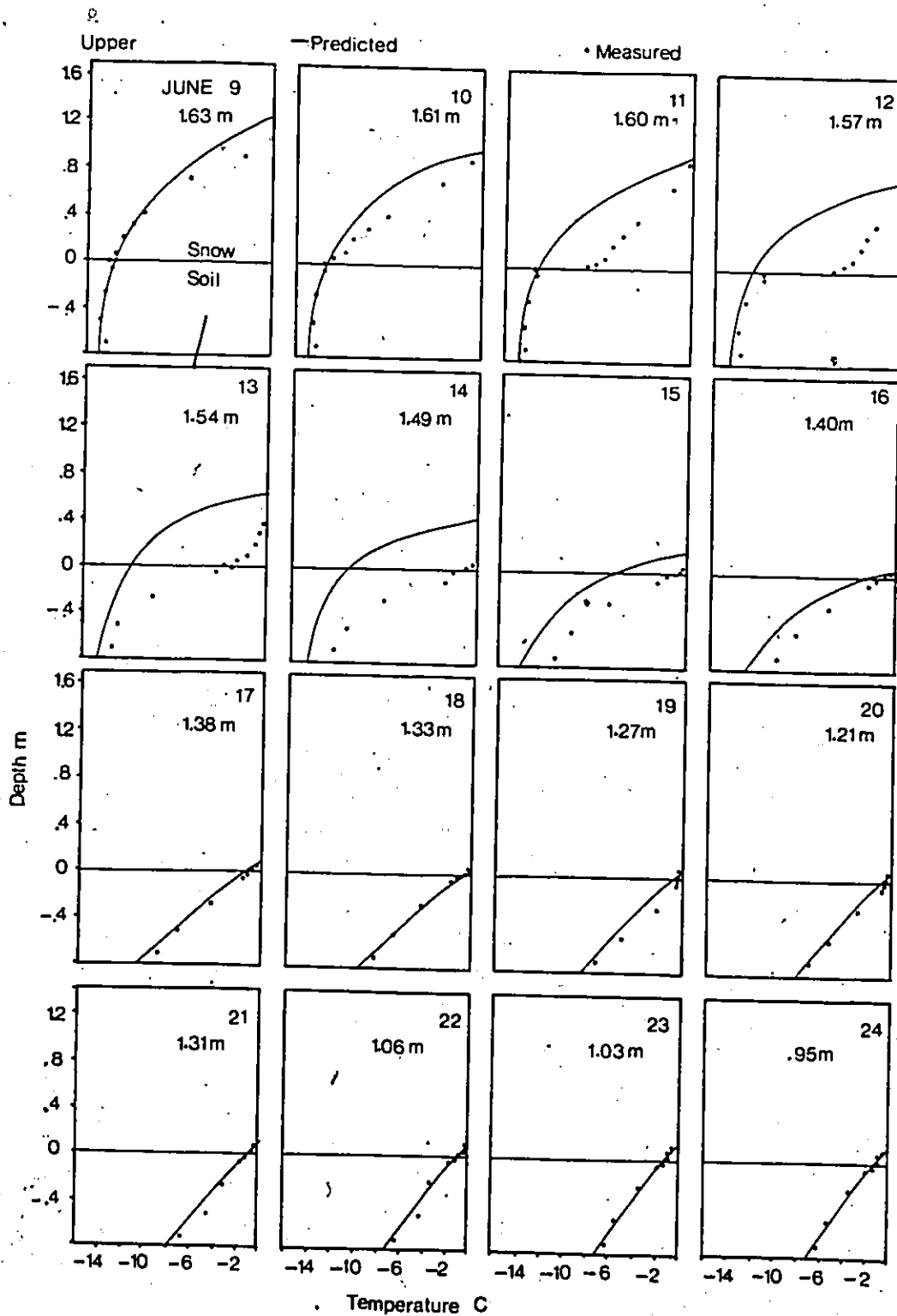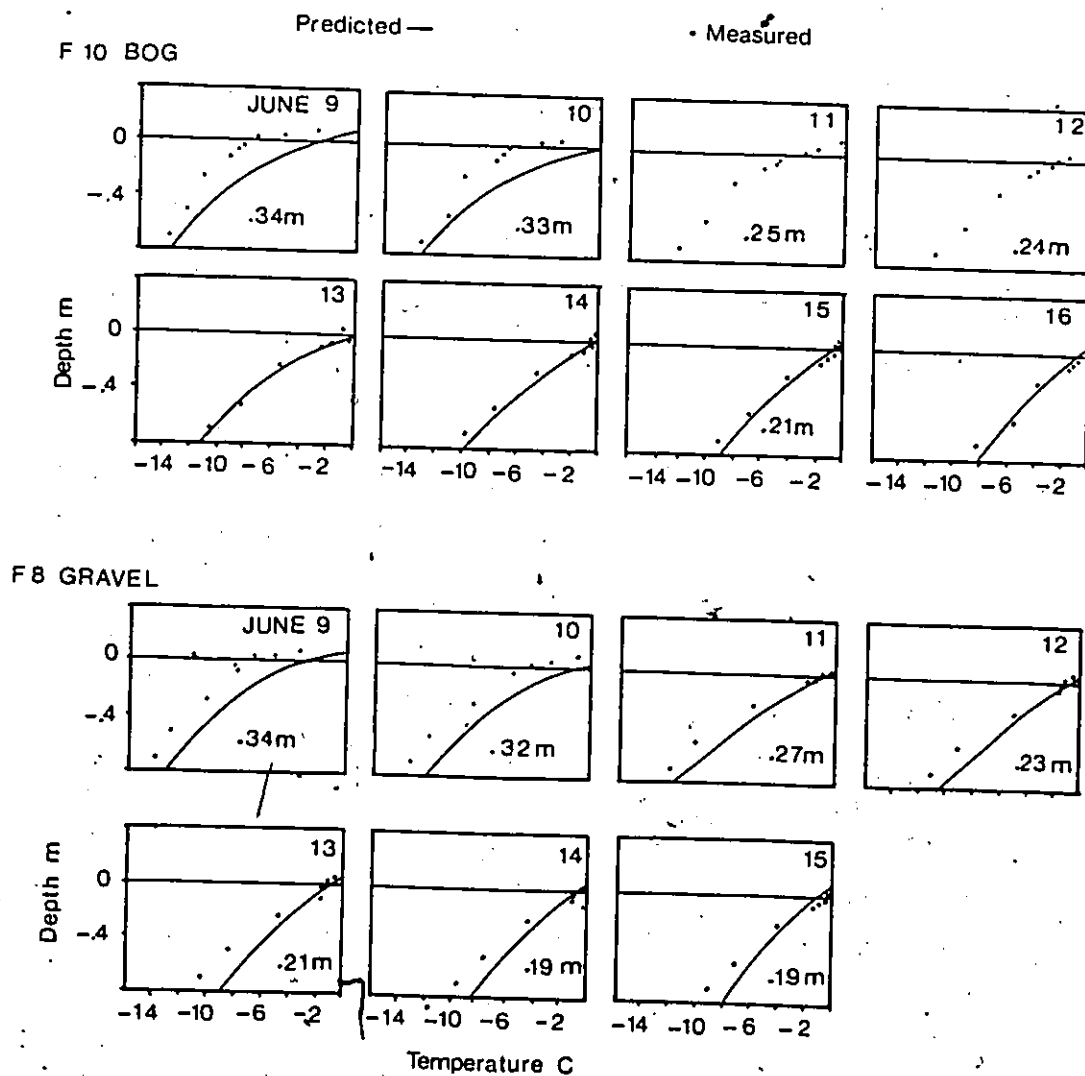
FIGURE 5.19b Predicted versus observed snow and ground temperatures at the bog and gravel thermistor sites during the snowmelt period, Resolute 1981. Snow depths are shown for each day.

down to a depth of 0.7 m.

The other thermistor rods, F10 and F8, were located in shallow snow which warmed rapidly. In both cases the predicted snow temperature increased more rapidly than the observed, due to the problem of over predicting the wetting front advance as discussed earlier (section 5.3). At site F8, the problem resulted in a maximum error of 2 C at some depths on June 10, after which the predicted gradually converged on the measured value with a maximum error of 1 C. At site F10, a maximum error of 3 C was observed on June 10. Because the predicted wetting front reaches the base two days early at this site, predicted basal ice growth also began early. In order to test the basal ice section of the model alone, the model operation was interrupted and restarted using the measured temperature data on June 12. In this case, predicted ground temperatures during basal ice growth were in agreement with the observed.

Snowpack water equivalent

To determine the daily change in snowpack water equivalent, the following information must be obtained: (1) snowpack conditions at the beginning of melt, (2) daily melt rate, (3) the time when water first reaches the snowpack base, (4) the soil infiltration capacity, and (5) daily basal ice growth. The calculated changes in pack water equivalent are therefore dependent on all the processes discussed earlier.

In all cases, the model accurately predicts changes in snowpack water equivalent. At pit CC6, for example the importance of basal ice may by observed (Figure 5.20). Firstly, the pack water equivalent decreases slowly during the first few days after the pack is isothermal. This is due to rapid basal ice growth which freezes a large portion of total surface melt (Table 5.5). Secondly, if basal ice growth is not included when calculating change in snowpack water equivalent, the pack water equivalent will be underestimated by up to 20 %. As a result, runoff will be overestimated, and the time when the ground becomes snowfree will be later than predicted.

CC6

* OBSERVED PACK WATER EQUIVALENT
— PREDICTED PACK WATER EQUIVALENT
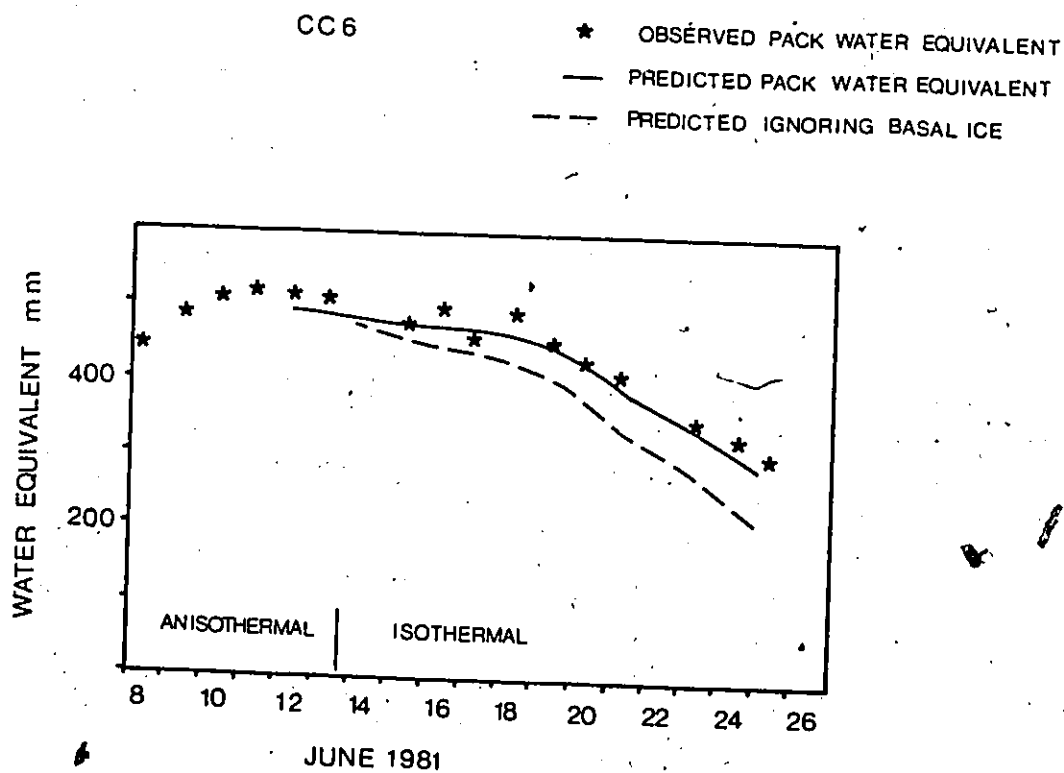— — PREDICTED IGNORING BASAL ICE

FIGURE 5.20 Predicted and observed changes in snowpack
water equivalent at pit CC6 after the pack becomes
isothermal, and the predicted change if basal ice is
not included. Resolute 1981.

CHAPTER SIX

WATER MOVEMENT THROUGH LAYERED SNOWPACKS

Many authors have described flow channels within wet snowpacks (eg. Gerdel 1954, U.S. Army 1956, Wakahama 1968). These channels facilitate meltwater flow and their presence makes it difficult to predict water movement in natural snowpacks. Little is yet known about their physical properties or the factors responsible for their development. This chapter will provide quantitative information on the variability of flow within a natural isothermal snowpack and relate this variability to the degree of metamorphism of the snowpack and to the melt rate, and develop a multiple flow path model for water movement in layered snowpacks, based on the homogeneous flow theory developed by Colbeck (1978).

6.1 Vertical, unsaturated flow in homogeneous snow

The vertical movement of water through homogeneous snow is governed by Darcy's Law for unsaturated flow in porous media (Colbeck 1971, Colbeck and Davidson 1972)

$$(6.1) \qquad U = -(k_{us}/v) \ (dP_c/dz - \rho_w \ g)$$

where U is the volume flux of water per unit area, k_{us} is

the unsaturated permeability, P_c is the capillary pressure, z is the depth, ρ_w and ν are the density and dynamic viscosity of the water, and g is the acceleration of gravity. Colbeck (1974) and Wankiewicz (1976) have shown that the pressure gradient term (dP_c/dz) is small compared to the gravity term ($\rho_w g$). The pressure gradient term is only important at low values of water saturation and at the leading front of the melt water wave. Colbeck (1978a, p172) suggested that "nonhomogeneous snow structures such as ice layers appear to distort the features of meltwater waves more than tension gradients" and that the tension gradients could be ignored without significant errors. As a result, equation 6.1 reduces to

$$(6.2) \qquad U = (k_{us}/\nu) \, \rho_w \, g$$

In most porous media (Colbeck 1972) unsaturated permeability (k_{us}) is related to the saturated permeability (k_s) by

$$(6.3) \qquad k_{us} = k_s \, S*^n$$

and the effective water saturation (S*) is calculated as

$$S* = (S_w - S_{wi}) / (1 - S_{wi})$$

where S_w is the water content and S_{wi} the irreducible water content. The value of the parameter n in equation 6.3 has been determined empirically. Colbeck (1971) postulated that n=2, while Colbeck and Davidson (1972) found that n=3.2 from measurements of water drainage in columns of homogeneous snow. Denoth et al (1978) found that n depends on the stage of metamorphism. Snow in the early stages of metamorphism had a mean n of 1.8, while snow in advanced stages had a mean value of 3.2. However, Denoth et al (1979) concluded that despite this general trend, "no clear relationship exists between any snow parameter and n." A value of n=3 will be used in this study since most previous work (Colbeck and Davidson 1972, Ambach et al 1981) showed that it provides sufficiently accurate results for ripe snowpacks. Substituting equation 6.3 into 6.2 gives

(6.4) $U = a \, k_s \, S*^3$

where a is a constant given by

$$a = (p_w \cdot g) / v$$

Colbeck and Davidson (1972) combined equation 6.4 with the continuity equation and solved to obtain the following relationship

(6.5) $[dz/dt]_u = 3 \, a^{1/3} (k_s^{1/3}/p_s) \, U^{2/3}$

where p_e is the effective porosity. For a given snowpack, the rate of movement of flux U ([dz/dt]$_u$) increases as meltwater flux increases. As a result, slow moving fluxes in the morning are overtaken by faster moving afternoon fluxes and a flow discontinuity or shock front develops (Colbeck 1978). This shock, which is bounded by small fluxes on one side and large fluxes on the other, propagates downwards at a rate (dSF/dt) given by (Colbeck 1978)

$$(6.6) \quad dSF/dt = a^{1/3}(k_s^{1/3}/p_e) \ (U^{+2/3} + U^{+1/3} \ U^{-1/3} + U^{-2/3})$$

where U+ is the larger flux overtaking the shock front and U- is the smaller flux overtaken by the shock front.

The diurnal melt wave may be routed through a snowpack using equations 6.5 and 6.6, using only the surface melt, snow permeability, and snow porosity. This technique describes the general shape of the flux wave at depth, but it underpredicts the arrival of the melt wave and overpredicts its peak value (Colbeck 1978a). These problems are generally attributed to the effects of ice layers and flow channels (Colbeck 1979) which redistribute the flow within the pack, concentrating it in certain areas and diminishing it in others. Since larger fluxes travel more quickly than smaller fluxes (equation 6.5) the effect of ice layers and flow channels is to disperse the rising limb of the flux wave

predicted by equations 6.5 and 6.6.

6.2 Flow variability in a natural snowpack

Previous work concerning the variability of flow within wet snowpacks relied extensively on the use of dye tracing experiments to follow the path of water movement (Gerdel 1954, U.S. Army 1956). Unfortunately, these experiments provided little quantitative information about the variability of flow within a snowpack. Daily monitoring of the multi-compartment lysimeter allowed both a direct measure of the range of flow conditions within the pack, and the effect of melt metamorphism on flow variability.

The multi-compartment lysimeter showed large variations in flow over its 0.25 m² area. On June 15, 1981 for example, the mean flow for all compartments was 9.8 mm/day, but the flow in individual compartments ranged from 0 to 24.6 mm/day (Figure 6.1a). From June 15 to 23 mean flow tended to increase, the range of flows also increased and the frequency distribution changed from negatively skewed to nearly symmetrical.

Expressing the daily total flow captured by each compartment as a percentage of the mean daily lysimeter flow, the effect of flow magnitude is removed and days with
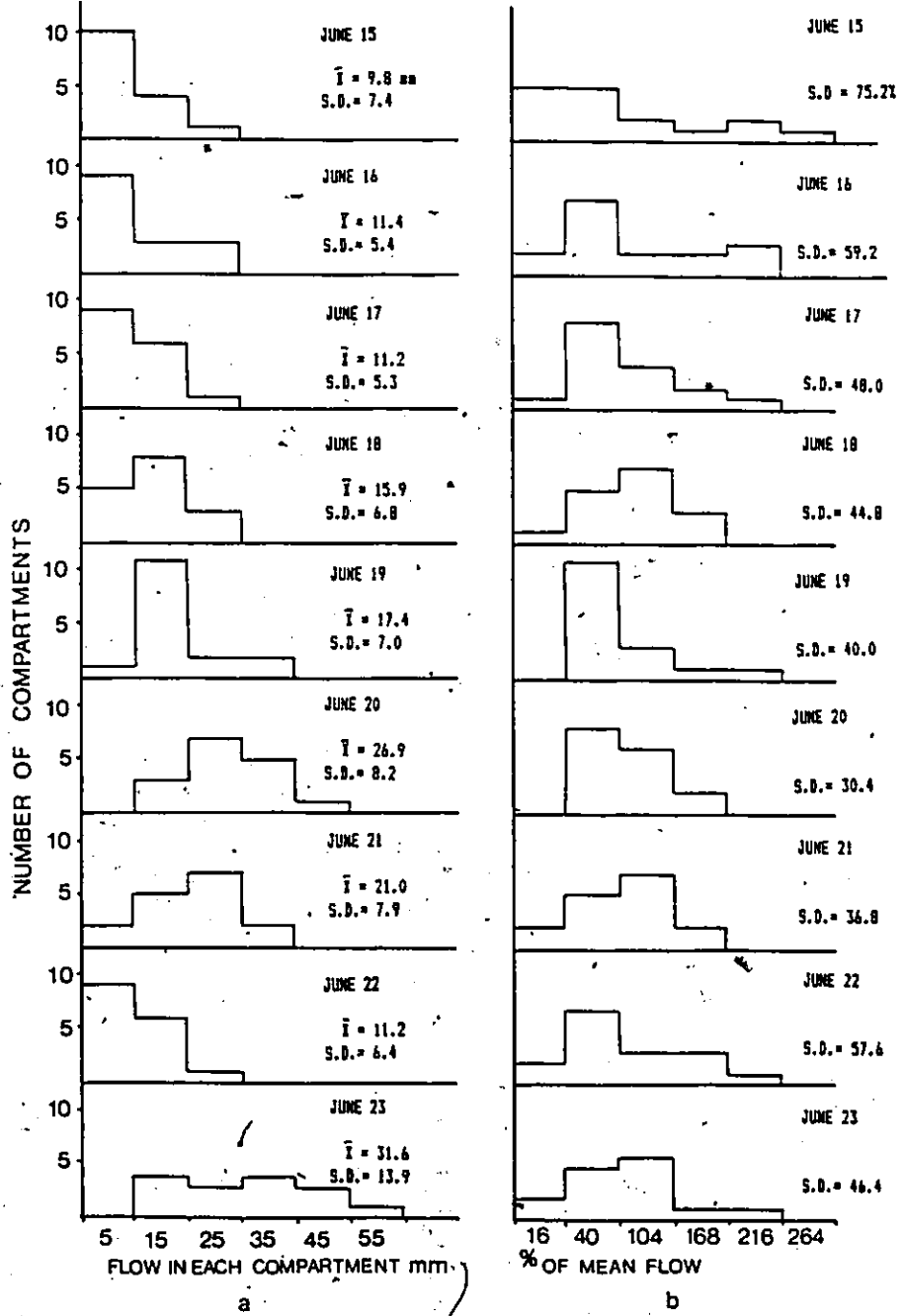
FIGURE 6.1 Total daily flow caught by each of 16 compartments in the multi-compartment lysimeter, expressed as actual flow (mm) and as a percentage of the mean flow.

different melt volumes may be directly compared. The flow in individual compartments ranged from 16 to 240 % of the mean flow (Figure 6.1b). Over the nine day study period the distribution of flows changed significantly. In the early period, the distributions are negatively skewed. Later, the distributions become more symmetrical, and the flow becomes more uniform with the standard deviation decreasing from 75.2% to a low of 30.4%.

Previous studies (Wakahama 1968) suggested that grain coarsening within the flow fingers at the initial wetting front produces vertical flow channels which are more permeable than the surrounding snow and can therefore carry larger volumes of water. The implication was that these features survive much of the melt period. However, as shown in the previous chapter, flow fingers in cold snowpacks are quickly overtaken by the general wetting front. For the small grain sizes common at the beginning of melt and the rate of grain growth (see Figure 6.9), differences in grain size between the fingers and non-finger areas disappeared within two or three days after the passage of the general wetting front. It seems unlikely therefore, that distinct flow channels with larger snow grains are responsible for the observed variations in flow.

Ice layers may also redistribute flow within the snowpack. Although all ice layers at strata boundaries are

continuous, their properties are highly variable. In the daily snow pit studies, properties of each ice layer observed across the 0.5 m snowpit width were described in the following general terms:

(1) solid ice — measured densities ranged from 630 to 950 kg/m³, and they appeared to have low permeability,

or

(2) granular ice → composed of loosely frozen snow grains of 0.2 to 3.0 mm in diameter. They were more permeable than the solid ice layers. In terms of ice layer morphology, all ice layers were classified as:

(1) variable ice — properties such as thickness and ice type varied over the 0.5 m width of the snowpit, or

(2) intermittent ice — small gaps existed in the ice layer over the 0.5 m width of the snowpit, or

(3) uniform ice.

At a typical snowpit (CC6), approximately 50% of all the observed layers were formed of granular ice and 50% of solid ice, and 55% were either variable and/or intermittent and only 45% uniform over the snowpit width. Note that when considered over their entire lateral extent, all ice layers were variable and intermittent. The properties of these layers are continuously varying. They do not have uniform sections separated by distinct drains, nor are there distinct breaks between sections of different properties. Instead

there are gradual transitions from low to high permeability and vice versa.

Depending on ice layer permeability, a portion of the water reaching it may pass directly through, while the rest will pond above the ice layer and flow horizontally until it reaches a more permeable section. As a result, the flux below a relatively impermeable section will be lower than that above it, while below permeable sections, or gaps, the flux increases. Since ice layer properties are continuously variable, the flux below it will also exhibit a wide range of values.

The frequent occurrence of permeable sections and gaps ensures that the water must travel a relatively short horizontal distance before it finds a vertical passage through the ice layer. As a result, the portion of the lag time between melt at the surface and that water reaching, the snow base which is due to vertical movement through the snow will far exceed the lag due to horizontal flow along the ice layer (Colbeck 1973).

As the snowpack undergoes melt metamorphism it becomes more homogeneous (ie. grain growth eliminates differences in grain size and the number of ice layers decreases (Figure 6.2)). As a result, it would be expected that the flow becomes more uniform through time. Over the period June 15 to 20 the standard deviation of the daily compartment flow,

using flow expressed as a percentage of the mean daily lysimeter flow (Figure 6.1b), decreased from 75.2% to 30.4% (Figure 6.2), but it increased on June 21, 22, and 23. This increase cannot be explained by physical changes in the snowpack structure. Over the June 15 to 20 period when the flow variability decreased steadily, daily melt rate increased from 8 to 27 mm/day (Figure 6.2). On June 21 and 22 the melt rate decreased and the flow became more variabile (Figure 6.2). It, seems therefore, that most of the day to day variations in flow may be explained by changes in the flow rate. The only exception was the observation for June 24.

6.3 Modelling water flux in layered snow

Colbeck's model for water movement through homogeneous snowpacks was modified to include the effects of ice layers. The complex nature of each ice layer makes the modelling of the interaction of flow with each ice layer impractical. Instead, a simplification was introduced by considering the snowpack to consist of a number of independent flow paths, each carrying a different portion of the total flow. Each path consists of uniform homogeneous snow and the water is routed directly from the snow surface to its base with no
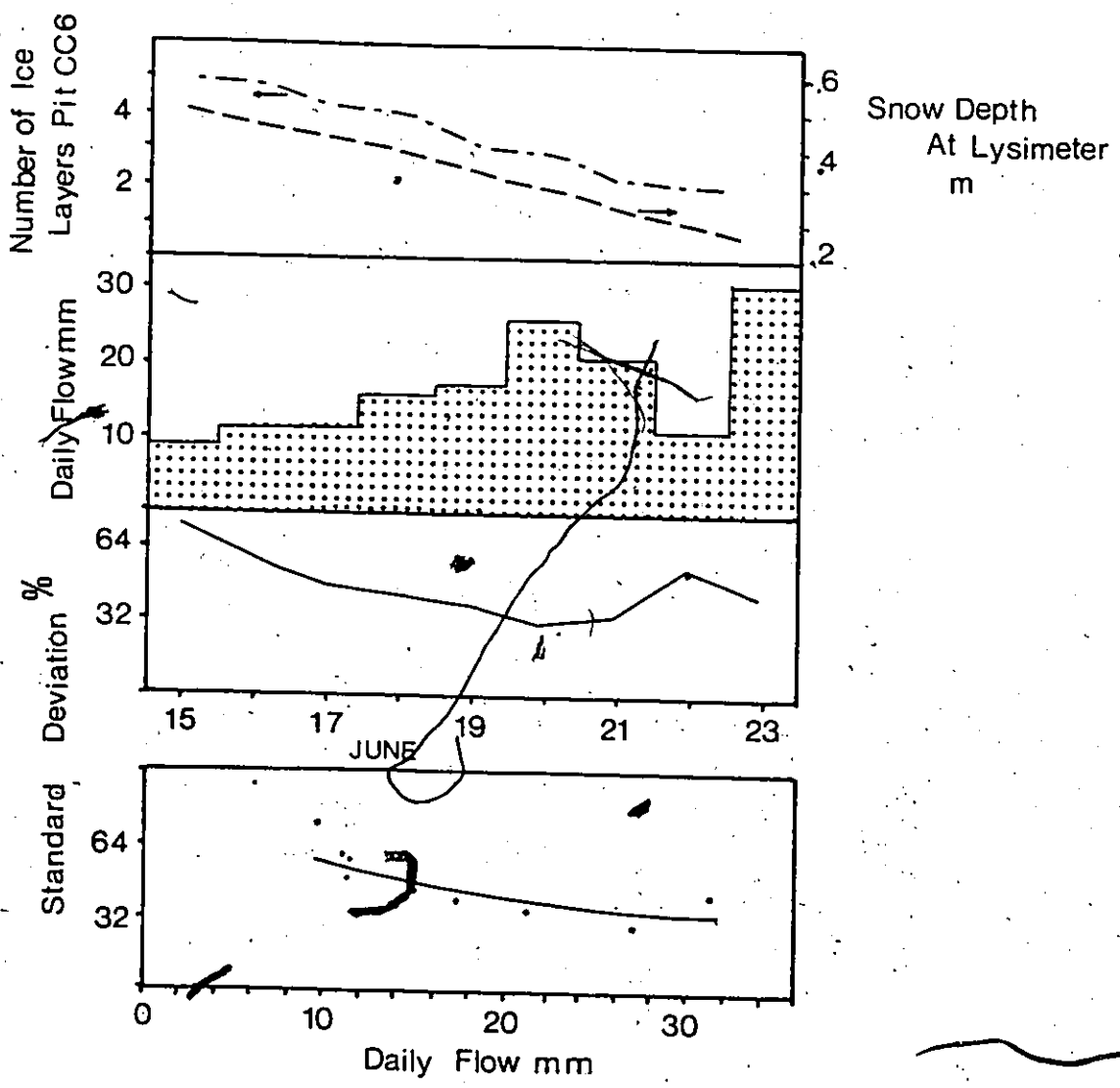
FIGURE 6.2 Daily changes in snowdepth, number of ice layers, total daily flow, standard deviation of the individual compartment flows expressed as a percentage of mean lysimeter flow, and the relationship between standard deviation of flow and daily melt.

direct interactions with the ice layers. The melt wave from each path may then be summed to determine the mean flux at the snowpack base. The following observations from the multi-compartment lysimeter suggest that these simplifications are realistic because:

(1) flow variability is insensitive to the number of ice layers or to snow depth, and therefore the flow distribution is similar at all levels within the snowpack

(2) the effect of each ice layer is to redistribute rather than to alter the flow. For example, each ice layer will redistribute the flow so that zones of high flow above it will not necessarily lie immediately above zones of high flow beneath. However, the distribution of flow conditions will be the same, and

(3) the lag time due to horizontal flow along the ice layer is minimal compared to the lag due to vertical drainage through unsaturated snow (Colbeck 1973).

The term multiple flow path model was first used by Colbeck (1979). The model presented in this paper (Figure 6.3) is similar in that it routes water down a number of independent flow paths, but it is considerably different in its conceptualization of the flow paths, particularly the distribution of flow among the different paths. The model employs the computer solution of equations 6.5 and 6.6 developed by Tucker and Colbeck (1977) to route melt water.
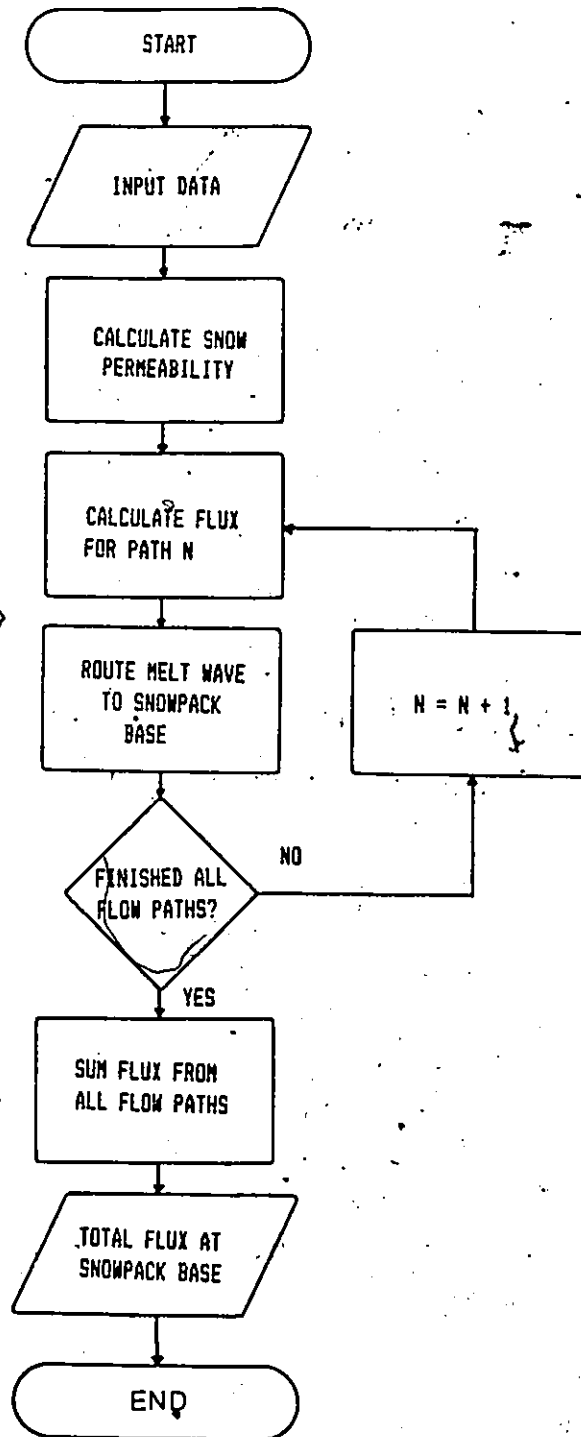
FIGURE 6.3 Simplified flow chart of the multiple flow path model

through a number of independent flow paths. Each flow path was assumed to have the same snow properties.

Using measured dry snow density(p_s) and grain size(g_s) the snow permeability(k_s) was determined from Shimizu (1970)

$$(6.7) \quad k_s = .077 \, g_s^2 \, \exp(-7.8 \, p_s/p_w)$$

where p_w is the density of water. The hourly values of snow melt (U) determined from the surface energy balance were adjusted to give the volume flux in each flow path (U_{FP}) by

$$(6.8) \quad U_{FP} = U \, (vol \, / \, siz)$$

and $\quad siz = 1/n_F$

where the flow path size (siz) is expressed as the fraction of unit area, and each flow path is the same size. Each path carries a different fraction of the total flow (vol), and n_F is the number of flow paths. Increasing the number of flow paths increases the accuracy of the model, but also increases the computational time. In this study all computations use ten flow paths. The flux values at the base of each flow path, for each hour j, were then summed to obtain the average flux for all flow paths (U_T)

$$(6.9) \qquad U_{T,j} = [\sum_{i=1}^{n} (U_{i,} \, siz)_i]_j$$

where n is the number of flow paths.

6.4 Model results

The multiple flow path model was tested for the period June 18 to 24, 1981. During this period there were continuous measurements of flow from the recording lysimeters and continuous prediction of surface melt from the energy balance. The total daily flow measured by both recording lysimeters was consistently 10 to 20% smaller than that estimated from the surface energy balance. It is not known if this problem was due to over-estimating surface melt, or an undercatch by the lysimeters due to either hydraulic factors or flow variability on a scale larger than the size of the lysimeters. But, the daily flow from each of the three lysimeters was always within +/- 10% of each other. This suggests that most of the error was due to overestimation of surface melt by the energy balance. Because the flow model is sensitive to the surface inputs, melt was adjusted so that daily melt equalled daily lysimeter flow. The other data required are snow depth, density, and grain size: values measured at pit CC6 were used. The

percentage of flow along each of the ten flow paths, was estimated from cumulative curves of percent of flow versus percent of area (Figure 6.4).

If the flow is assumed to be uniform (ie. along one flow path 100% of the area), the rising limb of the hydrograph occurs too late and is too steep (Figure 6.5). The multiple flow path model improves the prediction of the rising limb, because the flow paths carrying a high fraction of the total water reach the snow base before those carrying smaller fluxes. On June 20 for example, the path carrying the largest fraction of the total flow reaches the snow base approximately three hours before the path carrying the smallest flux (Figure 6.5). The overall effect is to diffuse the rising limb of the hydrograph, so its rise occurs earlier and is not as rapid. This effect is illustrated for three days chosen to represent a wide range of depth and melt conditions (Figure 6.6). In all cases, the predicted time of the hydrograph rise is accurate to within one hour without any systematic error in flow magnitude. In addition, the rate of rise to the peak, the peak flux, and the recession of the hydrograph are in agreement with measured results.

The independence of flow variability, and snow depth or the number of ice layers suggests that the multiple flow path model and the flow variability measured at Resolute may be extended to other environments. The model was tested
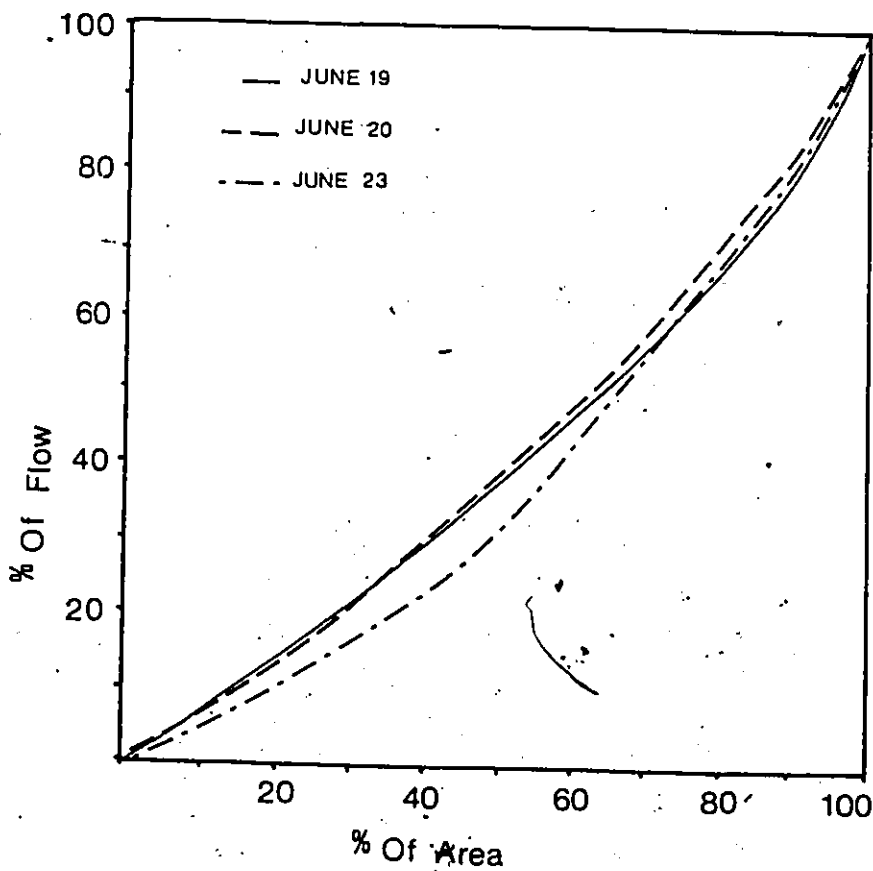
FIGURE 6.4 Cumulative percent of total lysimeter flow versus percent of lysimeter area, when compartments are added in a sequence of increasing flow per compartment.

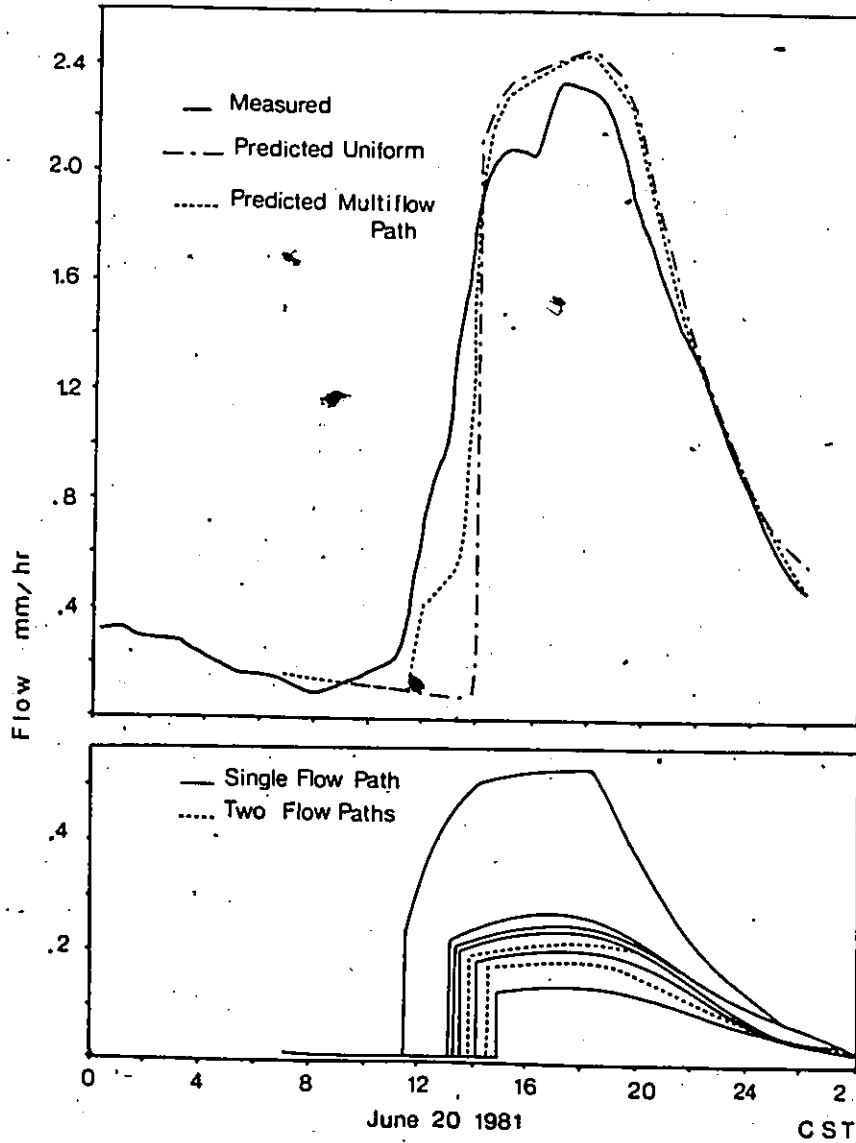FIGURE 6.5 Top – comparison of multiple flow path model, uniform flow model, and measured flow.
Bottom – Flow for the individual flow paths in the multiple flow path model. All of these are summed to get the total flow.
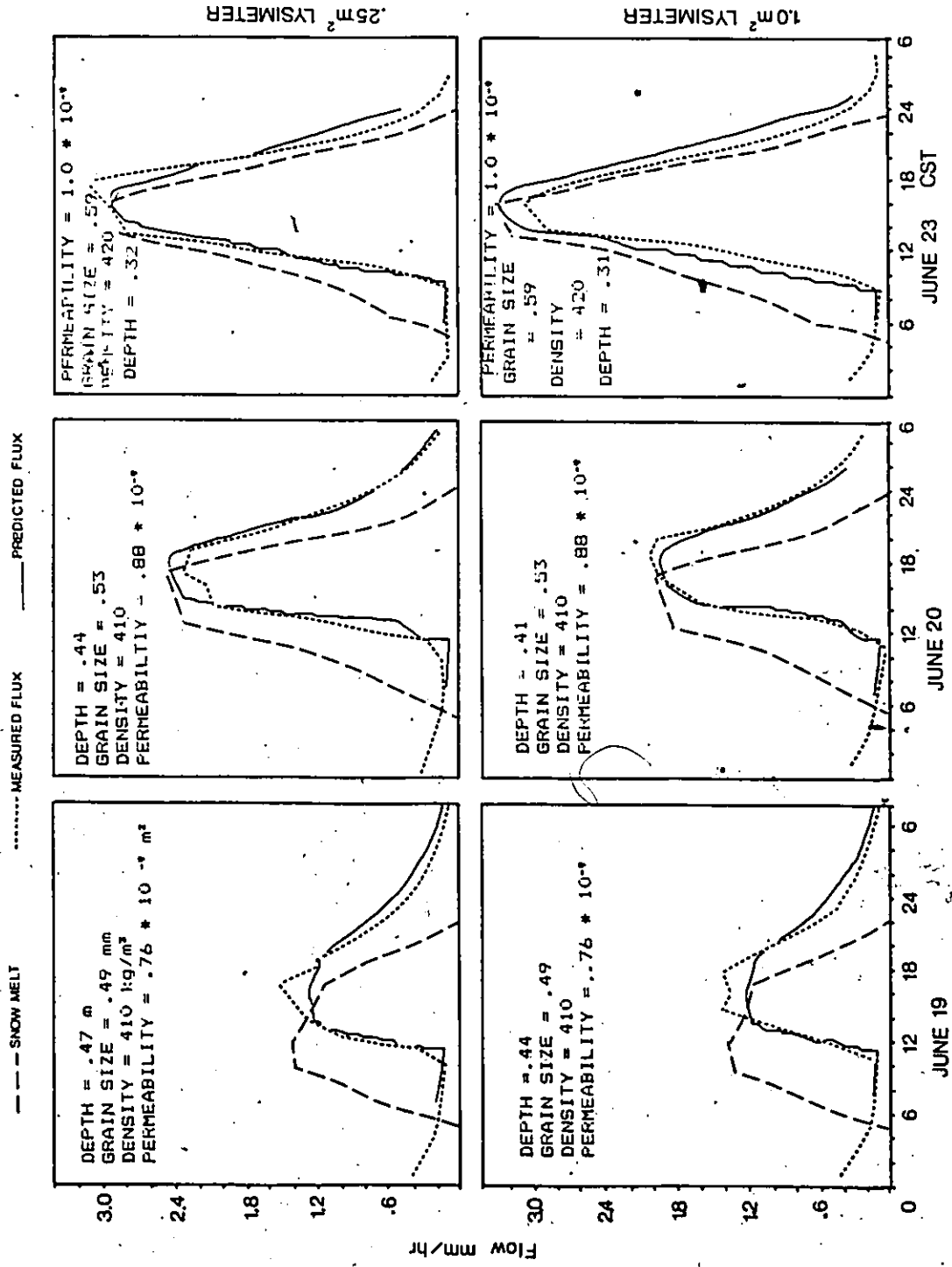
FIGURE 6.6 Comparison of the measured flux from both the 0.25 and 1.0 m² lysimeters and flow predicted by the multiple flow path model. The hourly surface melt from the energy balance is also shown.

using the melt and lysimeter data from the Central Sierra Snow Laboratory in California (Colbeck 1977), and the flow parameters obtained on the highest melt day at Resolute. The multiple flow path model predicts the flux significantly better than if uniform conditions are assumed (Figure 6.7). The predicted time of arrival of the melt wave is approximately one hour later than measured, but the rate of rise of the melt wave, peak flow, and the recession limb are predicted accurately. These results indicate that the multiple flow path model, using measured flow variability at Resolute, may be applied to different environments without requiring too much additional data.

The sensitivity of the multiple flow path model to changes in: (1) flow variability, (2) grain size, (3) density, and (4) snow depth were tested by varying each parameter while holding all others constant.

The importance of the day to day changes in flow variability were tested using both the most and least variable flow over the period June 15 to 23. Both cases provide significantly better predictions than the uniform flow model (Figure 6.8a). The melt wave reaches the base later, rises more steeply and peaks higher as the flow becomes progressivily more uniform. Since days with lower melt have more variable flow (Figure 6.2) they have a more diffused rising limb than days with higher melt.

Snow Depth 1.57 m
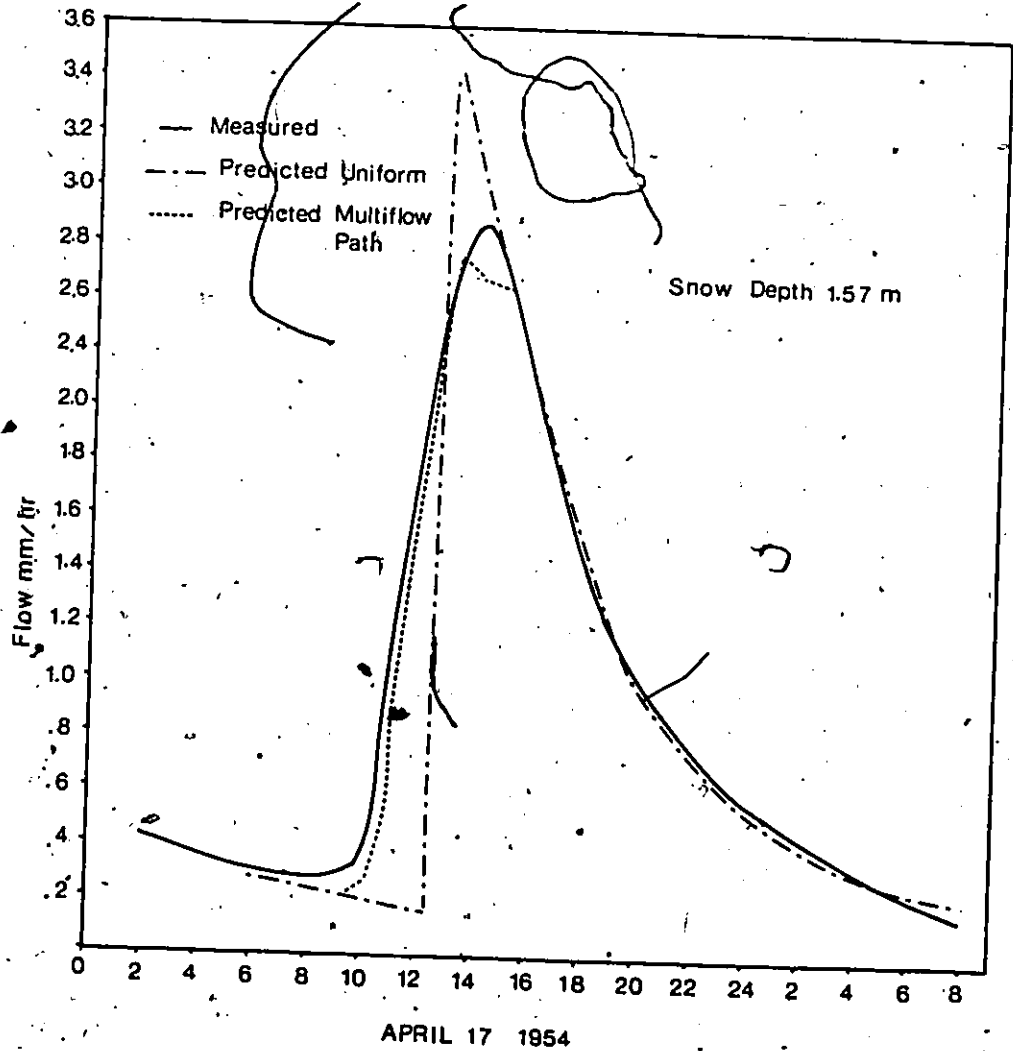
Flow mm/hr

APRIL 17 1954

FIGURE 6.7 Comparison of measured flow and predicted using the uniform flow model and the multiple flow path model. Melt and lysimeter flow data for the Central Sierra Snow Laboratory, California, April 17, 1954 from Colbeck (1977).
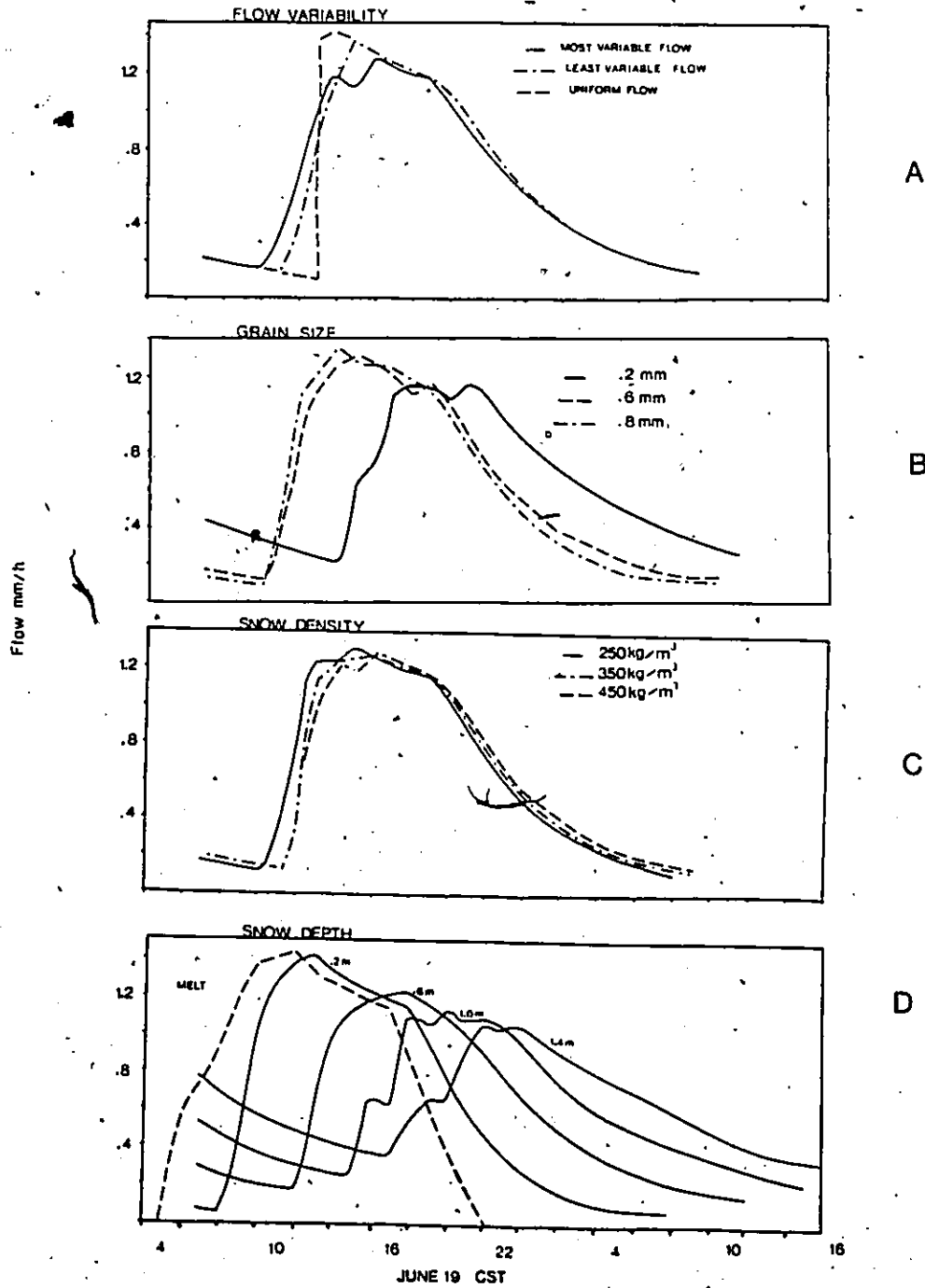
FIGURE 6.8 Sensitivity of the multiple flow path model to changes in flow variability, grain size, snow density, and snow depth.

Increasing the grain size from 0.2 to 1.0 mm, a range commonly found in melting snowpacks, increases the snow permeability from $0.13 * 10^{-9}$ to $2.0 * 10^{-9}$ m². This increase in permeability has a significant effect on flow within the pack. It decreases the low flows, increases the high flows, decreases the lag time to the hydrograph rise, steepens the rising limb, and increases the peak flow (Figure 6.8b). Since grain growth continues throughout the melt period, it is necessary to estimate grain size in order to accurately predict water flux in the snowpack. This requires a knowledge of the rate of grain growth and the time when the grains become wet. Colbeck(1975) estimated the rate of grain growth once the grains were wet by fitting the following curve to grain growth measured in the laboratory by Wakahama (1968)

(6.10) $\quad g_s = (g_s)_0 + b\ t^{1/2}$

where g_s is grain diameter, $(g_s)_0$ the initial grain diameter, t time in days, and b is dependent on the degree of saturation. Colbeck (1975) estimated $b=0.1$ would apply to the narrow range of water contents found in freely draining snowpacks, though it was never tested on grain growth under natural conditions. By using the predicted general wetting front at pit CC6 to determine when grains begin to grow,

equation 6.10 provides a reasonable estimate of grain size over the period June 8 to 25 for all strata within the snowpack (Figure 6.9). Grains within individual layers increased from about 0.20 mm to 0.57 mm after twelve days of growth. However, equation 6.10 over-predicts growth early in the grain growth period and under-predicts later on (Figure 6.9). One possible explanation is that radiation increases the growth of snow grains near the snow surface. This appears unlikely however, since the period of rapid growth (i.e. five to six days) after the beginning of growth) occurred when layer Six was only 0.1 m below the snow surface, but when layer Two was still 0.5 m below the surface. This analysis shows that the mean pack grain size increases from 0.2 mm to nearly 0.6 mm over a 16 day period. As indicated by Figure 6.8(b) this makes a significant difference, with the meltwave arriving at the snowpack base approximately two hours earlier, the peak flow is higher, and the low flow lower.

Snow density also affects water movement through the snowpack. Increasing the density from 250 to 450 kg/m^3 decreases the permeability from $2.6 * 10^{-9}$ to $0.6 * 10^{-9}$ m^2, and decreases the porosity from 0.73 to 0.51. As a result of these two offsetting factors, the water flux at depth is not
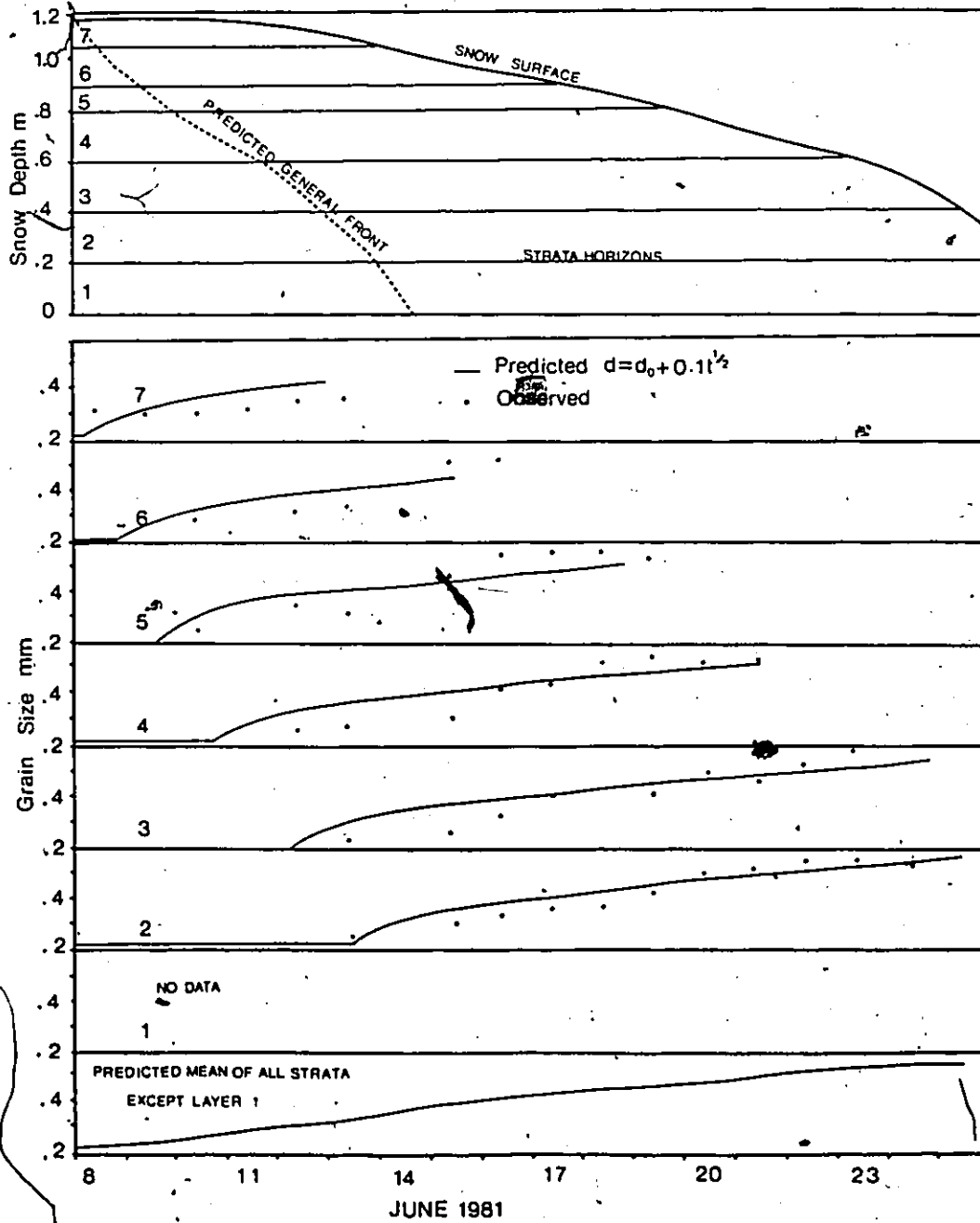
FIGURE 6.9 Measured versus predicted grain growth at pit
CC6 for each stratum. Predicted grain growth for
each stratum was started when the predicted general
wetting front reached the mid point of each strata.

very sensitive to changes in density (Figure 6.8c). For example, increasing the density from 250 to 450 kg/m^3 delays the arrival of the shock front by only one hour, and has a minor effect on the peak and low flows.

Snow depth is an important parameter controlling the melt water flux at the snowpack base. Of the parameters discussed in this section it has the greatest effect on flow. With increasing snow depth, the arrival of the melt wave is delayed, the rising limb flattens, the peak flow is lowered, and the minimum flow is increased (Figure 6.7d). Increasing the snow depth from only 0.2 to 0.6 m delays the peak flow by five hours and lowers the magnitude from 1.42 to 1.22 mm/hour.

Each of the four snowpack properties required to run the multiple flow path model change continuously throughout the melt season. The previous discussion however, illustrates that over the range of conditions which commonly occur, both flow variability and snow density are relatively unimportant. If insufficient information is available, single mean values may be used for the entire melt period without significant loss in accuracy. The other two snowpack properties, grain size and snow depth, are more important and their changes over the melt period must be included. Considering the large spatial and temporal variation in snow depth, changes in this parameter are extremly important when

considering the effects of vertical unsaturated percolation through the snowpack on meltwater runoff.

CHAPTER SEVEN

CONCLUSIONS

This study emphasizes the processes controlling the ripening of cold snowpacks underlain by a frozen substrate, and the implications of these ripening processes on the movement of water through wet, isothermal snowpacks.

The growth of ice layers plays an important role in snowpack ripening, controlling both the rate of advance of water into the dry snowcover, and the warming of the snow and ground during the ripening period. During ripening, 25 to 45% of all meltwater freezes within the snowpack, while the remainder is stored as liquid water. Of the water which refreezes, 85 to 90% of it freezes at premelt stratigraphic horizons to form continuous ice layers. Water is conducted below the general wetting front by vertical flow fingers. Ice layers only grow within the zone bounded by the deepest penetration of the finger wetting front and the general wetting front. Below the fingers, liquid water is not available, and above the general front the snow is isothermal and therefore no freezing can occur. The rate of ice layer growth is controlled by the rate of heat conduction into the cold snow both above and below the ice. The period of ice growth is controlled by the time difference between the

arrival of the finger front and the general wetting front at a given horizon. The growth rate varies from 3.3 to 3.6 mm water equivalent per day and they only grow for 24 to 36 hours. In this short period ice layers may reach up to 20 mm in thickness. While actively growing, ice layers remove water from the finger front, and in the cold Arctic snowpacks their rate of growth can retard the rate of finger front advance. As a result, the fingers may only advance 0.1 to 0.15 m ahead of the general wetting front. In warmer snowpacks, however, the ice layers grow more slowly and the finger front could quickly reach the snowpack base, and runoff may begin before the entire pack is isothermal.

The formation of ice layers releases latent heat which warms the surrounding areas, thus providing the primary mechanism by which energy is transferred from the snow surface into the underlying snow and soil. Since this heat is conducted ahead of the wetting front, ice layers grow in relatively warm snow (0 to −6 C), and much of the latent heat thus released (20 to 90%) is used to warm the soil. In order to raise the snowpack to an isothermal state, therefore, more energy is required than is necessary to satisfy the initial cold content of the snowpack. Even after the snowpack is isothermal, considerable refreezing of meltwater may occur at the snowpack base because there is a large ground heat flux into the frozen soil. This basal ice

growth may consume anywhere from 100% of the daily melt during its initial growth, to a low of 10% after seven to ten days of growth. As a result, daily runoff is always less than the daily melt, and the melt period is extended.

Modelling of the snowpack ripening shows an interdependence of the wetting front advance, ice layer growth, and the thermal conditions of cold snowpacks. Thus, the rate of ripening and the daily runoff volume can be predicted only if all the processes are considered. A simple cold content approach as developed for warm snowpacks is not applicable for cold snowpacks underlain by a frozen substrate.

Continuous ice layers also control water movement through the ripe snowpack. The properties of these ice layers are highly variable over short horizontal distances. For example, the permeability may vary from low to high within a horizontal distance of less than 0.5 m, leading to a concentration of flow below permeable areas. Instead of distinct flow channels carrying large fluxes separated by zones carrying smaller fluxes, there is a continuum of flow conditions. Since larger fluxes travel more quickly than smaller ones, a combination of various fluxes disperses the rising limb of the hydrograph. Measurements of water movement within the pack suggest that variations in flow are caused by ice layers, rather than by flow instabilities at

boundaries or by vertical flow channels along zones with coarser snow grains. Comparison of the measured flow and the predicted meltwave at depth using a multiple flow path model showed that the redistribution of flow by the ice layers, adequately explained the dispersion of the rising limb of the melt wave. This model was successfully applied to water flux data from California, suggesting that it may be applied to different environments using the measured flow variability from Resolute. This study therefore provides a simple model which, by taking into account the variability in flow due to ice layers, significantly improves the prediction of melt water flux at the snowpack base.

REFERENCES

Ahlmann,H.W. and Tveten,A.,1923. The recrystallization of snow into firn and the glaciation of the latter. *Geog. Ann.*, 5, 52-58.

Ahlmann,H.W.,1935. The stratification of the snow and firn on Isachsens's Plateau. *Geog. Ann.*, 17, 29-42.

Alexeev,G.A., Kaljuzhny,I.L., Kulik,V.Ya., Pavlova,K.K. and Romanov,V.V., 1972. Infiltration of snow melt water into frozen soil. *The Role of Snow and Ice in Hydrology*, I.A.S.H., 313-325.

Ambach,W., Blumthaler,M., and Kirchlechner,P.,1981. Application of the gravity flow theory to the percolation of meltwater through firn. *Jour. Glaciol.*, 27, 67-75.

Anderson,E.A.,1976. A point energy and mass balance model of a snowcover. *N.O.A.A.*, Tech. Report NWS 19, 150p.

Anderson,E.A.,1978. Streamflow simulation models for use on snow covered watersheds. *Proc. Modeling of Snow Cover Runoff*, ed. Colbeck,S.C. and Ray,M., C.R.R.E.L., 336-350.

Bagnold ,1941. *The Physics of Blown Sand and Desert Dunes*. Methuen, London, 265p.

Baird,P.D.,1952. Method of nourishment of the Barnes Ice Cap. *Jour. Glaciol.*, 2, 2-23.

Bengtsson,L.,1982. Percolation of meltwater through a snowpack. *Cold Regions Sci. and Technol.*, 6, 73-81.

Benson,C.S.,1962. Stratigraphic studies in the snow and firn of the Greenland Ice sheet. *S.I.P.R.E.*, Res. Report 70, 93p.

Benson,C.S.,1971. Stratigraphic studies in the snow at Byrd station, Antarctica, compared with similar studies in Greenland. in Crary,A.D. (ed), *Antarctic snow and ice studies II*, 333-353.

Benson,C., Holmgren,B., Trabant,D.,and Weller,G.,1974. Physical characteristics of seasonal snow cover in northern Alaska. *Proc. 42nd Western Snow Conf.*,58-63.

Berg,N.H.,1982. Layer and crust development in a central Sierra Nevada snowpack: some preliminary observations. *Proc. 50th Western Snow Conf.*

Bilello,M.A.,1969. Relationship between climate and regional variations in snow-cover density in North America. *C.R.R.E.L.*, Res. Report 267, 20p.

Bird,J.B.,1967. *The Physiography of Arctic Canada.* The Johns Hopkins Press, Baltimore, Md., 366p.

Cameron,R.L.,1971. Glaciological studies at Byrd station, Antarctica, 1963-1965. in Crary,A.D. (ed), *Antarctic snow and ice studies II*, 317-332.

Clarke,R.T.,1973. A review of some mathematical models used in hydrology, with observations on their calibration and use. *Jour. Hydrol.*, 19, 1-20.

Cogley,J.G.,1975. *Properties of Surface Runoff in the High Arctic.*, Ph.D. Thesis, McMaster University, Hamilton, Ont., 358p.

Colbeck,S.C.,1972. A theory of water percolation in snow. *Jour. Glaciol.*, 11, 369-385.

Colbeck,S.C.,1973. Effects of stratigraphic layers on water flow through snow. *C.R.R.E.L.*, Res. Report 311, 15p.

Colbeck,S.C.,1974. Grain and bond growth in wet snow, *I.A.S.H.*, Pub. 114, 51-61.

Colbeck,S.C.,1975. Analysis of hydrologic response to rain-on-snow. *C.R.R.E.L.*, Res. Report 340, 13p.

Colbeck,S.C.,1976. An analysis of water flow in dry snow. *Water Resources Research*, 12, 523-527.

Colbeck,S.C.,1977. Short-term forecasting of water runoff from snow and ice. *Jour. Glaciol.*, 19, 571-588.

Colbeck,S.C.,1978a. The physical aspects of water flow through snow. *Advances in Hydrosciences*, 11, 165-206.

Colbeck,S.C.,1978b. The difficulties of measuring the water saturation and porosity of snow. *Jour. Glaciol.*, 20, 189-201.

Colbeck,S.C.,1979. Water flow through heterogeneous snow. *Cold Regions Sci. and Technol.*, 1, 37-45.

Colbeck,S.C.,1982. An overview of seasonal snow metamorphism. *Reviews of Geophysics and Space Physics*, 20, 45-61.

Colbeck,S.C. and Davidson,G.,1972. Water percolation through homogeneous snow. *The Role of Snow and Ice in Hydrology*, I.A.S.H., 242-257.

Colbeck,S.C., Shaw,K.A. and Lemieux,G.,1978. The compression of wet snow., *C.R.R.E.L.*, Report 78-10, 17p.

Cook,F.A.,1958. Temperatures in permafrost at Resolute,N.W.T. *Geog. Bull.*, 12, 5-18.

Cruickshank,J.G.,1971. Soils and terrain units around Resolute, Cornwallis Is.. *Arctic*, 24, 195-209.

Denoth,A.,1980. The pendular-funicular liquid transition in snow. *Jour. Glaciol.*, 25, 93-97.

Denoth,A., Seidenbusch,W., Blumthaler,M., and Kirchlechner,P., 1978. Some experimental data on water percolation through homogeneous snow. *Proc. Modeling of Snow Cover Runoff*, ed. Colbeck,S.C. and Ray, M., C.R.R.E.L., 253-256.

Denoth,A., Seidenbusch,W., Blumthaler,M., Kirchlechner,P., Ambach,W., and Colbeck,S.C., 1979. Study of water drainage form columns of snow. *C.R.R.E.L.*, Report 79-1.

de Quervain,M.R.,1972. Snow structure, heat, and mass flux through snow. *The Role of Snow and Ice in Hydrology*, I.A.S.H., 203-226.

Dingman,S.L.,1975. .Hydrologic effects of frozen ground literature review and synthesis. *C.R.R.E.L.*, Special Report 218, 55p.

Dunne,T. and Black,R.D.,1971. Runoff processes during snow melt. *Water Resources Research*, 7, 1160-1172.

Dunne,T.,Price,A.G. and Colbeck,S.C.,1976. The generation of runoff from subarctic snowpacks. *Water Resouces Research*, 12,677-685.

Ebaugh,W.P. and DeWalle,D.R.,1977. Retention and transmission of liquid water in fresh snow.. *Proc. 2nd Conf. on Hydrometeorology*, 255-260.

Farouki,O.T.,1981. The thermal properties of soils in cold regions. *Cold Regions Sci. and Technol.*, 5, 67-75.

Fertuck,L.J., Spyker,J.W. and Husband,W.H.W.,1971. Numerical estimation of ice growth as a function of air temperature, wind speed and snowcover. *Can. Soc. Mech. Eng. Trans., The Engineering Jour.*, 14, I-VI.

Findlay,B.F.,1969. Precipitation in northern Quebec and Labrador: An evaluation of measurement techniques. *Arctic*, 22, 140-150.

Gerdel,R.W.,1945. The dynamics of liquid water in deep snow-packs. *Trans. American Geophysical Union*, 26, 83-90

Gerdel,R.W.,1948. Physical changes in snow-cover leading to runoff, especially floods. *I.A.S.H.*, Pub. 2, 42-51.

Gerdel,R.W.,1954. The transmission of water through snow. *Trans. American Geophysical Union*, 35, 475-485.

Glen,A.R.,1941. A sub-arctic glacier cap: the west ice of North East Land. *Geog. Jour.*, 98, 65-76.

Glennie,K.W.,1970. *Desert Sedimentary Environments.* Elsevier, Amsterdam, 232p.

Goodison,B.E., Ferguson,H.L., and McKay,G.A., 1981. Measurement and data analysis. in Gray, D.M. and Male, D.H. (ed), *Handbook of Snow Principles; Processes, Management and Use.*, Pergamon Press, Toronto, Ont., 766p.

Gold,L.W. and Williams,G.P.,1957. Some results of the snow survey of Canada. *National Research Council of Canada, Div. Building Research*, Res. Paper no. 38, NRC 4389, 15p.

Greenkorn,R.A. and Kessler,D.P.,1969. Dispersion in heterogeneous non-uniform anisotropic porous media. *Ind. Eng. Chem.*, 61, 14-32.

Guymon,G.L.,1978. A review of snow-soil interactions. *Proc. Modeling Snow Cover Runoff*, ed. Colbeck,S.C. and Ray,M., C.R.R.E.L., 297-303.

Hare,F.K. and Hay,J.E.,1971. Anomalies in the large-scale annual water balance over North America. *Can. Geographer*, 15, 79-94.

Hare,F.K., Lama,U.,and Lin-Sien,C.,1975. Annual heat and water balances over North America and their relation to evaporation theory. *Proc. Canadian Hydrol. Symp:75* ,Assoc. Comm. Hydrol., Nat. Res. Council of Canada, 490-510.

Heron,R. and Woo,M.K.,1978. Snow melt computations for a High Arctic site. *Proc. 35th Eastern Snow Conf.*, 162-172.

Hill,D.E. and Parlange,J.-Y.,1972. Wetting front instability in layered soils. *Soil Sci. Soc. America, Proc.*, 36, 697-702.

Hills,R.C.,1970. The determination of the infiltration capacity of field soils using the cylinder infiltrometer. *British Geomor. Res. Group*, Tech. Bull. 3, 25p.

Holmgren,B.,1971. Climate and energy exchange on a sub-polar ice cap in summer. Arctic Institute of North America Devon Island Expedition 1961 -1963. Part F. On the energy exchange of the snow surface at ice cap station. *Meddelanden fran Uppsala Universitets Meteorologiska Institution*, Nr 112.

Horton,R.E.,1915. The melting of snow. *Mon. Weather Rev.*, 43, 599-605.

Jackson,C.I.,1960. Snowfall measurements in northern Canada. *Quart. Jour. Royal Meteor. Soc.*, 86, 273-275.

Johansen,O.,1975.*Thermal Conductivity of Soils*, Ph.D. Thesis, Trondheim, Norway.

Jordan,R.P.,1978. *The Snowmelt Hydrology of a Small Alpine Watershed*. M.Sc. Thesis ,University of British Columbia, Vancouver, B.C., 200p.

Koerner,R.M.,1964. Firn stratigraphy studies on the Byrd-Whitmore Mountains traverse, 1962-1963. in Mellor,M. (ed), *Antarctic Research Series*, 219-235.

Koerner,R.M.,1970. Some observations on superimposition of ice on the Devon Island Ice Cap, N.W.T. Canada. *Geog. Ann.*, 52A, 57-67.

Koerner,R.M.,1971. A stratigraphic method of determining the snow accumulation rate at Plateau station, Antarctica, and application to South Pole - Queen Maud Land traverse 2, 1965-1966. in Crary,A.P. (ed), *Antarctic Snow and Ice Studies II*, 225-238.

Kojima,K.,1967. Densification of seasonal snow cover. *Physics of Snow and Ice*, International Conference on Low Temp. Sci., Sapporo, Japan, 929-951.

Kuroiwa,D.,1968. Liquid permeability of snow. *I.A.S.H.*, Pub. 79, 380-391.

LaChapelle,E.R.,1969. *Field Guide to Snow Crystals* . J.J. Douglas Ltd, Vancouver, B.C., 101p.

Linsley,R.K., Kohler,M.A. and Paulhus,J.L.H.,1949. *Applied Hydrology*. McGraw Hill, N.Y.,N.Y., 689p.

Longley,R.W.,1960. Snow depth and snow density at Resolute, N.W.T. *Jour. Glaciol.*, 3, 733-738.

Male,D.H. and Gray,D.M.,1981. Snow cover ablation and runoff. In Gray,D.M. and Male,D.H. (ed), *Handbook of Snow Principles, Processes, Management and Use*. Pergamon Press, 766p.

Marsh,P.,1978. *Water Balance of a Small High Arctic Basin*. M.Sc. Thesis, McMaster University, Hamilton, Ont., 108p.

Marsh,P. and Woo,M.K.,1979. Annual water balance of small High Arctic basins. Proc. *Canadian Hydrol. Symp:79*, Assoc. Comm. Hydrol., Nat. Res. Concil of Canada, 536-546.

Maxwell,J.B.,1980. *The Climate of the Canadian Arctic Islands and Adjacent Waters*, vol 1. Env. Canada, Atmospheric Env. Service, 532p.

McCuen,R.H.,1973. The role of sensitivity analysis in hydrologic modeling. *Jour. Hydrol.*, 18, 37-53.

Mellor,M.,1965. Blowing snow. *C.R.R.E.L.*, Monograph 3, A3c, 79p.

Miesner,A.D.,1955. Heat flow and depth of permafrost at Resolute Bay, Cornwallis Is., N.W.T., Canada. *Trans. Amer. Geophys. Union*, 36, 1055-1060.

National Atlas of Canada,1974. Dept. of Energy, Mines, and Resources. 254p.

Ozisik,M.N.,1980. *Heat Conduction*. Wiley, New York, 687p.

Parlange,J.-Y.,1974. Water movement in soils, *Geophysical Surveys*, 1, 357-387.

Penner,E.,1970. Thermal conductivity of frozen soils. *Can. Jour. Earth Sci.*, 7, 982-987.

Price,A.J. and Dunne,T.,1976. Energy balance computation of snowmelt in a subarctic area. *Water Resources Research*, 12, 686-694.

Raymond,C.F. and Tusima,K.,1979. Grain coarsening of water − saturated snow. *Jour. Glaciol.*, 22, 83-105.

Rundle,A.S.,1971. Snow accumulation and firn stratigraphy on the East Antarctic Plateau. in Crary,A.P. (ed), *Antarctic Snow and Ice Studies II*, 239-255.

Schytt,V.,1949. Re-freezing of the meltwater on the surface of glacier ice. *Geog. Ann.*, 31, 222-227.

Seligman,G.,1936. *Snow Structure and Ski Fields*. International Glaciological Society, Cambridge, 555p.

Seligman,G.,1941. The structure of a temperate glacier. *Geog. Jour.*, 97, 295-315.

Sellers,W.D.,1965. *Physical Climatology*. The University of Chicago Press, Chicago,'Il., 272p.

Sharp,R.P.,1951. Features of the firn on upper Seward Glacier, St. Elias Mountains, Canada. *Jour. Geol.*, 59, 599-621.

Shimizu,H.,1970. Air permeability of deposited snow. *Contributions from the Institute of Low Temperature Science*, Series A No. 22, 32p.

Shumskii,P.A.,1964. *Principles of Structural Glaciology*. Dover Publ., N.Y., N.Y., 497p.

Sommerfeld,R.A. and LaChapelle,E.,1970. The classification of snow metamorphism. *Jour. Glaciol.*, 9, 3-17.

Sverdrup,H.U.,1935a. The temperature of the firn on Isachen's Plateau and conclusions regarding the temperature of the glaciers on Spitzbergen. *Geog. Ann.*, 17, 53-88.

Sverdrup,H.U.,1935b. The ablation on Isachsen's Plateau and on the 14th of July Glacier in relation to radiation and meteorological conditions. *Geog. Ann.*, 18, 145-166.

Tabler,R.D.,1975. Predicting profiles of snowdrifts in topographic catchments. *Proc. 43rd Western Snow Conf.*, 87-97.

Taylor,L.D.,1971. Glaciological studies on the South Pole traverse, 1962-1963, in Crary,A.P. (ed), *Antarctic Snow and Ice Studies II*, 209-224.

Tucker,W.B. and Colbeck, S.C.,1977. A computer routing of unsaturated flow through snow. *C.R.R.EL.*, Special Report 77-10, 39p.

U.S. Army.,1956. *Snow Hydrology*, Summary report of the snow investigations, Corps of Engineers, North Pacific Division, Portland, Oreg., 437p.

Wakahama,G., Kuroiwa,D., Hasemi,T. and Benson,C.S.,1976. Field observations and experimental and theoretical studies on the superimposed ice of McCall Glacier, Alaska. *Jour. Glaciol.*, 16, 135-149.

Wakahama,G.,1968. The metamorphism of wet snow. *I.A.S.H.*, Pub. 79, 370-379.

Wankiewicz,A.C.,1976. *Water Percolation Within a Deep Snowpack - Field Investigations at a Site on Mt. Seymour, British Columbia*. PH.D. Thesis, University of British Columbia, Vancouver, B.C., 177p.

Wankiewicz,A.C.,1978a. A review of water movement in snow. *Proc. Modeling of Snow Cover Runoff*, ed. Colbeck,S.C. and Ray,M., C.R.R.E.L., 336-350.

Wankiewicz,A.C.,1978b. Hydraulic characteristics of snow lysimeters. *Proc. 35th Eastern Snow Conf.*, 105-116.

Ward,W.H. and Orvig,S.,1953. The heat exchange at the surface of the Barnes Ice Cap during the ablation period. *Jour. Glaciol.*, 2, 158-168.

Woo,M.K.,1982a. Upward flux of vapor from frozen materials in the High Arctic. *Cold Regions Sci. and Tech.*, 5, 269-274.

Woo,M.K.,1982b. Snow hydrology of the High Arctic. *Proc. 50th Western Snow Conf.*

Woo,M.K. and Heron,R.,1981. Occurrence of ice layers at the base of High Arctic snowpacks. *Arctic and Alpine Research*, 13, 225-230.

Woo,M.K., Heron,R. and Marsh P.,1982. Basal ice in High Arctic snowpacks. *Arctic and Alpine Research*, 14.

Woo,M.K., Heron,R.,and Steer,P.,1981. Catchment hydrology of a
    High Arctic lake. *Cold Regions Sci. and Tech.*, 5,
    29-41.

Woo,M.K. and Marsh,P.,1977. Determination of snow storage for
    small eastern High Arctic basins. *Proc. 34th Eastern
    Snow Conf.*, 147-162.

Woo,M.K. and Marsh,P.,1978. Analysis of error in the
    determination of snow storage for small high Arctic
    basins. *Jour. App. Meteorol.*, 17, 1537-1541.

Wooding,R.A. and Morel-Seytoux,H.J.,1976. Multiphase fluid flow
    through porous media.*Ann. Rev. Fluid Mech.*, 8,
    233-273.

Work,R.A.,1948. Snow layer density changes. *Trans. American
    Geophysical Union*, 29, 525-545.

Yosida,Z.,1973. Infiltration of thaw water into a dry snow
    cover. *Low Temp. Science*, Ser. A, 31, 117-133.

Young,G.J.,1969. *Snow Cover Variations, Axel Heiberg Is.,
    N.W.T.*, M.Sc. Thesis, McGill Univ., Montreal, Que.,
    87p.